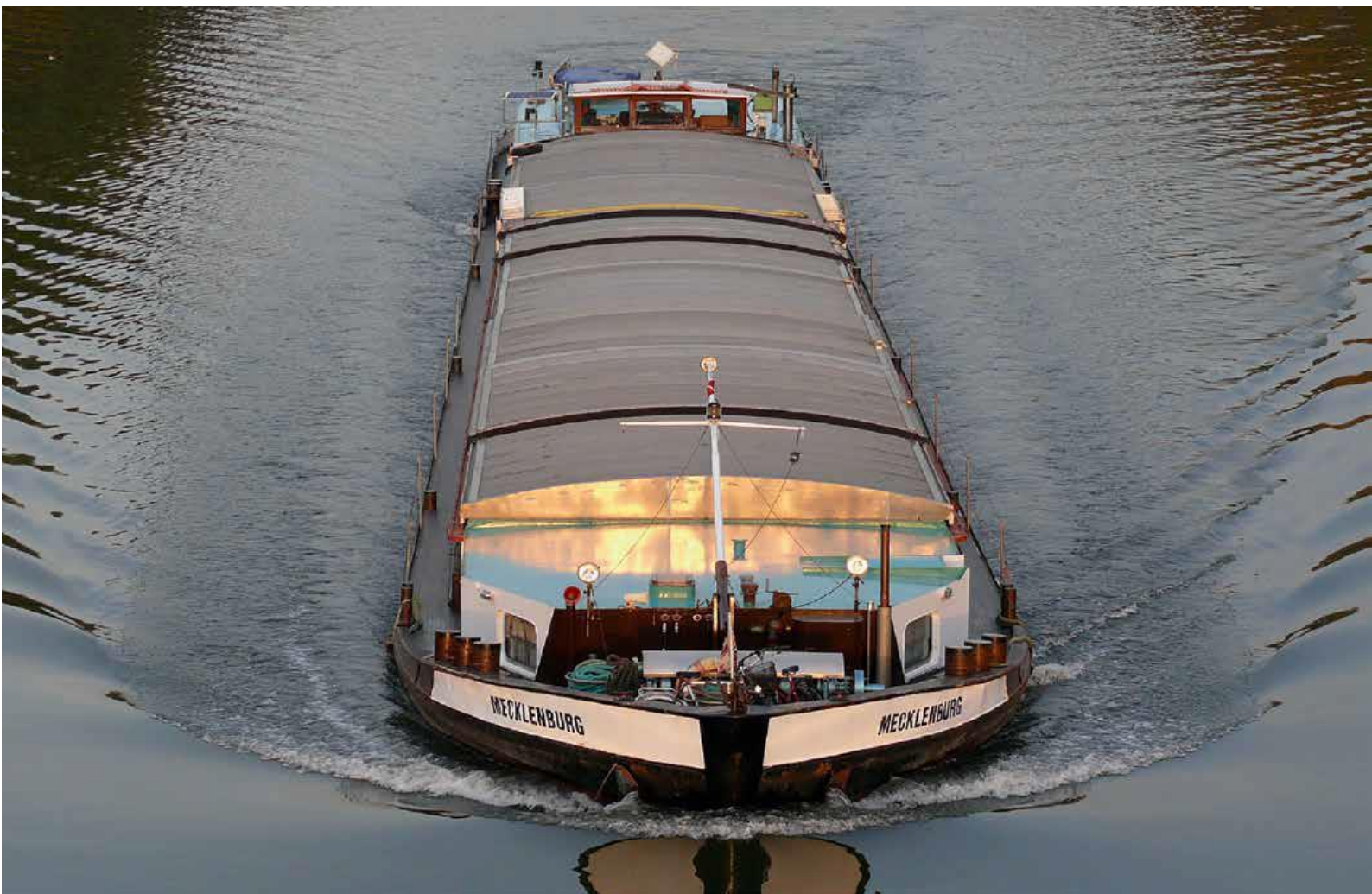


Investigation of the power estimation for inland barges

Master's Thesis
Despoina Gkioka

Date of submission 2023



Rijkswaterstaat
Ministry of Infrastructure
and Water Management

 TU Delft

Investigation of the power estimation for inland barges

by

Despoina Gkioka

Student number: 5294533

Master thesis submitted to Delft University of Technology
in partial fulfilment of the requirements for the degree of

MASTER OF SCIENCE

In Hydraulic Engineering

Faculty of Technology, Policy and Management

To be defended publicly on Wednesday June 28, 2023

Graduation committee:	Prof.dr.ir. M. van Koningsveld	TU Delft, chair
	Ir. E. Bolt	Rijkswaterstaat
	Drs. O.C. Koedijk	TU Delft, Rijkswaterstaat
	Dr.ir. H. de Koning Gans	TU Delft
	MSc. M. Jiang	TU Delft, supervisor

An electronic version of this thesis is available at <http://repository.tudelft.nl>



Preface

This thesis is a result of nine months research at Delft University of Technology & the Ministry of Infrastructure and Water management, i.e., Rijkswaterstaat. The first three months were dedicated to a literature analysis considering a variety of methods that calculate the required power either for inland barges or seagoing vessels. More specifically, the study focused on the existing method that Rijkswaterstaat uses to compute both the resistance that a sailing ship encounters and the required power, this is the Bolt (2003) method. Then similar theories were analyzed in order to get all the required background information for understanding the shallow water effects. The remaining six months were used to implement the Bolt (2003) method and the options for improving it, in Python, to evaluate the results and then to compare with the real data and as a last step to write the thesis report.

At the beginning of my internship at Rijkswaterstaat, Ernst Bolt and Otto Koedijk explained to me that Backer van Ommeren, the initiator of my thesis topic, studied the existing power method and discover that some simplifications and assumptions adversely affect the accuracy of the method in resistance and power estimations. Finally, during the kickoff meeting the chair of this thesis, Mark van Koningsveld, proposed to me that not only sailing of barges in shallow water is important but also behavior of motor vessels in these water conditions would be an asset to inland navigation. So, it was decided to conduct a literature study on the available power estimation methods which in turn were coded in python notebooks and uploaded to OpenTNSim repository. The evaluation of the power methods were achieved through the Academic and the Real-world test cases and taking into account the results of the tests the best practice(s) were selected.

During my thesis, a lot of people were actively involved in guiding, helping and teaching me. First of all, many thanks go out to all committee members: prof. M. van Koningsveld, dr. Ir. H. de Koning Gans, drs. O. Koedijk, ir. E. Bolt and Phd. M. Jiang were accepted to staff it. Especially to Man Jiang, thanks for all the time you made available for me at any time. Secondly, I would like to thank my parents that offered me the opportunity to do my master abroad and for the everlasting support and your encouragement as without then I could not be standing here. Also, many thanks go out to my friends who supported me and helped with my struggles both personal and academic.

Despoina Gkioka
Delft, June 2023

Summary

Inland shipping is widely acknowledged as a sustainable mode of transportation due to its low energy consumption and emissions in comparison to road and rail transport. However, with growing concerns around reducing emissions in the transportation sector, there is pressure to address environmental issues associated with inland shipping. In the Netherlands, a Green Deal has been formulated to outline the goals for reducing CO₂ emissions by 2030 and other environmental pollutants by 2035 in inland navigation, to enable us to take the next step towards a climate-neutral society by 2050. This increasing pressure raises the question of how to get insight of the energy consumption and the associated emissions from inland shipping. To date, an accurate method is lacking that is able to estimate the total resistance, the propulsive power and in turn the energy consumption in shallow water and thus to quantify the CO₂ emissions. Over the years, several power estimation methods have been developed for inland vessels, with the Rijkswaterstaat power estimation method being one of the most widely recognized. Recently, Backer van Ommeren (2019) investigated the Rijkswaterstaat power estimation method and found that certain assumptions and parameters used in the method were not well-founded, and that some approximations were unnecessary.

The main objective of this study to conduct a comprehensive literature analysis on Backer van Ommeren (2019) comments and recommendations regarding the Rijkswaterstaat (RWS) or Bolt (2003) method in order to clarify to what extent these recommendations will indeed improve the Bolt (2003) method or if an alternative power method should be proposed instead. This will be accomplished through a comparison process of the power results as a function of sailing speed, water depth, and channel dimensions for various types of inland vessels, utilizing the selected methods that will be derived from the literature study along with Backer van Ommeren (2019) recommendations applied to the original method. After coding these methods in Python and analyzing their results, the best practice(s) that will be derived from the test cases, will be implemented on two classes of motor vessels an M6 and an M8 to estimate the resistance and the power and then they will suggest to Rijkswaterstaat for potential future use.

To achieve the main research objectives, the following research was conducted. Initially, a literature analysis on the available resistance methods, how they consider and divide the several resistance components, and which are the shallow water effects that affect them, was done in order to evaluate their performance in terms of power estimations. Secondly, the comments made by Backer van Ommeren were presented and analyzed. Specifically, he investigated various formulations for calculating the return flow, water level depression, and characterizing the waterway as normal, narrow, wide, or very wide. This study was accomplished through the use of specific power efficiency and resistance coefficients. Based on his study, he derived a method, the Backer method (Backer van Ommeren, 2019) and suggested a number of formulas to be further tested. After completing the literature review, the findings lead to the selection of the power methods that will be treated in this thesis and the kind of improvements that will be applied to the original Bolt (2003) method.

Subsequently, from the literature study and Backer van Ommeren (2019) review, four methods were derived to be simulated and tested in this thesis. These methods include the TU Delft method, Bolt method with speed correction, Bolt method modified by Backer, and Backer method. The simulation was achieved with two rounds of tests that are conducted, firstly the “Academic test case” and secondly the “Real-world test case”. In the “Academic test

case” five methods were simulated and the most promising that met specific criteria are selected. Then, in the “Real-world test case” the selected methods as they were derived from the “Academic test case”, were further evaluated for the selection of the best practice(s). The first round of tests is applied to two classes of motor vessels in narrow and wide waterways with shallow, intermediate and deep water depth conditions and the results include the total resistance and the brake power while the second round simulates only one motor vessel of class six in wide waterways for the same depth conditions as previously and the outcome includes the delivered power. The “Real-world test case” is divided in two parts. The first part includes the comparison between the estimated and the measured delivered power in order to assess the performance of the methods with the real data. The second part evaluates the performance of the methods in the presence of a current flow, by comparing the fuel consumption in upstream, downstream and round trips.

The evaluation of the methods in a real-world test case led to a number of conclusions, and the best practices were recommended accordingly. It should be noted that the comparison process was based solely on a single real-world case, utilizing a singular set of real data. It is important to be conducted additional comparisons across multiple real cases in order to increase the understanding of the accuracy of the various methods being compared. In the context of power estimation in shallow water, both the Bolt (2003) method and TU Delft method (Jiang, Baart & van Koningsveld, 2022) have demonstrated remarkable accuracy in their predictions while Backer method and Bolt method modified by Backer are not recommended for power predictions. Notably, Bolt (2003) method has proven to be effective in estimating power within a speed range of 2.5m/s to 3.5m/s while TU Delft method (Jiang, Baart & van Koningsveld, 2022) showed accurate predictions within a speed range of 2.5m/s-4m/s (accurate as defined within 20% of the observed value). Regarding the intermediate and deep water conditions, only TU Delft method (Jiang, Baart & van Koningsveld, 2022) showed acceptable performance in power estimation again for sailing speeds varying 2.5 m/s – 5 m/s. The power demand at very low speeds for all the three methods display a considerable deviation between the estimated power output and the actual values, surpassing the acceptable rate of 20%. This can be attributed to two reasons. At low speeds, the interaction between a sailing vessel and the boundary layer becomes more pronounced, causing the ship to experience turbulent effects that dominate the boundary layer more intensively. As a result, the vessel experiences increased resistance, requiring more power. Secondly, in actual operating conditions, a ship has a minimum power engine setting that is dependent on the engine characteristics. So, when the ship is moored and the "hotel mode" is on, as the ship not having a separate auxiliary power unit, a propeller brake is used to allow the turbine to continue running and generate power without the propeller spinning. This effect does not consider by the power estimation methods that rely on parameters such as sailing speed and water depth. The Backer (2019) method demonstrated satisfactory performance in predicting resistance and power for both types of motor cargo vessels within narrow waterways. This method effectively accounted for the variations in depth by accurately estimating lower resistance and power demand as the depth increased. However, Its accuracy in wide waterways diminished due to the equations' unsuitability for such conditions, by generating nearly identical resistance and power estimations for the three different water depths. Based on the aforementioned restriction, it is not recommended to employ this particular approach for subsequent power estimations. As regards the Bolt method modified by Backer performs poorly in estimating resistance and power across narrow and wide waterways with varying depths. It consistently yields similar results for shallow, intermediate, and deep depths at a specific sailing speed. Therefore, it is not recommended as an improvement to the Bolt method. In the presence of current flow, three methods have shown promising results. Specifically, the TU Delft method (Jiang, Baart & van Koningsveld, 2022) is recommended for

motor vessel, as it produces deviations from real measurements of 0.93% for upstream, 1.36% for downstream, and 0.45% for round trips. Also, TU Delft method (Jiang, Baart & van Koningsveld, 2022) is recommended in case of pushed and coupled convoys as it has been found to produce the smallest deviations in upstream sailing, with a maximum of 3.9% while the deviations observed for downstream sailing and round trips are around 1.9%. Bolt (2003) method and Bolt method with speed correction, were found to produce acceptable deviation rates of around 7% for upstream trips, with the benefit that these methods require less detailed input data. Nevertheless, for downstream and round trips, the deviations were much higher, reaching up to 80% and 30%, respectively and event that requires additional investigation and validation.

Contents

Investigation of the power estimation for inland barges.....	0
List of Symbols.....	14
1. Introduction.....	16
1.1. Background information.....	16
1.2. Inland shipping & modal split.....	16
1.3. Problem description	19
1.3.1. Pressure to acquire a power method for inland shipping & to reduce emissions19	
1.3.2. Research gap	20
1.3.3. Problem statement.....	21
1.4. Research objectives.....	21
1.5. Research question	22
1.5.1. Research Sub-questions	23
1.6. Approach and methodology.....	23
1.7. Thesis outline.....	25
I Literature review.....	27
2. Theoretical background.....	28
2.1. Resistance description.....	28
2.1.1. Power & energy consumption.....	31
2.1.2. Power model	31
2.2. Flow description	33
2.3. Bolt method.....	34
2.3.1. Explanation of velocities that used in Bolt method	34
2.4. Backer van Ommeren comments	36
2.4.1. Analysis of Backer van Ommeren comments.....	37
2.4.2. Proposed formulas for wide & very wide waterways	41
2.4.3. Selected equations	42
2.5. Options to improve Bolt method	43
II Methods implementation.....	47
3. Materials & methods.....	48
3.1 Modelling concept.....	48
3.2 Implementation of the five studied methods	48
3.3 Academic test case with evaluation criteria.....	49
3.4 Real-world test case with evaluation criteria.....	50

3.4.1.	Real-world data introduction	50
3.4.2.	Delivered power evaluation process	51
3.4.3.	Fuel-use evaluation process	52
III	Results.....	54
4.	Academic test case	55
4.1.	Bolt method.....	55
4.2.	Backer method	58
4.3.	Bolt method modified by Backer.....	61
4.4.	Bolt method with speed correction for shallow water	62
4.5.	TU Delft method	65
4.6.	Evaluation of the performance of the 5 studied method	67
4.7.	Selection of the three most promising methods.....	69
5.	Real-world test case	71
5.1.	Three methods tested by real power-speed data of a single barge	71
5.1.1.	Bolt method.....	71
5.1.2.	Bolt method with speed correction.....	73
5.1.3.	TU Delft method	75
5.2.	Three methods tested by fuel report with current influence and vessel type variation.....	76
5.3.	Selection of the best practice(s).....	78
5.3.1.	Selection based on power-speed results.....	78
5.3.2.	Selection based on fuel-use results.....	80
5.4.	Summary.....	80
III	Discussion, conclusions & recommendations.....	82
6.	Discussion Part A: Application of the best practice(s) in shallow water depth.....	83
6.1.	Resistance and Power results for a motor vessel M6 (CEMT IVa).....	83
6.2.	Resistance and Power results for a motor vessel M8 (CEMT Va).....	85
7.	Discussion Part B	88
8.	Conclusions & Recommendations.....	90
8.1.	Conclusions.....	90
8.2.	Recommendations.....	95
	List of figures	98
	List of tables.....	101
	Bibliography.....	104
	Appendix A:Waterway classification	109
	Appendix B:RWS vessel classification.....	111

Appendix C:Backer method-2 nd approach	112
Appendix D:Comparison between power from survey data & estimated power according to Bolt method.....	114
Appendix E: Data for the evaluation of the fuel consumption.....	116
Appendix F:Fuel consumption.....	118
Appendix G: Background physics	120
Theories for confined waterways.....	120
Appendix H: Algorithms.....	124
Bolt method.....	124
Backer method	127
Bolt method with speed correction	128
Bolt method modified by Backer.....	128
Reference formula for implementing TU Delft method.....	129

List of Symbols

Symbols	Description
$1 + k$	Form factor
α	Wave amplitude (m)
B_s	Beam of a ship (m)
r	Blockage coefficient
C_B	Block coefficient
C_f	Frictional resistance coefficient
C_p	Pressure coefficient
C_r	Residual resistance coefficient
C_t	Total resistance coefficient
C_{vp}	Viscous pressure resistance coefficient
C_v	Viscous resistance coefficient
C	Wave celerity (m/s)
Fr_h	Depth Froude number
G	Acceleration of gravity (m/s^2)
H	Wave height (m)
h	Water depth (m)
L_s	Length of ship (m)
L_{pp}	Perpendicular length of ship
R_f	Frictional resistance
R_v	Viscous resistance
R_{vp}	Viscous pressure resistance
R_w	Wave-making resistance
Re	Reynolds number
S	Wetted surface (m^2)
V_s	Sailing velocity (m/s)
U	Flow velocity (m/s)
U_r	Return flow velocity (m/s)
U_{maxb}	Maximum Boundary layer _{bed} velocity (m/s)
U_{maxs}	Maximum Boundary layer _{ship} velocity (m/s)
Λ	Wavelength (m)
N	Kinematic viscosity (m^2/s)
P	Water density (kg/m^3)
P_e	Effective power (kW)
P_b	Brake horsepower (kW)
P_d	Delivered horsepower (kW)
a^*	Karpov's coefficient, _{friction}
a^{**}	Karpov's coefficient, _{residual}

1. Introduction

1.1. Background information

Climate change has major consequences for humanity, nature and the environment. If greenhouse gas emissions continue to increase at the same rate, the temperature on Earth will keep rising. Scientists claim that this increase will continue for decades, largely due to the greenhouse gases produced by human activities (NASA, 2020). The Paris Agreement was drawn up in 2015, with the aim to ensure the global response to the threat of climate change and to pressure to reduce emissions in the six main sectors namely buildings, industry, energy, transportation, nature-based solutions, and agriculture (UNFCCC, 2020). European Union has demonstrated significant progress in reducing greenhouse gas emissions by 23% between 1990 and 2018, but the goal is continuous by cutting emissions by at least 55% by 2030 in order to set Europe on a responsible path to becoming climate neutral by 2050 (European Commission, 2020). The analytical goals for the reduction of the environmental pollutants are summarized below:

- 2024: A reduction of CO₂ emissions of at least 20% compared to 2015, and a reduction of environmental pollutants of at least 10% compared to 2015
- 2030: A reduction of CO₂ emissions of 40% to 55% compared to 2015
- 2035: A reduction of environmental pollutants of 35% to 50% compared to 2015
- 2050: To have realized emission-free and climate-neutral inland shipping

The Smart Mobility Strategy (SSMS) in line with the EU Green Deal, emphasizes the crucial role of Inland Waterway Transport as a sustainable means of transportation within the broader transportation sector, playing a crucial role in achieving future sustainability objectives. In particular, the SSMS highlights the potential of inland waterway transport to reduce emissions in the transportation sector and support the EU's transition to a carbon-neutral economy. Specifically, the extension is focused to increase the share of Inland Waterway Transport (IWT) by 25 % by 2030 and by 50 % by 2050 as a sustainable mode of transport, so as to follow Green Deal goal of 90% reduction in transport-related greenhouse gas emissions by 2050 (Fumuso, 2021). To achieve the aforementioned objectives, it is essential to implement "green policies." This requires the quantification of greenhouse gas emissions, which is strongly related with the accurate estimation of the shaft power as well as can enhance the effectiveness of the policies. By utilizing the estimated power as an input value, emissions can be quantified through various methods that calculate different types of emissions, or by determining energy efficiency design indexes for different ship types.

This chapter provides some background information on the inland shipping sector in general, and more specifically on inland shipping in the Netherlands. Afterwards we dive into the problem description of this study and the research gap, followed by the definition of the research objective, scope and the research questions that are going to be answered.

1.2. Inland shipping & modal split

There are four major types of transport namely air, road, sea and rail. Inland waterway transportation, also known inland refers to the movement either of goods or people between different locations through the use of waterways such as rivers and canals. This transportation system typically involves ships or barges that navigate into the inland waterways. During the Industrial Revolution, the waterway network was significantly improved since canals were

constructed and hence the water transports were extended. Moreover, the ever-growing world trade and the constant increasing in the transportation of goods through water in the last centuries shows an additional acceleration rate in the recent decades as a result of the advancements in technology. Large sea-going vessels have become an indispensable part of the intercontinental transport, but it also applies to the inland transport rates.

Waterborne transport is considered one of the significant modes of transportation within the logistic chain internationally and particularly in Europe. Specifically, over 37,000 kilometers of waterways interconnect various European cities and industrial regions, therefore these trade routes play a significant role in supporting industry and facilitating the movement of goods. The River Rhine can be considered the perfect example to present this trend, as it covers approximately 1000 kilometers and flows from Basel to Rotterdam. Moreover, with the Mannheim Convention of 1868, the river Rhine became an economic asset for the Rhine region and now is the busiest river in Europe and a very crucial transport axis in West-Europe (Bureau Voorlichting Binnenvaart, 2017).

Inland waterway transport is a competitive alternative to other modalities like road or rail transport. At first, this is because inland navigation is environmental-friendly compared to its alternatives: it has a relatively low energy consumption per ton kilometer, and it has low noise emissions. Secondly, inland shipping is a relatively safe mode of transport, especially when you consider the transportation of dangerous goods (European Alternative Fuels Observatory, 2023). In the third place, inland waterway transport is characterized by its reliability and major capacity for increased exploitation, compared to other modes of transport which are often confronted with congestion and capacity problems (Bureau Voorlichting Binnenvaart, 2017). Because of these advantages of inland shipping and the increasing pressure to reduce emissions, considering climate change and environmental damage, the transport sector is experiencing a modal shift towards inland shipping. There is a potential of increasing this modal share even further, and the European Commission aims to promote and strengthen the competitive position of inland waterways in the transport system, and to facilitate its integration into the intermodal logistics chain (Bureau Voorlichting Binnenvaart, 2023). It is mentioned that the transport performance as illustrated in Figure 1.2.1 shows a steady recovery trend for inland waterway freight transport in Europe, starting in the third quarter of 2020. A weakening in this upward trend occurred in the quarter of 2021, which can be attributed to the extreme floodings (climate change) in the Rhine region. This period of high water was followed by a period of low water during the fourth quarter of 2021 (CCNR., 2022).

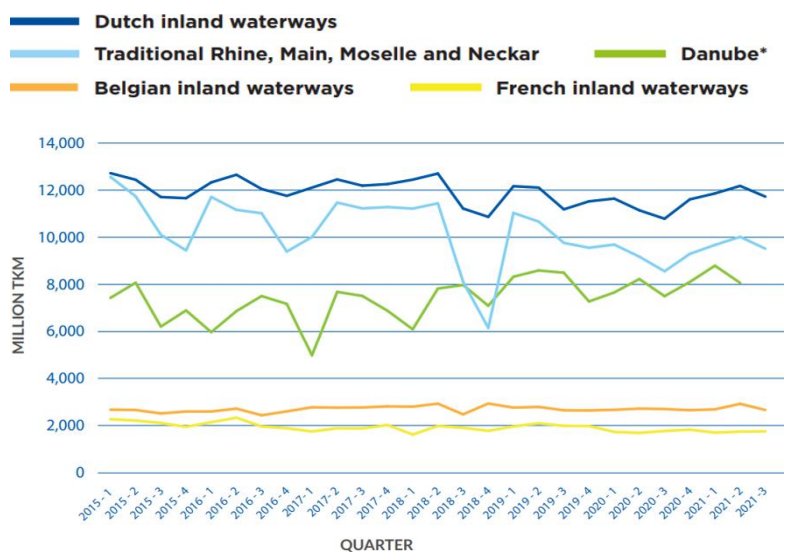
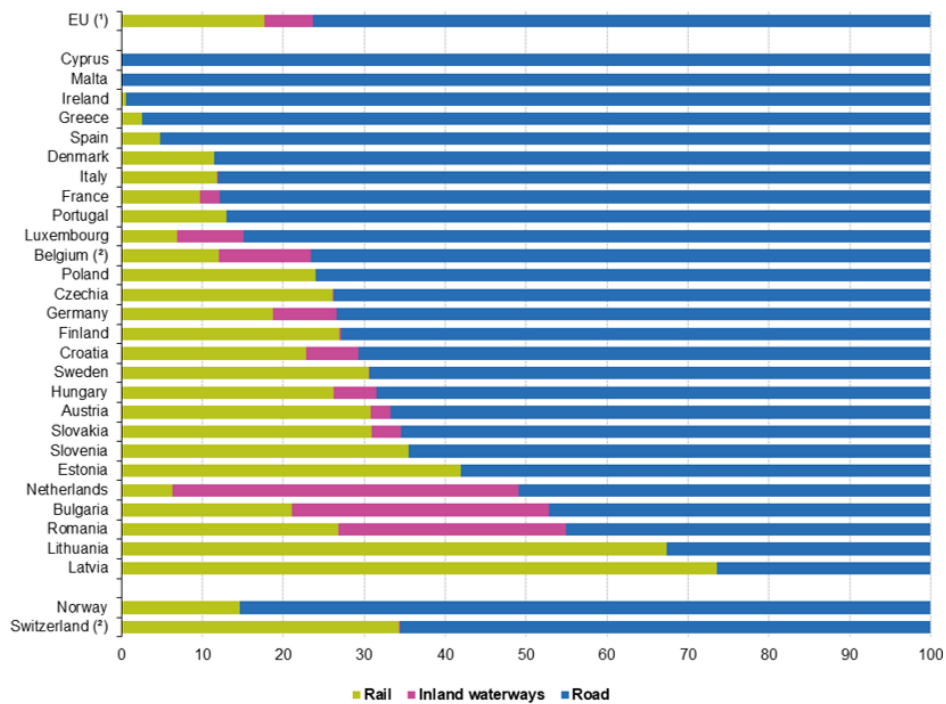


Figure 1.2.1: Inland waterway transport performance in Europe by region & quarter (CCNR., 2022)

Modal split is the distribution of the transportation modes, that depends on both factors the industrial activity of an area and the geographical location. Regarding the latter, the geographical location has a large influence on the share of different modalities. Across the Europe, rail, road, shipping, and inland navigation are the main modes of transportation of goods. Underground pipelines are used in case of fixed routes, transporting large volumes of liquids. In case of urgent delivery of small cargo, cargo airlines are preferred. Figure 1.2.2 shows the modal split around the Europe. Notably, in 2019 shows that the modal share of inland navigation is by far the highest in the Netherlands. The freight that is being transported in the Netherlands by inland shipping amount to 45% in 2019 while currently a decrease of around 3% has been observed. With a fleet of 8000 inland ships, the Dutch fleet is the biggest and most modern fleet of Europe (Sipotra, 2021).



Note: Countries are ranked based on the share of road transport.
 (*) EU includes rail transport estimates for Belgium and road freight transport estimates for Malta.
 (**) Estimated values.

Figure 1.2.2: Modal split of freight transport in 2019 data (Sipotra, 2021)

Figure 1.2.3 illustrated the amount of goods that are transported per modality type in the Netherlands with a transport share of over 45% in comparison with the other modalities. Also, comparing Figure 1.2.2 and Figure 1.2.3, nowhere else in Europe is the share of inland shipping in this chain as large as in the Netherlands and combined with the extensive network of rivers and canals connects major industrial areas and ports to each other, making inland shipping an efficient and cost-effective mode of transport.

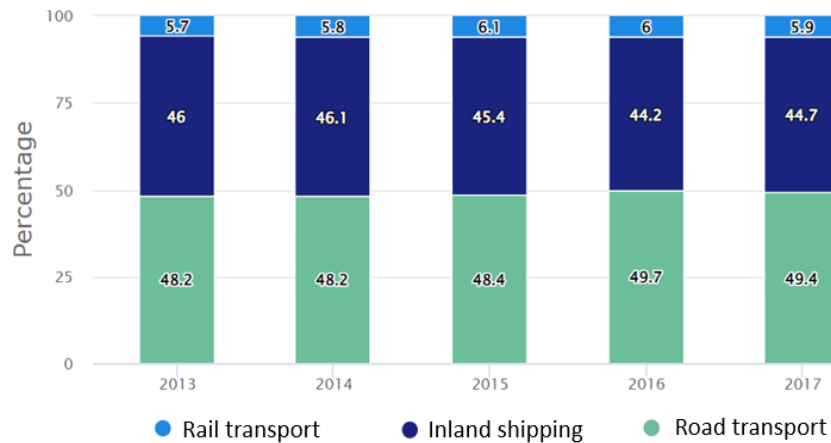


Figure 1.2.3: Percentage of freight transport by modality in the Netherlands (Percentage Goedertransport per Modaliteit in Nederland, Binnenvaartcijfers, 2023b)

1.3.Problem description

1.3.1. Pressure to acquire a power method for inland shipping & to reduce emissions

Now that significance of shipping in cargo transportation becomes increasingly apparent and the emerging emissions policies are known, it is crucial to recognize the importance of precise quantification methods. The quantification of emissions is strongly related with the required power that a vessel needs in order to overcome the ship resistance and sails to its destination at specific time. Over the years, several methods have been developed to predict the propulsive power but most of them were based on conventional vessels and in deep water conditions while the inland shipping has some limitations (water depth & channel width, hull shape). As a result, these limitations hinder the direct applicability of the methods to inland vessels and affect the accuracy of the power results. Consequently, there is a need to develop a new method that is specifically applicable to the inland sector.

In 2003, Bolt taking these considerations into account developed a method for the estimation of the ship resistance, the required power, and the energy consumption that account for the shallow water effects and the shape of inland vessels. The idea of Bolt (2003) method lies in that does not specialize to an individual inland ship type, but it has a more general application, so an estimate should be made on the basis of the “average” characteristic main dimensions per ship class. The advantage of the method is that needs a small number of input parameters to conduct the calculations and the equations are relatively simple and solve algebraically. This method has been used for several years from Rijkswaterstaat for the corresponding calculations in the entire inland fleet. Moreover, Rijkswaterstaat considering the European vision to reduce the emissions from inland shipping, developed a model, BIVAS model, which performs a network analysis on inland water transport to compute the different types of emissions. For the development of this model, Bolt method was used to calculate the resistance and the required power in order to estimate the energy consumption and to translate it to emissions.

Recently, in 2019 Bolt (2003) method was reviewed by Backer van Ommeren and Rijkswaterstaat received some critical comments that revise its accuracy. According to Backer van Ommeren, simplifications and assumptions in key equations and power efficiencies, adversely affect the accuracy of the resistance and power estimations. Consequently, Backer van Ommeren along with a detailed description of the weak points that he detected in Bolt

method, he also proposed two recommendations. Especially, he suggested the use of another power method and some recommendations of how to improve the accuracy of the current method.

Taking into account the commitments of the European vision to be climate-neutral by 2050 and the increase of the share of the Inland Waterway Transport as a sustainable mode of transportation, reducing inland emissions has become crucial. However, it is raised the question of how to achieve this goal, without an accurate prediction power method to quantify inland emissions along the waterway network. Therefore, the challenge will be to acquire a power method that can combine the shallow water effects with the special shape of the inland vessels, and it is directly applicable on these ships. Developing a reliable predictive method that can address these challenges will be essential in achieving meaningful reductions in inland emissions.

1.3.2. Research gap

The process of calculating energy consumption and emissions in inland shipping is complex and strongly related with accurately predicting ship resistance and required power. There are numerous factors that influence these parameters, including ship and waterway dimensions, sailing speed, and current flows. For example, ships navigating through narrow and shallow waterways experience greater resistance, requiring more propulsive power, which in turn increases energy consumption and emissions. Therefore, it is crucial to look for a method that considers both ship and waterway characteristics to estimate resistance, propulsive power, energy consumption, and corresponding emissions.

Over the years, various methods and tools have been developed to quantify emissions, which can be achieved by computing either CO₂ emissions or estimating different types of transport emissions. In 2009, the International Maritime Organization's (IMO) Marine Environment Protection Committee developed measures to reduce greenhouse emissions in international shipping, which were later expanded in 2013 to include inland navigation. To measure the amount of CO₂ emitted per capacity mile (tone-mile) by a sailing ship, IMO proposed the modified Energy Efficiency Design Index (EEDI*) (Radojčić, Simić, Momčilović, Motok & Friedhoff, 2021b). However, with the European Green Deal signed in December 2019, there is additional pressure to control and reduce emissions to achieve carbon neutrality by 2050 (European Environment Agency, 2023). As a result, another method was developed in 2019 that focuses on quantifying emissions per type, such as nitrogen oxides, in addition to CO₂. Regardless of the differences in criteria and processes used to quantify emissions, all of these methods rely on the required ship power as a fundamental factor.

To date, numerous studies have been conducted to estimate the ship resistance and the propulsive power but most of them were developed in deep and unrestricted water conditions. Also, methods that are related to the inland vessels are based on tradition and the personal wishes and experience of the skippers than on a scientific approach. Consequently, these methods do not account shallow water effects and they are not directly applicable to inland ships navigating in such conditions. Starting from 1945, Karpov (van Terwisga, 1989) was developed an approximate method that was described in literature of van Terwisga, for practical calculations of the total ship resistance. The transformation of the method in order to be applicable to shallow water was based on the depth Froude number and the substitution of the actual speed of the ship with a notional speed. Specifically, Karpov determined that the total resistance can be divided into two components the frictional and the residual and according to that he defined the corresponding notional speeds and the

related coefficients for these speed calculations. However, the use of the deep sailing speed in the Froude number reduce the accuracy of the method in shallow water. A few years later, in 1974, Gulddammer proposed a model to calculate resistance, where in turn was used to estimate propulsive power. This model was developed on conventional ships and, through corrections to the friction coefficient, was applied to inland navigation vessels. More specifically, the friction correction was made by increasing the original friction proportionally to the increased wetted surface due to appendages. Almost ten years later, (Holtrop & Mennen, 1982) developed a method that was based on the regression analysis of a wide range of model tests and trial data which give broad applicability. The method estimates the total resistance by making a clear breakdown into different resistance components. Again, the simulations were conducted on deep-water conditions.

Another power estimation method was developed in 2003 by Bolt which takes into account the effects of shallow water by adjusting sailing velocity in narrow and shallow conditions. For the development of the method simplifications were done for the calculation of the return flow and the limit speed. This method was used from Rijkswaterstaat in order to conduct power calculations, to estimate the energy consumption and to quantify the different types of emissions from inland navigation. However, in 2019 this method was assessed from Backer van Ommeren and showed that the use of assumptions and simplifications adversely affect its accuracy. This statement triggered the interest either to improve the original method or to substitute it with a more advanced and accurate one.

1.3.3. Problem statement

The aim of this dissertation is to perform a literature review and analysis of the available resistance-power methods, the Bolt (2003) method, the Backer method, and Backer van Ommeren (2019) recommendations. The purpose is to identify to what extent Backer van Ommeren recommendations will indeed improve Bolt (2003) method or a substitution with an alternative power method is necessary. The analysis will assess the strengths and weaknesses of these methods and recommendations, as well as their practical applicability. Ultimately this study aims to suggest the best practice(s) that accurately calculate the ship resistance, the propulsive power and then the energy consumption which are the fundamental components to emission calculations and policies to reduce environmental impact.

1.4. Research objectives

The goal of this study is to conduct a comprehensive literature analysis on the resistance or the different resistance components that affect inland shipping and determine the power use, in order to acquire an accurate power prediction method. Specifically, Backer van Ommeren comments and recommendations regarding the Rijkswaterstaat (RWS) or Bolt (2003) power estimation method will be investigated, to clarify to what extent these recommendations will indeed improve the method or if an alternative power method should be applied instead. This will be accomplished through a comparison of power as a function of sailing speed, water depth, and channel dimensions for various types of inland vessels, utilizing either available power methods from the literature or by modifying Bolt method with well-developed formulas from the literature material. The derived results will be evaluated with real power and fuel-use data and the best practice(s) will be proposed to Rijkswaterstaat for potential future use and the implementation of the European vision for zero CO₂ emissions by 2050. Based on that, the following research objectives are presented as follows:

First objective: To study which are the available resistance methods in the literature and which of them are applicable to inland vessels, how they consider and divide the total resistance into several resistance components and how this distinction affect the power estimation.

To accomplish the first objective, a literature study on the available resistance methods will be conducted. It will be discussed how each method considers the ship resistance and how each component interact with the vessel and obstacle its sailing. The relationship between resistance and power, as well as the various types and characteristics of power efficiencies, will also be explored. Based on the findings of the literature review, methods will be classified according to the type and number of resistance components, in order to assess their performance in achieving the third objective of the study.

Second objective: To evaluate Backer van Ommeren recommendations and clarify to what extent these recommendations will indeed improve the Bolt method.

This will be achieved, by studying the Backer van Ommeren technical report which contain an alternative power method and recommended formulations for several parameters. More specifically, the proposed formulas and coefficients will be applied to the Bolt (2003) method in order to test to what extent these recommendations improve the accuracy of the current method. The comparison and the validity of these two methods will be implemented in the third objective of the study.

Third objective: To analyze and evaluate the performance of the selected resistance-power methods from literature and from the Backer van Ommeren recommendations.

The methods that will be derived from the previous two objectives will be evaluated in two stages. Originally, all the derived methods will be coded in python notebooks in order to execute resistance and power calculations for different water depths and channel widths. In the initial stage, each method will undergo an assessment based on specific criteria for resistance and power calculations, with the aim of selecting those that satisfy the established requirements. In the second stage of evaluation two round of test will be conducted. Firstly, the power as a function of speed, water depth and channel dimensions will be compared with real power data and secondly the performance of each method will be tested in the presence of current flows.

Fourth objective: To draw conclusions on this comparison in order to recommend the best practice(s) and to be applied for a number of inland vessels.

The results that will be derived from the evaluation process will be analyzed and the best practice(s) will be suggested to Rijkswaterstaat.

1.5. Research question

The research objectives that are defined and presented in detail previously will be achieved through the following main research question.

“What resistance and power related estimation methods are available in literature, how can objectively evaluate how these methods perform and how can these evaluation results be used to provide Rijkswaterstaat with the best practices?”

To answer the main research question, five sub-questions are formulated and are presented in the following section.

1.5.1. Research Sub-questions

To achieve the defined research objectives, the following research questions has been defined and further elaborated in the following section:

1. What methods are available in literature for the estimation of the total resistance and the propulsive power and how these resistance methods consider the resistance components?
2. What are Backer van Ommeren recommendations to improve Bolt method, and to what extent these recommendations will indeed improve Bolt method?
3. What are the available options to improve the current power method in terms of resistance and propulsive power estimation for inland ships?
4. How can the performance of these methods best be compared and what criteria should be applied to enable the objective selection of the most promising methods?
5. Based on these criteria what can be recommended as a best practice moving forward for the Rijkswaterstaat?

1.6. Approach and methodology

To answer the different sub-questions of this research, the approach and methodology of each question will be presented.

Sub-question 1: *“What methods are available in literature for the estimation of the total resistance and the propulsive power and how these resistance methods consider the resistance components?”*

The determination of the resistance faced by a ship and the propulsive power required is a complex process that involves various contributing factors such as the ship type, sailing environment, and other effects like shallow water. Although the literature offers several models for calculating resistance components to estimate total resistance, most of them are developed for seagoing vessels. Therefore, this thesis will begin with a literature review to analyze how basic resistance components are categorized, their relationship with power, and the efficiency factors considered in these calculations. Based on this categorization, the first method to be studied will be the Bolt (2003) method, which is also applicable to inland ships. The goal of this current literature review is to categorize methods in terms of the number of resistance components, in order to evaluate how analytical or simplified models affect the accuracy of prediction results.

Sub-question 2: *“What are Backer van Ommeren recommendations to improve Bolt method, and to what extent do these recommendations will indeed improve Bolt method?”*

The second sub question involves the literature study into Backer van Ommeren (2019) proposed power method and recommendations for the substitution of specific formulas and coefficients to the original Bolt (2003) method. Following the findings of this analysis, it will be decided to investigate and evaluate the performance of two methods. The first method will be the Backer (2019) method as it was derived from his study while the second is related to the application of the proposed formulas and coefficients to the original Bolt method which will be introduced as “Bolt method modified by Backer”. The simulation of both methods will be realized through algorithms in python notebooks, and the calculations will include the total resistance as well as the required power as a function of the sailing speed, the channel width and the depth. The validity of these methods will be further handled in Sub-question 4.

Sub-question 3: *“What are the available options from the literature to improve the current power method in terms of resistance and propulsive power estimation for inland ships?”*

According to the literature study that is initially conducted on the encountered ship resistance and the available resistance-power methods, it is derived two investigate two scenarios, an ultimately different power method and the application of advanced return flow equations to the Bolt (2003) method. The former scenario includes the TU Delft method (Jiang, Baart & van Koningsveld, 2022) and the latter an improvement of the original theory, “Bolt method with speed correction” which together constitute the other two theories that will be studied and analyzed in terms of improvement the current power method. More specifically, TU Delft method (Jiang, Baart & van Koningsveld, 2022) is originated by the original Holtrop and Mennen (1982) theory with power efficiencies for shallow water and “Bolt method with speed correction” incorporated the return flow formulas for shallow water as they were derived by Robijns (2014). For the evaluation of these methods, two separate python models will develop to simulate these theories and estimate the resistance and the propulsion of the inland vessels. It is mentioned that the review of these methods will be treated in detail in in Sub-question 4.

Sub-question 4: *“How can the performance of these methods best be compared and what criteria should be applied to enable the objective selection of the most promising methods?”*

The evaluation of the aforementioned five methods will be conducted in two rounds of test cases. The first case which is called “Academic test case” will be applied to M6 and M8 motor cargo vessels, for the calculation of total resistance and propulsive power for narrow, wide, shallow, intermediate and deep waterway conditions. By reviewing the results of the first case the most promising methods will be selected for the second round of tests. The second case, “Real-world test case”, will be applied only to M6 inland vessel for wide, shallow, intermediate and deep water conditions and the delivered power will be computed. In that test case the methods will be compared with real power data and the most reliable theory that converges with the real values will be selected. In the Real-world test case, an additional comparison process will be held to evaluate the performance of the most promising methods in the presence of current flows. Each of the method will estimate the fuel consumption in upstream and downstream trips as well as in round trips and the results will be compared with the real fuel-use.

The evaluation process of the most promising methods will be based on 3 criteria for the election of the best practice.

- Accurate representation of important theoretical concepts
 - effect of changing water depth
 - effect of changing channel width
 - effect of changing velocities
 - effect of changing currents
- Predictions compared with real-world data fuel use data considering an acceptable deviation rate of 20%
- Practical applicability
 - Easily applied
 - Enough accuracy for the application purpose (annually overall rough estimation, lower accuracy is acceptable, other purposes, may need higher accuracy)

- Not dependent on hard to acquire input data (engine rpm, propeller characteristics, diameter, number of blades etc.)

By applying these criteria to the most promising methods will be selected as the best practice(s).

Sub-question 5: “Based on these criteria what can be recommended as best practice moving forward for the Rijkswaterstaat?”

The selected method(s) will be presented in a comprehensive table. The table will contain the results of the resistance and the power components in shallow water conditions, for the most representative motor vessels in the Netherlands, an M6 vessel. Rijkswaterstaat can use these results for specific cases to select the most suitable method to compute fuel consumption and CO₂ emissions. While this thesis has done important groundwork to enable this selection, the work here focused on a limited number of both ships and dataset. Additional effort is needed to create similar tables for the entire inland fleet.

1.7. Thesis outline

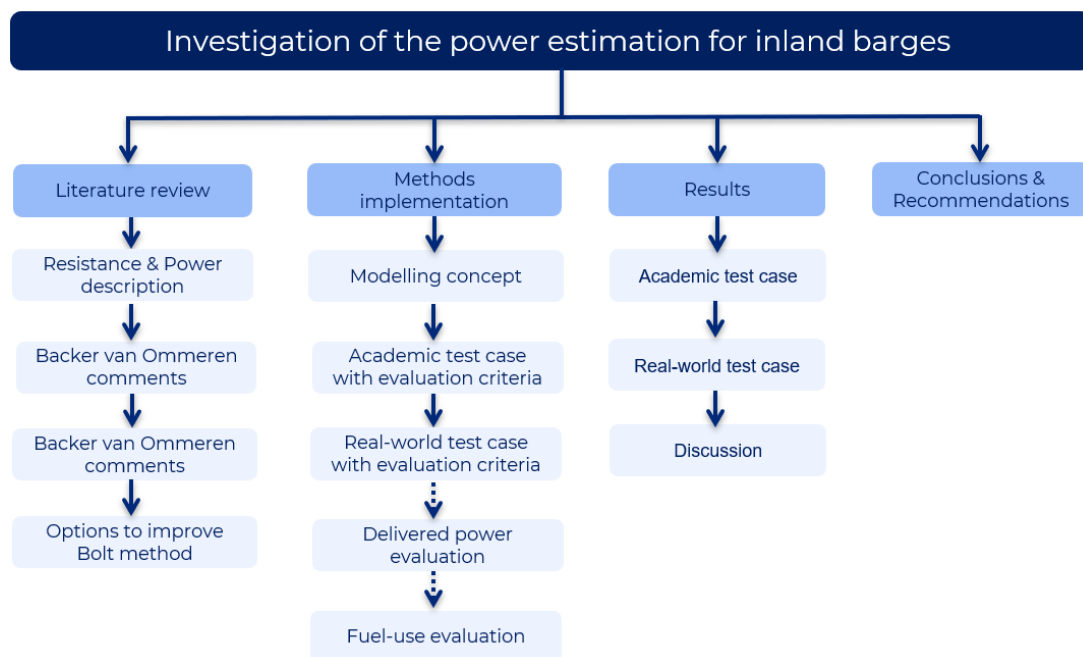


Figure 1.7.1: Flow of the outline of the Master Thesis

The structure and the outline of the Thesis project are presented in Figure 1.7.1, including a schematization graph.

In Chapter 2 of this report, a literature review was performed for the main components of the ship resistance and power and the flow pattern around the ship. Then the Bolt (2003) method is presented and explained along with the related comments from Backer van Ommeren and the options of improving it.

In Chapter 3 of this report, the methodology that is used to tackle the problem step by step is described.

In chapters 4 and 5, the results from the Academic and the Real-world test cases are presented, explained, and analyzed respectively.

In Chapters 6, 7 and 8, a discussion is performed about the studied methods and the results. Following that the conclusions of the study are summarized, including recommendations for future research.

I Literature review

2. Theoretical background

In this chapter the basic knowledge on the fundamental factors that impact a sailing ship and determine the required power in inland shipping is presented. The aim is to introduce the different resistance components and the flow pattern around a sailing ship, as well as the relationship between power and energy consumption.

Taking into account the pressure to address the climate change and reduce greenhouse gas emissions is also putting pressure on the inland shipping sector to reduce its emissions. To achieve this, an accurate power prediction method is required. To date, Bolt (2003) method is used for the power estimation in the inland shipping sector as the most suitable. However, a study conducted by Backer van Ommeren reviewed the accuracy of this method and yield important findings. This chapter also introduces some information about flow behavior around the ship Section 2.2, the Bolt (2003) method in Section 2.3, followed by a summary of Backer's comments in Section 2.4. Finally, the proposed options for improving the current approach are presented in Section 2.5.

2.1. Resistance description

The total resistance of an inland vessel determines the total required power and so the energy consumption. The most important ship resistance components would present in this section. There are many different methods ITTC57 - Model ship correlation line values of frictional resistance coefficient (Morrall, 1970), Holtrop and Mennen (1982), etc., to estimate the resistance but it is quite complex to make a good estimation as the resistance of a ship depends on many variables. Even so, the principal factors affect ship resistance are:

- friction and viscous effects of water acting on the hull
- required energy to create and maintain the ship's characteristic bow and stern waves
- water level depression results resistance

This thesis would investigate only the first two aforementioned factors as inland vessels do not expose to extreme air effects during sailing in waterways. Each of the previous factors have special properties and behave in a different way in shallow water. So as the region is confined, the effect of limited water depth should be taken into account in the transformation of resistance components

How does each factor work on the sailing ship?

Firstly, it is important to define how a viscous fluid affect the ship. When the fluid flows around the vessel, there is a pressure distribution normal to the body. At the bow there is a component of pressure resisting motion while in the stern there is a component of pressure assisting motion. Then water particles stick to the ship resulting in the formation of a boundary layer where the flow rapidly changes speed from zero speed to the free-stream speed. Two forms of resistance happen as a result of viscosity Friction Resistance and Viscous Pressure Resistance (Figure 2.1.1). Concerning the former, acts tangential to the and over the entire wetted surface of the hull by causing a net force that opposes to the sailing ship. Frictional resistance depends on the roughness of the ship's surface and the water viscosity. Viscous pressure resistance acts normal to the hull but in the aft of the ship the boundary layer reduces the forward acting component of pressure. This reduction in the forward acting component results in a net resistance force due to pressure acting on the hull. This increase in resistance due to pressure is called viscous pressure drag.

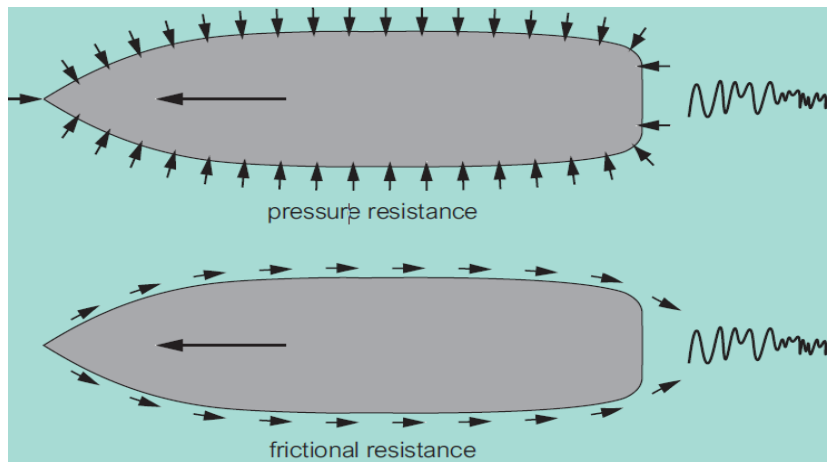


Figure 2.1.1: Frictional and pressure resistance and their direction (Van Koningsveld, Verheij, Taneja & De Vriend, 2021)

The second major component that would be studied in this dissertation is the resistance due to wave making or generated waves (Figure 2.1.2). The creation of waves requires energy and as the sailing speed increases then the produced waves (by the ship) also increases and therefore the energy required to produce these waves increases too. This loss of energy is known as wave making resistance and often becomes a limiting factor in the speed of a ship.

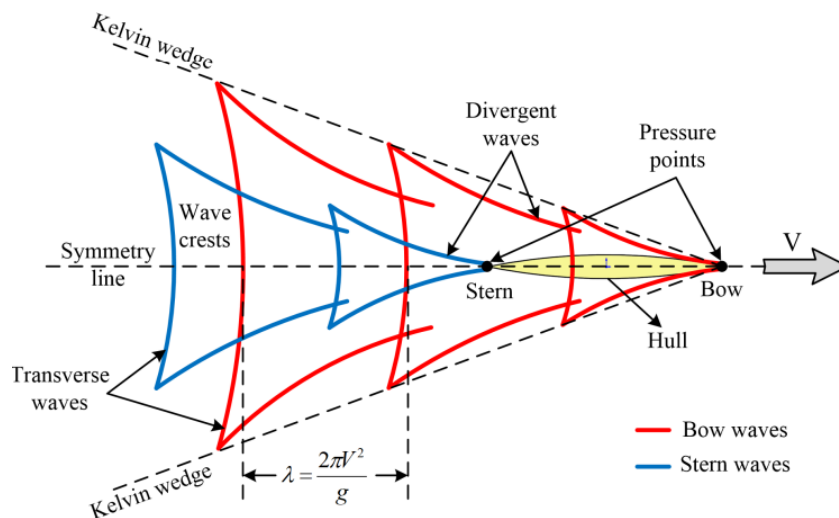


Figure 2.1.2: Wave interference of an actual ship hull. V and λ denote the velocity and the wavelength (Du, Ouahsine, Sargent, & Hu, 2020)

The motion of a ship through water requires energy to overcome resistance, i.e., the force working against movement, so it should be designed to move efficiently with a minimum of external force. As the resistance of a ship cannot be measured directly, the knowledge about the resistance of ships comes from model tests or empirical calculations. As it is mentioned in the introduction, water depth and channel width play a major role on the resistance that a ship encounters. For the ships that are designed to operate in shallow water, it is essential to consider the effects of water depth on ship resistance from the aspects of both ship design and hull formation. In Figure 2.1.3 is shown the magnitude of each resistance component as a function of sailing speed. It is obvious that at low speeds viscous resistance dominates, and at high speeds the total resistance curve turns upward dramatically as wave making resistance begins to dominate.

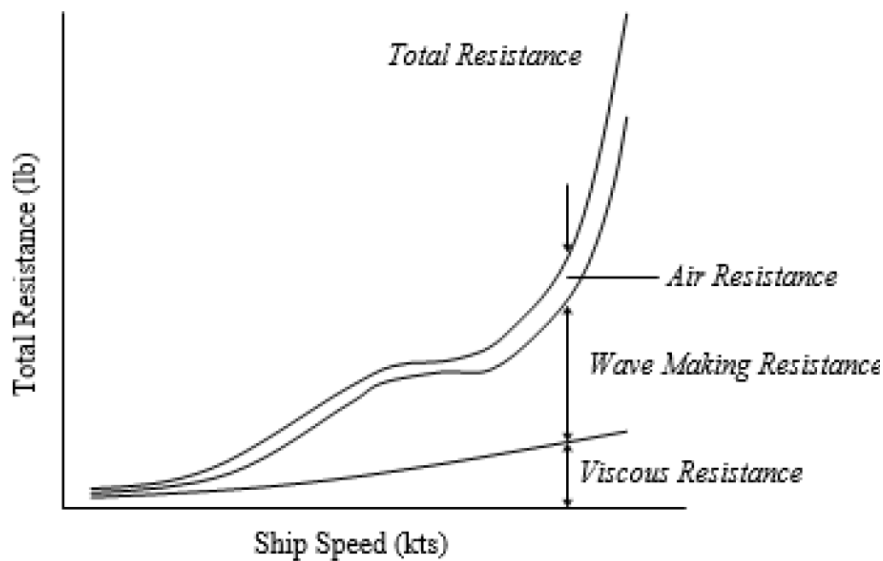


Figure 2.1.3: Components of Hull resistance (The United States Naval Academy, 2001)

As it is mentioned in the start of this section, there are several methods for the calculation of the total resistance. However, each method follows a different approach concerning the resistance components that constitute the total resistance. Specifically, estimation methods are roughly divided into two groups, on the one hand the group of methods that do not separate frictional and wave resistance and on the other hand methods that do separate between wave and frictional resistance. It is now more widely known that the lack of this separation can result in wrong resistance corrections while the separation yields much lower corrections and are considered a better alternative. Three approaches can be identified in terms of breaking down the several resistance components that form the total resistance.

- **1st Approach - Classical treatment of resistance:** This approach divides the total resistance into two components, the skin frictional resistance, which is governed by the Reynolds' number and the residuary resistance (taken mainly to be the wave making). For instance, Karpov approximate method (van Terwisga, 1989) that was developed in 1945 for practical calculations was based on this approach. Also Bolt, (2003) method follows this approach, taking also the shallow water effects into account by introducing an extra resistance term, the resistance due to water level depression (detailed analysis in Section 2.2). Another method that was also based on this approach is the one by Guldhammer (1974). This method was developed for conventional vessels, but it is also applicable to inland vessels through a correction on the friction coefficient, by increasing the original friction proportionally to the increased wetted surface due to appendages.
- **2nd Approach:** An alternative approach for determining total resistance involves accounting for both frictional and viscous effects, as well as wave resistance as a secondary term. This approach incorporates the product of the friction coefficient and the form factor to represent viscous-friction resistance. The ITTC57- Model ship correlation line values of frictional resistance coefficient (Morrall, 1970), applied this approximation.
- **3rd Approach:** A third approach that was found in the literature for the estimation of the total resistance based on the combination of the two aforementioned approaches

and the consideration of three additional components. Specifically, the total resistance (Equation 2.1) is split into frictional resistance R_F multiplied by the form factor $(1 + k_1)$, the appendage resistance R_{APP} , the wave resistance R_W , a bulbous bow R_B (additional pressure resistance of bulbous bow), the additional pressure resistance of the immersed transom at the stern R_{TR} and the model-ship correlation resistance R_A which includes effects such as hull roughness and air drag.

$$R_{tot} = R_f \cdot (1 + k_1) + R_{APP} + R_W + R_B + R_{TR} + R_A \quad (2.1)$$

This approach was originally followed by Holtrop and Mennen (1982) and recently was modified in terms of two variables the shallow friction coefficient (Zeng et.al, 2018) and the hydrodynamic power efficiency for shallow water (Jiang et al, 2022). Appendix H contains the analytical calculation of Holtrop and Mennen (1982) method, which includes all the relevant computations required for implementing of the TU Delft method discussed in Section 2.4.

2.1.1. Power & energy consumption

One of the most important considerations for a naval architect is the determination of the required power for a ship. The designing phase apart from the selection of the hull form, it is necessary to determine the amount of engine power that will enable the ship to meet its operational requirements. Once the power required to propel a ship is found, then the type of engine should be selected, the determination of the required amount of fuel storage and the estimation of the ship's center of gravity should be done. It is obvious that the propulsion system in a ship converts the fuel energy into thrust power to propel it. However, after tests that were done both on full-scale and model-scale ships to determine the required power, it is found that power is directly related to the amount of resistance a hull experiences when moving through the water.

The power of a ship refers to several parameters, such as brake, shaft and delivered horsepower (Section 2.1.2). The propeller converts the rotational power of the shaft into useful thrust and the ship moves through water. Another term that is also used in this dissertation is the effective horsepower. This is the power required to move the ship at a given speed in the absence of propeller action. It is equal to the product of the resistance of a ship and the speed of the ship. This power is equal to the brake horsepower minus the losses due to the gearbox, shafting and propeller, as well as interaction between the propeller and the hull.

Energy and power are closely related but are not the same physical quantity. A ship needs energy to sail, but the rate at which this amount of energy is consumed, i.e., the sailing speed, determines the power. Worded differently, energy equals to the product of power and the operating time. So, the ship's engine determines how much power it can produce, while the amount of fuel available determines how much energy the engine has available. As a result, energy consumption causes pollutants, and each energy increase causes greater amount of CO₂ emissions.

2.1.2. Power model

The greenhouse gas emissions that are produced by a ship during its sailing is directly related to the power required to achieve a certain speed. Worded differently, this is the power demanded by the vessel and is depended by several factors, including the resistance of the ship, transmission efficiency, and propulsive efficiency. As a result, by reducing the brake horsepower necessary to achieve a given speed is of great importance for mitigating the environmental impact of inland shipping. The total required power of an inland ship can be subdivided into two components: the power required for hotel systems on board, and the power required for propulsion.

$$P_{tot} = P_{hotel} + P_{propulsion} [kW] \quad (2.2)$$

The hotel systems on board require heat and electrical power (lighting, heating of cabins). The hotel power component (P_{hotel}) takes this required energy into account. In general, this component is relatively low for inland ships, since the scale of these ships is relatively small and there are not so many activities on board of the ship. When vessels become larger, the hotel power component increases. Therefore, the hotel power is estimated as a percentage of the total installed power (taking into account the scale of the ship): the hotel power is estimated to be 8% of the installed engine power (Baldasso et al., 2019). Please note that this component does not consider the idling of the engine in a stationary stage.

$$P_{hotel} = 0.08 \cdot P_{installed} [kW] \quad (2.3)$$

Originally, it is mentioned that propulsive power depends on the resistance of ship that needs to be overcome and especially for inland vessels depends on their dimensions and shape, the velocity of the ship and waterway characteristics. To translate the resistance to total required power, you have to take into account propulsion characteristics and different losses in the system. The Effective horsepower (EHP), or effective power P_e , is the power that is needed to travel with a certain speed, overcoming its resistance (Watson, 1998). The EHP, delivered by the ship's propellers, can be defined as follows:

$$P_e = V_s \cdot R_{tot} [kW] \quad (2.4)$$

The delivered horsepower (DHP) is the power that is delivered to the propeller and can be expressed as the power required to sail with a certain speed (EHP plus the losses at the propeller), open water efficiency of the propeller, relative rotative efficiency and the hull efficiency. Therefore, the delivered horsepower (DHP) should be larger than the effective horsepower (EHP).

$$P_d = \frac{P_e}{\eta_0 \cdot \eta_r \cdot \eta_h} [kW] \quad (2.5)$$

The brake horsepower (BHP) is the power required to sail with a certain speed (EHP plus the losses at the propeller that already considered in the DHP), plus shaft and gearbox losses. Therefore, holds that the brake horsepower (BHP) is always larger than the other two power components. The Brake horsepower is the total power required for propulsion.

$$P_b = \frac{P_d}{\eta_t \cdot \eta_g} = P_{propulsion} [kW] \quad (2.6)$$

Figure 2.1.4 depicts the various power components and their corresponding efficiencies. These components and efficiencies, along with the equations presented earlier, form the foundation of the power calculations that will be carried out in the upcoming chapters.

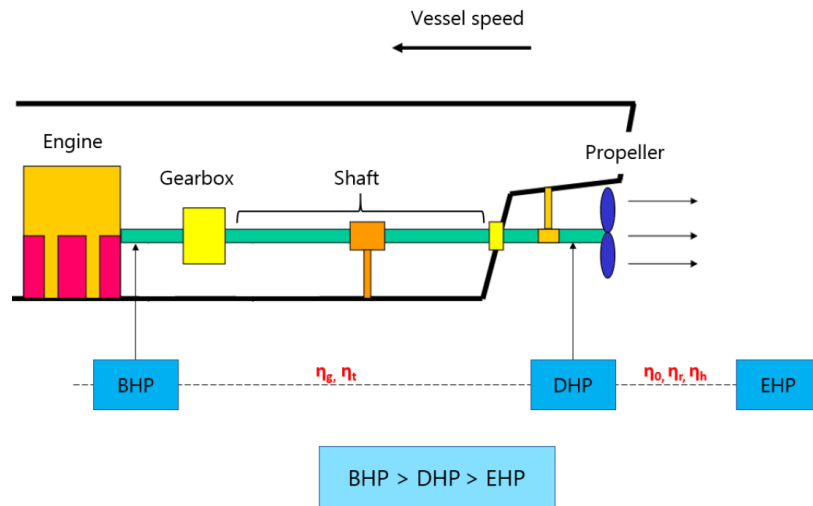


Figure 2.1.4: Schematization of a ship to illustrate different power components and efficiencies (Seger, 2021)

2.2. Flow description

The main hydrodynamic phenomena of a sailing ship are ship waves and ship-induced flows, which are getting prominent when entering on a shallow or narrow canal. These water motions have a visible effect on sailing vessels by water level depression along the ship and return flow. Because water motions affect navigation, so many models have been developed to determine the return current and water level drawdown and predict the effects, from simple analytical models, for instance the methods of Schijf (1949) or Bouwmeester (1986) to advanced computer simulations. But what is the reason behind these effects? A detailed analysis would be explained in the next paragraph.

When the sailing vessel enters a waterway mainly restricted both at depth and width, it is known that there is an increased return velocity beneath the ship just after the passage of the bow, due to contraction of the flow lines by separation at the bow. In a ship-based coordinate system, the water streaming from the bow with direction to the stern will be diverted besides and beneath the ship. The fraction of the flow which passes under the bow is mainly determined by the bow shape and draught of the ship. Part of the water at the bow is forced down and will separate from the hull just after passing the bow. As a result, contraction will occur, and the velocity will increase but this effect more or less depends on the shape of the bow. Worded different, more streamlined bows reduce the contraction and in turn lead to lower velocity. After the contraction at the bow, flow velocities will decrease and boundary layers on the ship and bed will start to develop. With direction from bow to stern these boundary layers will grow in thickness, reducing the effective underkeel clearance, and consequently the velocities should increase or the water discharge under the keel should decrease. The only way the discharge can decrease is if water is flowing away to the sides of the ship. This flow process is called fanning out. Concerning the stern of the ship, the rotating propeller will induce an area of low pressure in front of the propeller. Therefore, the flow will be directed upward and after the passage of the vessel the flow will be mainly determined by the influence of the propeller jet.

It is mentioned that the flow pattern that is described previously lead to increased sailing velocities and results into higher ship resistances and propulsive power. Despite the number of available methods and models to determine flow circumstances around sailing vessels, it appears hardly any of them can predict flow velocities beneath a ship. It is of great importance

to acquire a better insight to these velocities in order to estimate with greater accuracy the amount of energy that is consumed per voyage.

2.3. Bolt method

In 2003 a method for the estimation of the ship resistance, the required power and the energy consumption was derived from Bolt. The idea of Bolt approach lies in that does not specialize to an individual inland ship type, but it has a more general application to inland fleet. So, an estimate should be made on the basis of the “average” main, characteristic dimensions per ship class.

The Bolt method is developed according to the “1st Approach-Classical treatment of resistance” with an additional resistance term in order to be applicable in shallow and confined waterways. Therefore, less resistance components are considered for the determination of the total resistance compared to the “3rd Approach”. This assumption will be reviewed in terms of accurate resistance and power estimations through comparison of other power methods and with real power data.

Having considered that the usual resistance calculation methods are based on seagoing vessels, he defined the reasons that make these theories not automatically applicable to inland navigation.

1. Seagoing vessels tend to sail at higher speeds relative to their length, which makes wave-making resistance a significant factor in their total resistance. In contrast to inland ships that typically sail at relatively low speeds, which means that the impact of wave-making resistance on their total resistance is not so important. Consequently, the frictional resistance of inland ships considers more important than the wave-making, although the latter is still a factor that contributes to the total resistance, so it includes to the residuary resistance. Overall, wave resistance has a lesser effect on inland ships compared to friction, but it is still a factor that affects the sailing.
2. Regarding the shape of the ships, there is a discrete difference between the bow of a motor vessel with a hull of “V” shape and put it differently streamlined ships encounter less resistance and barges that are more prismatic/rectangular and displace a larger amount of water. This larger amount of water that is displaced leads to higher total resistance. Next, seagoing vessels usually sail on deep and wide waters in contrast with inland vessels move on shallow and narrow conditions. It is mentioned that it is the most important different that renders existing methods not suitable. Meanwhile seagoing vessels have extra resistance to overcome as a result of sea waves, higher wind speeds on average and generally greater windage in proportion.

The analytical calculation process for the implementation of Bolt (2003) method is described in Appendix H.

2.3.1. Explanation of velocities that used in Bolt method

For the estimation of resistance and power components several velocities are presented, and it may cause misunderstandings. So, in this paragraph each velocity type would be analyzed and explain further.

- Sailing velocity V or V_s

Sailing velocity or service speed is the velocity maintained by a ship under normal load and weather conditions in deep and unrestricted waters. Also sailing velocity could be considered one of the most representative factors of inland vessels in the required power and in the energy consumption. From the results in Chapters 4 and 5 will be seen that the relationship between the speed and the required power is nonlinear, and when it sails in shallow water depths this relationship will even be more asymptotic. Based on this variable, the depth Froude number and the Reynolds number were computed.

- Limit speed V_{lim}

Limit speed is the theoretical maximum or attainable velocity for conventional ships. Specifically limit speed is determined by the specific characteristics of a channel and its dimensions along with ship dimensions.

- Return current or return flow velocity U_r

As it was already analytically explained in the previous paragraph, when the ships encounter restricted or shallow or both conditions the velocity of water, the so-called flow velocity is further accelerating during flowing in the fairway.

- Effective velocity V_{eff}

A ship sails in shallow waterways encounters greater resistance than in deeper depths. This resistance is getting higher in narrower waterways as the blockage factor increases while it reduces in wider waterways (more width for sailing). As a result, this effect is captured by the sum of the return flow and the sailing speed. For the narrow case the return flow equation either from (Schijf, 1949) or from (Tuck, 1966) theories can be used and then to add in the sailing speed. However, in wide waterways the Schijf (1949) theory cannot apply as it leads to underestimated return flow velocities. So, in Bolt (2003) method a different formula for such extreme conditions was proposed, the effective velocity, which considers the effect of the return in wide channels and constitutes the second term of the relative velocity. This mathematical formula multiplies sailing speed with the shallow water factor so as to capture the magnitude of shallow water conditions in wide channels.

- Relative velocity U_{rel}

Relative velocity is regarded as the flow velocity that is experienced by the ship and is used for the calculation of frictional resistance. It is composed of the sailing speed and the return flow according to Schijf on a restricted fairway or the effective velocity due to shallow water, whichever is largest. The main components that constitute relative velocity are the return flow and the sailing or the adjusted speed. What does it mean adjusted speed?

Bolt by taking into account the great effect of restricted or wide and shallow water conditions proposed a group of equations each of which depend on the dimensions of waterway. More specifically V_{adj} stands for adjusted velocity and the goal was to adjust the default velocity (sailing speed) in such a way that the required power was more or less constant when the waterway dimensions change. The three equations that in turn constitute the adjusted velocity are the sailing speed as it is measured in unrestricted and deep water (1st term), then the limit speed (Equation 2.7, 2nd term) that is certain for each ship in restricted waterway of given dimensions and can be reached when the return current has maximum as a function of the water level depression. It is recommended to work with the 90% of the limit speed as it is considered the most efficient related to required power and fuel consumption. The last term is the shallow water velocity that is structured as a function of shallow water factor in order

to reduce the sailing speed and demonstrate the magnitude of shallow water factor to counteract the increasing power in shallow water.

$$V_{lim} = \begin{cases} 0.78 \cdot \sqrt{g \cdot h} \cdot \left(1 - \frac{A_m}{A_c}\right)^{2.25}, & \text{if } 0.1 \leq \frac{A_m}{A_c} \leq 0.3 \\ \sqrt{8 \cdot g \cdot h} \cdot \left(\cos \frac{\pi + \cos \left(1 - \frac{A_m}{A_c}\right)^{-1}}{3}\right)^{1.5} & \end{cases} \quad [m/s] \quad (2.7)$$

$$V_{adj} = \min \begin{cases} V \\ 90\% \cdot V_{lim} \\ V_{sh} = 1.18 \cdot V \cdot swf^{-1 \cdot \left(0.75 + \frac{A_m}{A_c}\right)} \end{cases} \quad [m/s] \quad (2.8)$$

$$U_{rel} = \max \begin{cases} V_{adj} + U_r \\ swf \cdot V_{adj} \end{cases} \quad [m/s] \quad (2.9)$$

$$\text{Shallow water factor: } swf = \frac{1}{1 - e^{-4 \cdot 4 \cdot \max\left\{\frac{h/T}{(h/T)_{lim}}\right\}}} \quad [-] \quad (2.10)$$

The selection of which equation would be used from the group of limit velocities depends on the above criterion. However, in Bolt (2003) method the second formulation was selected. As far as the $(h/T)_{lim}$ value in Equation 2.10, it is a cut-off value to prevent excessive high relative velocities and consequently too large increase of power needed. Most of the cases the selection of this limit depends on the ship draft and the available water depth, and it is not a constant value for ship and type classes. Concerning the adjusted velocity and which formula would be applied for the resistance components, the following classification was done. The waterway is regarded narrow when the speed adjustment is governed by the limit velocity, as shallow when the speed adjustment follows from the shallow water factor and deep when there is no speed adjustment, and it is equal to sailing speed.

$$\begin{aligned} \text{if } V_{sh} \leq 90\%V_{lim} \quad & \& \quad V_{sh} \leq V \xrightarrow{\text{yields,shallow}} V_{adj} = V_{sh} \\ \text{if } 90\%V_{lim} \leq V \quad & \& \quad 90\%V_{lim} \leq V_{sh} \xrightarrow{\text{yields,narrow}} V_{adj} = 90\%V_{lim} \\ \text{if } V \leq 90\%V_{lim} \quad & \& \quad V \leq V_{sh} \xrightarrow{\text{yields,deep}} V_{adj} = V \end{aligned}$$

For the calculation of friction resistance, the relative velocity is selected, while for the pressure and the resistance due to water level depression the adjusted velocity was needed. In contrast with the traditional power estimation methods, in this theory the adjusted velocity again was used for the calculation of the depth Froude number, but the relative velocity is applied to Reynolds number.

2.4. Backer van Ommeren comments

In 2019 Backer van Ommeren conducted an extensive study on Bolt (2003) or RWS method and he investigated that several assumptions and simplifications adversely affect the accuracy of the method. It is mentioned that this method also were used from TNO and CE Delft. In his report, the main problem was detected in the assumptions and simplifications that were done in several equations while on the other hand he proposed the review of some information that are given in Waterway Guidelines, TU Delft Repositories (2020) and would be analyzed in suggested Comment 3. The solutions/recommendations that were proposed are summarized

in the list below. These solutions could be considered as a way in order to maintain the usability of this method or to substitute with a more accurate method. It is mentioned that this master thesis will only investigate the comments that are relevant to the Bolt (2003) theory.

1. Lack of source in some equations, documents and data used for the model.
2. Fix the error(s) in the model.
3. Unnecessary simplifications & Estimations with significant inaccuracy.
4. Test the data used for plausibility, logical coherence, and consistency.
5. Use the same data in all applications.
6. Make sure that the data used is recognizable to readers who are not very familiar with this matter.
7. Use of an alternative model for power estimations.

2.4.1. Analysis of Backer van Ommeren comments

1. *Lack of source in some equations, documents and data used for the model.*

The first weak point that was found in Bolt (2003) method is the lack of source in several equations. To be more specific, in Bolt theory were analyzed the equations for resistance components, the required power and the losses that happen over the ship shaft as well the formulas for the energy consumption. Normally, each formula depends on several factors and coefficients each of which has a specific role and use. One of these factors is the velocity or velocity equations that would be used for the calculations almost in all terms.

In the method different velocities were presented but there was not a clear explanation of each one or it did not define the bibliography or the author. In addition to that there are equations that suggested by Bolt but again a clear and well-defined reasoning is absent. Nevertheless, the main problem was focused on equations of velocity that were used in the method which have already presented in Section 2.3 and further will be analyzed in Appendix H where the method is analytically explained.

2. *Fix the error(s) in the model.*

By studying the Bolt (2003) theory and the description of his approach, a survey was done. To be more specific, Bolt tried to check the validity of his method by taking into account the velocity and the brake power as they were given from Skipper's interview. Then he simulated the same motor vessels and produce the same parameters. However, by studying the relative table the values of brake power as they were computed from his model gave bigger brake power for an empty vessel and smaller for a loaded one. The same pattern also was shown in the resistance components, higher values at empty ships instead of loaded. So, Backer van Ommeren in his analysis recommended to fix the error(s) that lead to these strange results. The relative table is presented in Appendix D.

3. *Unnecessary simplifications & estimations with significant inaccuracy.*

According to Backer van Ommeren comments, the simplifications in specific equations adversely affect the accuracy of Bolt (2003) method. Notably, the simplifications in the equations of the limit speed and the return flow velocity and in turn in the water level depression led to underestimated results. In Bolt (2003) theory, instead of solving the general equation with iterations for the determination of the limit velocity a simplified formula was suggested that would be solved algebraically. Starting from that and given the result of the

limit speed (simplified version), the return flow is defined again algebraically. The effect of these simplifications is supported through plots that show the value of the return flow calculated with the original (iterations) and the simplified formula. Apart from this, engine power used is also plotted in order to give a clear perspective of how simplifications and assumptions underestimate (for this case) and affect fundamental parameters in a method. In the following graph, red line depicts the computations that made iteratively (no simplifications) while the blue line related with Bolt approach and simplified equations. From the graph it is obvious that simplified model calculates values for both return flow and engine power also with speeds that exceed the limit one. Based on the results that are shown, speeds above limit speed or 10 km/h would be possible with a reasonable engine deployment, however in reality once the limit speed (maximum speed) is reached when the return current has also reached its maximum a further increase does not suggested as the water movement next to the ship passed from subcritical to critical zone. The effect of modifications at ninety percent of the limit speed led to a reduction of 7% in the return flow while in power used is approximately 20%.

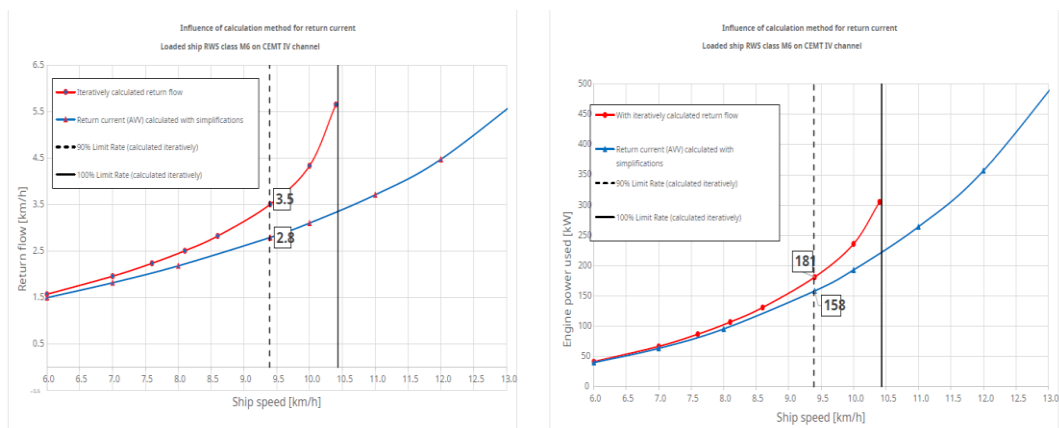


Figure 2.4.1: Comparison between simplified and iteratively calculations for return flow & power (Backer Van Ommeren, 2019)

- If $V_0 \leq 75\%V_{lim}$ the divergence between original & simplified method are small.
 - If $75\%V_{lim} \leq V_0 \leq 90\%V_{lim}$ increase underestimation of the U_r , z , E

Concerning the estimations that was done in order to derive the simplified equations are summarized below.

- $U_r / V_s \ll 1$: assumed that U_r is too small compared to sailing speed meaning that has little influence on the resistance that a ship encounters.
- $A_s / A_c \ll 1$: assumed unrestricted conditions and the ship is able to sail with the limit speed (maximum sailing velocity) according to Schijf (1949).

In Appendix H where Bolt calculation process is presented, the equations that were used for the calculation of resistance components, total resistance and then propulsive power and energy consumption, contain several velocity types. For example, the factor 1.18 that used to determine the adjusted velocity in shallow water is a process of trial and error and there is not an exact motivation of how it was derived. In addition to that a formula for a shallow water factor was structured and was based on the ratio of depth over the draft. However, in this formula a limit in this ratio of 1.1 was set as a cut off value to prevent the extremely large values of power in low depths. Again, the selection of this limit was a trial and error process.

Moreover, another simplification that affect the accuracy of Bolt (2003) method was found in the selection of the water depth and the channel width. More specifically these two factors are strongly related with the shape of the cross section of the channel, rectangular or trapezoidal. In Bolt (2003) method the cross section was assumed as rectangular and therefore the maximum water depth and width were used. The result of the aforementioned choices show varying results an event that indicate that the selection of the channel dimensions have significant effect both in return flow and power calculations. According to Backer, it is recommended do not work with the maximum waterway depth in the calculations, but with the average depth over the cross-section of the waterway. The graphs below show that calculating with the maximum depth of the fairway leads to an underestimation of the required engine power. At a sailing speed of 90% of the limit speed the power deviation is approximately 3%.

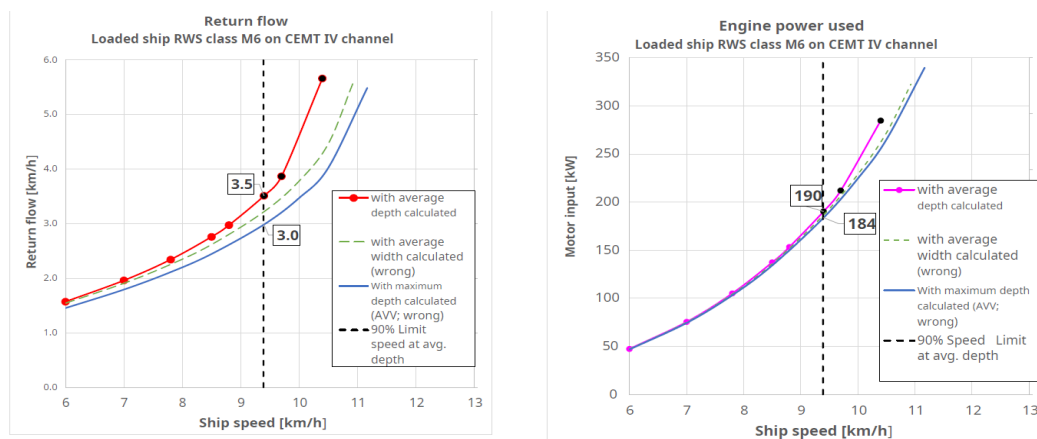


Figure 2.4.2: Effect of maximum depth and width in return flow and required power calculations (Backer Van Ommeren, 2019)

Furthermore, Backer van Ommeren analyzed the effect of a narrow, a wide and a very wide waterway on the return flow and water level drop calculations. More specifically one precondition for the application of the Schijf (1949) model is that the return flow and thus the drop in the water level is uniform in the cross-section of the fairway. According to measurements (Blaauw & Knaap, 1985), it seems that Schijf (1949) model accuracy is reduced in the calculation of the water level in normal channels while it cannot be used in case of a (very) wide waterway.

Based on these measurements that were executed by Blaauw (1983), Bolt applied a formula in order to predict the return flow effect on wide waterways, but the background of this formula cannot be found. To test the validation of this formula, Backer van Ommeren did some simulations, the outcome of which sometimes did not correct. He simulated an M8 motor vessel on a fairly wide waterway of 171m for two water depths of 5m and 7.5m respectively. In the first case, five meters water depth was considered shallow for an M8 while in the second simulation the conditions were considered comfortable. In 5m depth(shallow) the Bolt equation showed very high values compared to the original formula with iterations. Interestingly enough is the result in wide and deep conditions where the exponential formula present almost zero return flow while the analytical gives higher values.

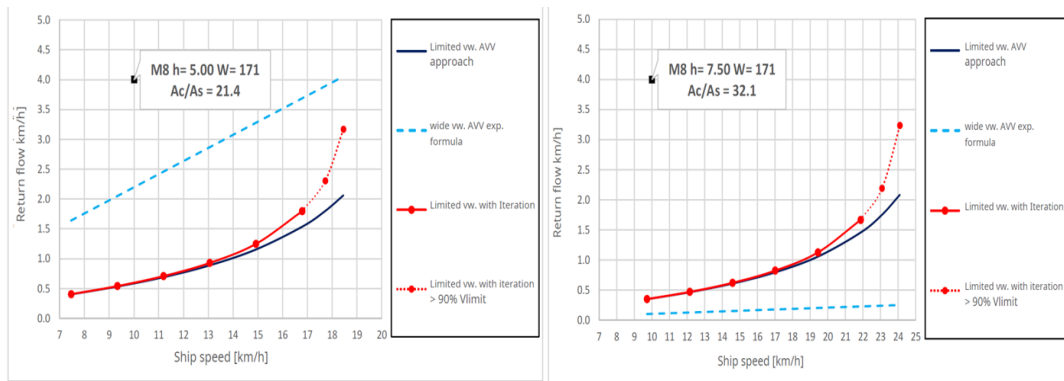


Figure 2.4.3: Left picture M8 at 5m, Right picture M8 at 7.5m (Backer Van Ommeren, 2019)

4. Data selection, plausibility, logical coherence, and consistency

The last three comments that were proposed from Backer, data selection & plausibility, logical coherence, and consistency, are relevant with the waterway guidelines and in turn with the input data that were used from power estimation methods. Specifically, he suggested how the important input parameters should be presented in guidelines. Also, he advised to be cautious when selecting the input data since most of the methods simulate with the velocity relative to water while others with velocity relative to the ground. These comments would present and summarize next.

Waterway Dimensions:

He proposed some modifications that are relevant to the width and the depth of the waterways. To be more specific according to Waterway Guidelines, TU Delft Repositories (2020) (Appendix A), the fairway width for commercial navigation is specified at three different levels either with the minimum waterway depth that is required on the channel bottom or at the keel plane of the laden vessel or at the keel plane of an unladen vessel plus the extra width that needs in the event of side winds or longitudinal currents or both phenomena. However, Backer van Ommeren suggested in the next version of waterway guidelines to include the width on the water level surface. Concerning the depth in canals and rivers, he proposed to be included in the revised guidelines also the use of average depth instead of the minimum one that is already available in guidelines (Waterway Guidelines, TU Delft Repositories, 2020, Table.18) of the existing guidelines. Additionally, he recommended for channels that are not listed in the waterway guidelines such as Princess Margriet Canal, Twente Canal and Juliana Canal, to determine the depth at the centerline and be $1.4 \cdot$ locally permitted maximum draft.

Water depth, Sailing speed & Current speed :

To determine the depth of the waterways, it would be useful to collect historical data of the variation that water depth presents over the years and based on that information to define the average value for Dutch rivers. Additionally, he recommended the entire Dutch network waterways, to be included waterway guidelines.

Subsequently, he recommended cautious in the selection of the sailing speed. This is mentioned because data from AIS are speeds over the ground, so they should first be converted to velocities through the water for most of the power estimation methods.

Backer van Ommeren suggested that the flow velocities of rivers be substantiated with calculations based on historical data (statistical data) in order to be connected with the

substantiation of the corresponding water depths. He supported this suggestion since the effect of the current flows is important as it leads to larger gas oil consumption compared with the cases where they did not consider. As far as, the effect of tidal currents, it is recommended not to include in the calculations because the reverse in tide direction is determined and is realized every 11.5 hours.

2.4.2. Proposed formulas for wide & very wide waterways

Backer studied the effect of the channel width on the flow profile, on the magnitude of the return flow and on the water level drop at the ship, at the bank and in middle between ship and shore. According to the results that were derived from the width variation on the return flow and the water level drop, he proposed to test the use of alternative formulas for the return flow and the water level depression. Initially, he studied the formula that was developed by Hydraulic Laboratory in Delft University, which was derived by a large series of model tests. More specifically, the water level drop at the ship, at the bank and halfway was measured and the measurement results are presented as ratios of channel width to ship width. Through regression analysis and by selection 2nd order polynomial, the following equation was derived.

$$z_{ship} = z_{avg}(-2 \cdot 10^{-5} \cdot W_B^3 + 6.2 \cdot 10^{-3} \cdot W_B^2 - 7 \cdot 10^{-3} \cdot W_B + 0.9927) [m]$$

$$\left\{ \begin{array}{l} z_{avg} = \text{water level depression in the middle of the shore the ship} \\ \text{correction factor} = (-2 \cdot 10^{-5} \cdot W_B^3 + 6.2 \cdot 10^{-3} \cdot W_B^2 - 7 \cdot 10^{-3} \cdot W_B + 0.9927) \\ W_B = \frac{B_c}{B_s} \end{array} \right.$$

For the application of the above formula, (Schijf, 1949) method has been chosen to compute z_{avg} and the return flow. Concerning the correction factor, the value varies as a function of width ratio.

if $W_B \cong 1$ narrow waterway \rightarrow correction factor $\approx 0 - 1$ no difference between shore & ship

if $W_B \cong 20 - 23 \rightarrow$ correction factor ≈ 2 no water level drop on the bank

Blaauw and Knaap (1985) suggested a formula for the estimation of water level depression in very wide fairways, the basis of which came from Tuck (1966) theory. Backer van Ommeren before the proposal of the next equation, test its validation with 3D calculations that have been done in a loaded barge (Pacuraru & Domnisoru, 2017).

$$z = 1.36 \cdot \frac{v}{L_s^2} \cdot \frac{Fr_h^2}{\sqrt{1 - Fr_h^2}} [m]$$

In Figure 2.4.5 the comparison of the two methods was done for two different water depths. Admittedly, the fit in this example appears to be very good, as the results of the Tuck (1966) method reasonably correspond with the results of the model tests. It is mentioned that the previous formula is valid for $6.5 < B_c / B_s < 8$, afterwards studies show reasonable results for wider waterways.

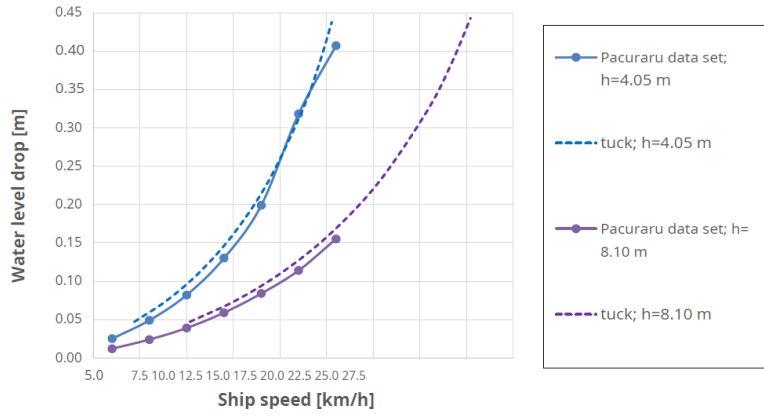


Figure 2.4.4: Comparison between (Tuck, 1966; Pacuraru & Domnisoru, 2017)

2.4.3. Selected equations

Backer van Ommeren in his study tested several formulas either for the return flow calculations or for the water level drop estimations along with the use of alternative coefficients for the resistance and the power calculations. Specifically, apart from the formulations that were used in Bolt (2003) method, he also tested the following formulas:

$$1 - \frac{A_s}{A_c} + \frac{1}{2} \cdot \left(\frac{V_{lim}}{\sqrt{g \cdot h}} \right)^2 - \frac{3}{2} \cdot \left(\frac{V_{lim}}{\sqrt{g \cdot h}} \right)^3 = 0 \left[\frac{m}{s} \right] \quad (2.11)$$

$$U_r = (V_s + U_{r,o}) \cdot \left(\frac{(V_s + U_{r,o})^2 + V_s^2}{2 \cdot g \cdot h} + \frac{A_s}{A_c} \right) \left[\frac{m}{s} \right] \quad (2.12)$$

$$z = \frac{(V_s + U_r)^2}{2g} - \frac{V_s^2}{2g} [m] \quad (2.13)$$

$$U_r = \sqrt{2 \cdot g \cdot z + V_s^2} - V_s \left[\frac{m}{s} \right] \quad (2.14)$$

$$\text{Water level drop narrow \& wide: } \frac{z_{ship}}{z_{avg}} = (-2 \cdot 10^{-5} \cdot W_B^3 + 6.2 \cdot 10^{-3} \cdot W_B^2 - 7 \cdot 10^{-3} \cdot W_B + 0.9927) \quad (2.15)$$

$$z = z_{avg} = \frac{(V_s + U_r)^2}{2g} - \frac{V_s^2}{2g} [m]$$

$$\text{Water level drop, very wide channels: } z = 1.36 \cdot \frac{V}{L_s^2} \cdot \frac{Fr_h^2}{\sqrt{1 - Fr_h^2}} [m] \quad (2.16)$$

According to previous equations, Backer van Ommeren concluded that it is a good choice to opt for the Equation 2.12 for return flow calculation and Formulas 2.15 and 2.16 for the water level depression. Moreover, he suggested two formulas for the classification of a waterway as narrow, wide or very wide and the substitution friction coefficient, pressure coefficient, and water level drop coefficient with different values and use of alternative power efficiency coefficients. Additionally, the use of the latest version of Waterway Guidelines, TU Delft Repositories (2020) in terms of waterway dimensions and to consider the flow currents in the sailing speed were proposed.

Limits for the classification of waterways:

$$\text{Normal, Narrow, Wide: } \frac{A_c}{A_s} \leq 5.45 \cdot h + 0.56 \cdot A_s - 17.68$$

$$\text{Very wide: } \frac{A_c}{A_s} > 5.45 \cdot h + 0.56 \cdot A_s - 17.68$$

$$\left\{ \begin{array}{l} \text{20\% surcharge for friction resistance} \\ C_p = 0.1 \\ C_z = 0 \text{ for motor vessels} \end{array} \right.$$

$$\left\{ \begin{array}{l} \eta_h = 1.07 \\ \eta_g = 0.91 \end{array} \right.$$

In this dissertation the proposed equations and coefficients will be combined to introduce the "Backer method" and the equations of water level depression along with the several proposed coefficients will be applied to Bolt (2003) method to compose the "Bolt method modified by Backer".

2.5. Options to improve Bolt method

To address the recommendations made by Backer van Ommeren for improving the Bolt (2003) method four potential solutions investigated. First, by combining the selected and most suitable formulas from Backer van Ommeren study for resistance and power computations the Backer method introduced as the first solution. Second, the 3rd comment regarding simplifications in return flow estimation was considered and two specialized formulas for shallow water conditions applied to original Bolt method. Third, it is explored how the Bolt (2003) method can be modified by using the equations proposed by Backer van Ommeren while maintaining the simplified return flow formula that can be solved algebraically, with the goal of improving the overall performance of the current method. Finally, it is evaluated an alternative power estimation model known as the TU Delft method (Jiang, Baart & van Koningsveld, 2022), to determine its suitability as a replacement for the Bolt (2003) method.

1. Backer van Ommeren method

Backer van Ommeren, who is credited as the initiator of this thesis topic and the one that review the Rijkswaterstaat theory or Bolt (2003) method, conducted a detailed investigation on it. In his study, he investigated several equations for the calculation of the return flow velocity, the water level depression and he tested the use of alternative coefficients in resistance and power. Subsequently, he compared the results of the return flow velocities obtained from different equations and selected the most appropriate to be used. A similar procedure was also applied to choose the most suitable formula for calculating the water level depression. According to the findings, he developed a methodology, the Backer method to the resistance components and the required power.

Backer van Ommeren method was developed according to the following theories. The equation of the limit speed (2.11) and the return flow (2.12)¹ are obtained by using Schijf (1949) theory. For the calculation of the water level depression two equations were used. In the case of a narrow or a wide waterway the water level drop is computed from Equations 2.13 & 2.15 (Schijf, 1949; Blaauw, 1983; Blaauw & Knaap, 1985) while for a very wide waterway the Equation 2.16 as it presented in the study of Blaauw & Knaap (1985) based on Tuck (1966) potential theory for slender bodies was used. Also, he decided to reduce the increase of the frictional resistance from 40% to 20% and the pressure coefficient from 0.15 to 0.1. In Appendix H the steps for the analytical calculations are described.

¹ Backer method with the return flow equation (Bouwmeester et al., 1985) was investigated by computing the resistance and the brake power. However, the results by using the formula came out slightly lower than that with (Schijf, 1949) formula (Appendix C).

2. Bolt method with speed correction

The velocity of flow under the keel changes when the vessel moves from deep to shallow water. This change occurs due to the riverbed effect. In shallow water, the velocity of flow under the keel increases due to the limited depth, resulting in a significant drop in pressure. Consequently, the buoyancy, which is the upward force of the ship, decreases, causing the ship to sink further (larger draft).

Resistance calculations require well-defined velocity profiles and its transformation in shallow water. Several methods predict maximum flow velocity at the boundary layer of the bed, but the development of the boundary layer from ship bottom was first introduced in 2014 by Robijns in Delft Laboratories. This is an empirical flow model, which is able to predict the flow field directly above the bed and beneath the sailing vessel. First, this flow model is developed for conventional vessels and then the model is adapted, to predict the flow field underneath barges. This order has been chosen, since there were more experiments with conventional vessels than with barges (Robijns, 2014). After model setup and experiments the Equations 2.17 and 2.18 were derived. The application range for the empirical flow model is restricted near to the riverbed at a range of $1.1 \leq h/T \leq 1.6$. So, in case that ratio of depth to draft is diverted from the previous range, it was shown that the interaction between the riverbed and the ship is minimal. In the same research study, another formula for the return flow also investigated. This formula originally initiated by Maynard (1990) while Stolker and Verheij (2006) modified the original equation in order to improve its accuracy. Maynard (1990) equation based on model research on push-tow units to predict this maximum return current beneath a sailing barge which is dependent on the water depth, the draft, the ship width, and the sailing speed. So, the original formula is created by a regression analysis of the physical model data on dimensionless ratios. The range of applicability of this formula is $h/T > 1.6$. The following equations will be applied to original Bolt (2003) method to test if they can improve its accuracy. The analytical process of the calculations is shown in Appendix H.

$$\text{For motor vessel: } U_{x,max} = 0.6 \cdot \left(\frac{T}{h}\right)^{1.2} \cdot V_s - 1.5 \cdot \left(\frac{h}{B_s}\right)^{1/3} \cdot U_o \left[\frac{m}{s}\right] \quad (2.17)$$

$$\text{For barges: } U_{x,max} = 1.36 \cdot \left(\frac{T}{h}\right)^2 \cdot V_s - 1.7 \cdot \left(\frac{h}{B_s}\right)^{1/3} \cdot U_o \left[\frac{m}{s}\right] \quad (2.18)$$

$$U_r = 1.07 \cdot (V_s + U_o) \cdot \left(\frac{T}{h}\right)^{0.08} \cdot \left(\frac{B_s}{h}\right)^{1.82} \left[\frac{m}{s}\right] \quad (2.19)$$

3. Bolt method modified by Backer

The third solution that it is studied and simulated is the modification of Bolt theory according to Backer's suggestions or "Bolt method modified by Backer". To be clear Backer van Ommeren in his study except for an alternative solution for the calculation of the resistance components and the brake power, also he suggested to test some proposed formulas in the original Bolt (2003) theory as a trial to improve it. These suggestions are presented in Section 2.4.3 and for this solution the formulas that describe the water level depression, the characterization of the waterway's class as well as the power efficiencies were used. In Appendix H the analytical calculation procedure is presented.

4. TU Delft method

The last solution that is investigated is the TU Delft method (Jiang, Baart & van Koningsveld, 2022). Recently, in 2022 Jiang, Baart, and van Koningsveld have developed a comprehensive emissions and RES demand quantification method for IWT vessels, of which the variation of vessel types and engine types, actual transport volume, and dynamic navigation conditions, operation behavior in upstream and downstream trips are considered. The method is validated by real world data, were obtained from inland vessel fuel reports. The main reason for the development of this method originated from the policy on the energy transition, the reduction management of the inland waterway transport emissions and the applicability of renewable energy sources (RES). It is mentioned that the transition to renewable energy sources (RES) and the related investments require a comprehensive and a reliable quantification of emissions and RES demand. Therefore, a corresponding simulator OpenTNSim - Energy (Jiang et al., 2022) of the method is created.

The resistance and power calculations in TU Delft method based on the Holtrop and Mennen, (1982) theory, with shallow water effect corrections. Notably, it is about a set of empirical equations, derived from a large number of model test results and ship trial data in deep calm water condition. It is considered one of the most accurate methods for predicting resistance with wide applicability (Lothar, 2019). The main idea of this theory as it is already mentioned in Section 2.2, is the total resistance is subdivided into different resistance components. Therefore, it computes a dimensional total resistance (R_T) according to Equation 2.1, which is broken down into several components: frictional resistance (R_f), appendage resistance (R_{app}), wave-making resistance (R_w) and residual resistance (R_{res}). The residual resistance includes resistance due to bulbous bow near the water surface (R_B), pressure resistance due to immersed transom (R_{TR}) and model-ship correlation resistance (R_A). In the IWT vessel resistance estimation, the bulbous bow resistance is not considered as most of the IWT vessels do not have a bulbous bow.

As it has already mentioned, TU Delft method (Jiang, Baart & van Koningsveld, 2022) includes corrections that capture the shallow water effects so in resistance calculations as in power estimations. Regarding the frictional resistance, that originally estimated according to ITTC-57 formula which is a function of Reynolds number with the assumption of infinitely deep and wide water condition, in the case of shallow water navigation, the speed of water flow around and beneath the ship increases and thus influence the Reynolds number and thereby the frictional resistance coefficient (C_f). To improve the prediction of the frictional resistance and include these effects, CFD computations were done. In 2018, Zeng et al. (2018) analyzed the flow between two flat plates at different Reynolds numbers ($105 < Re < 109$) and different distances between the plates ($0.01 < D/L_S < 1.00$) and proposed a modification of the ITTC-1957 correlation line. This new proposed C_f is used for the frictional resistance estimation by substituting the C_f according to ITTC-1957 in Holtrop and Mennen method (1982). The detailed calculations are presented in Appendix H.

Regarding the sailing speed correction that is used in shallow water conditions, Karpov's approach was used (Karpov, 1946; Van Terwisga, 1989). This approach involves the derivation of two speed correction coefficients. The first coefficient accounts for the impact of the return flow around the ship hull, which affects friction estimations. The second coefficient addresses the increased resistance caused by wave-making in shallow conditions. The former is represented by α^* and was developed for different ratios of the water depth to ship draft (h/T), at different froude depth number conditions. So, the corrected speed is obtained by

Equation 2.20 and was used for the frictional resistance estimation. The latter coefficient for the increased wave-making resistance in shallow depths is represented by α^{**} . Again it was developed for different ratios of the water depth to ship draft (h/T), at different Froude depth number conditions but the corrected velocity V_2 is derived according to Equation 2.21. It should be noted that the direct application of V_2 , for wave-making resistance estimation leads to overestimation since its estimated power has already exceeded installed engine power at IWT vessel normal sailing speed. Therefore, it was found by real world sailing data validation, the V_2 correction is partially adopted in IWT vessels as follows:

$$V_2 = \begin{cases} 75\% \text{ of the correction, } h \leq 3m \\ 85\% \text{ of the correction, } 3m < h \leq 9m \\ 95\% \text{ of the correction, } h > 9m \end{cases}$$

$$V_1 = \frac{V_s}{a^*} \quad (2.20)$$

$$V_2 = \frac{V_s}{a^{**}} \quad (2.21)$$

The equations that were used for the power calculations in TU Delft method (Jiang, Baart & van Koningsveld, 2022) are the one that described in Section 2.1.2 while the power efficiencies with the corresponding values are presented next. The η_g , η_t , η_o , η_r , η_h are a series of power efficiencies according to vessel power plant layout, which are gearing efficiency, transmission efficiency, open water efficiency, relative rotative efficiency of the propeller, hull efficiency, respectively. The η_g commonly ranges between 0.95 and 0.99 and η_t between 0.5 and 1, as described by (Klein, 2002). The product of η_o , η_r and η_h is also expressed as hydrodynamic efficiency, η_D .

The key distinction of this approach from the original Holtrop and Mennen (1982) method lies in its hydrodynamic efficiency values, which are influenced by the water depths and incorporate the impacts of shallow water. The hydrodynamic efficiency η_D requires correction for shallow water operation, as it is influenced by water depth, waterway width, and vessel sailing speed (Simic & Radojicic, 2013; MoVe IT! 2014). For seagoing vessels sailing in deep open sea, the value of it is commonly between 0.6 and 0.7. While research projects on shallow water operation vessel power efficiency (Bilen & Žerjal, 1999; Simic & Radojicic, 2013; MoVe IT! 2014; Marin, 2020; Radojicic et al., 2021) indicate that the η_D of vessels in shallow water is usually ranges between 0.4 to 0.5 but can be as low as 0.2 to 0.3. Most of the pushed convoys have a relatively low η_D of around 0.3 to 0.4 (Bilen & Žerjal, 1999), though this can also be lower and depends on several factors. Following Equations 2.4 to 2.6, the power components will be computed according to TU Delft method (Jiang, Baart & van Koningsveld, 2022). Again, the analytical calculation process for the implementation of the TU Delft method are described in Appendix H.

II Methods implementation

3. Materials & methods

This chapter aims to provide insights into improvements of Bolt (2003) method namely Bolt method with speed correction, Bolt method modified by Backer as well as Backer method and the TU Delft method that were presented in Chapter 2, Section 2.5, with the goal of improving the reliability of the Bolt (2003) method or its substitution with another power model. Also, the implementation and testing of these methods will be discussed in terms of their effectiveness in resistance and power calculations. Finally, the comparison process between the methods in the first test stage and with the real data in second test stage will be described, by following specific evaluation criteria.

1. Accurate representation of important theoretical concepts
2. Accurate results compared to real-world power and fuel use data considering the acceptable deviations rate that was determined to 20%
3. Practical applicability

3.1 Modelling concept

To calculate the different resistance components, the total resistance and then the propulsive power of an inland vessel the python notebooks will be used. Specifically, four notebooks will be developed in order to simulate the original Bolt method, Backer method and Bolt's improvements. Then these notebooks will be uploaded to the open-source Transport Network Simulation (OpenTNSim) repository. The package is available at the Github of the Hydraulic Engineering Department of TU Delft (van Koningsveld, 2019) . Regarding the simulation of TU Delft method (Jiang, Baart & van Koningsveld, 2022) and the resistance and power calculations, the energy module from the OpenTNSim will be applied.

The calculations of the resistance power components require several input data. Therefore, the notebooks were designed to allow users to modify input parameters and generate corresponding results effortlessly. These results are presented through graphs that enable easy comparison of resistance and power fluctuations across various waterways.

3.2 Implementation of the five studied methods

The importance to acquire a power prediction method for inland shipping in shallow and confined waterways led to the investigation of Bolt (2003) method according to Backer van Ommeren recommendations. In this section will be explained how the aforementioned methods were implemented in python notebooks.

Originally the Bolt method was developed. According to excel spreadsheet that was provided from Rijkswaterstaat showing a comprehensive study of inland vessels in terms of resistance and power estimation and following the description of Bolt (2003) method that was presented in Chapter 2, Section 2.2, the first notebook was structured. This script contains all the necessary equations to calculate friction, pressure, and residual resistance, along with their corresponding coefficients and sailing speed formulas. Additionally, it includes equations for effective, delivered, and propulsive power. Following that the input parameters for the calculations were defined. Specifically, the ship characteristics including the length, the width and draft, the waterway dimensions namely the water depth and the width, the sailing speed over the water and then the maximum installed power per inland ship type were given. By combining the equations with the input parameters, the resistance and the power components were computed. Regarding the presentation of the results, graphs for the total

resistance and the propulsive power as a function of the sailing speed and the water depth were produced.

Based on Backer van Ommeren comments regarding the Bolt (2003) method and the goals outlined in the (Green Deal Zeevaart, Binnenvaart En Havens, Green deals, 2019) in Chapter 1, Section 1.1, for an accurate power method for inland ships, four methods were investigated in Section 2.5. These methods include the Backer method, the Bolt method with speed correction, the Bolt method modified by Backer, and the TU Delft method. For the simulation of the four methods a similar procedure as in Bolt method were applied.

The simulations aim to produce consistent outcomes across all the methods under investigation, enabling an objective evaluation of their performance in various waterways and with different types of the inland fleet. Two distinct test cases were established for both the evaluation and validation procedures: the Academic test case and the Real-world test case.

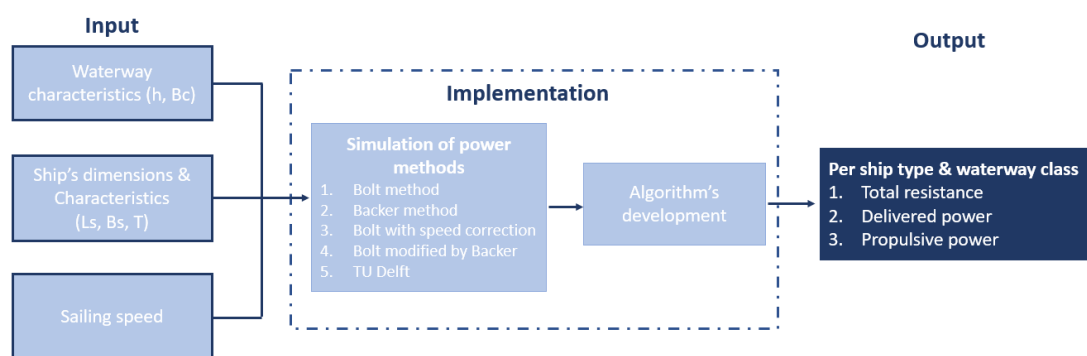


Figure 3.2.1: Resistance & power calculation process

3.3 Academic test case with evaluation criteria

In this section, the first round of the validation process would be introduced from a theoretical point of view. The goal of this test will be to select the most well-performed methods according to the first criterion “Accurate representation of important theoretical concepts (changing depth, width & sailing speed)”. For this test case two motor cargo vessels were selected, an M6 (CEMT IV) and an M8 (CEMT Va). The choice of these two classes was done according to (Identify Typical Fleet Families and Operational Profiles on European Inland Waterways and Canals – Prominent-IWT, n.d.) as the most common motor vessel types on the North-South corridor. The drafts are 2m and 2.7m respectively.

The five methods will be simulated for two scenarios of waterway conditions and for the two types of motor cargo vessels the M6 and the M8. The first scenario will simulate a narrow waterway for three different water conditions namely shallow, intermediate, and deep. For the narrow case, the channel width is selected equal to be 50m as a representative value according to Waterway Guidelines, TU Delft Repositories (2020), while the depth varies in between 3 – 10 m for the M6 vessel and 4 -10 m for the M8 vessel. Therefore, the minimum water depth to ship draft ratio studied is 1.5 for both ships.

The second scenario will simulate a wide waterway for the three different waterway depths similar to the first scenario. For this scenario the selected channel width is determined equal to 150m while the depth variation is constant and equal to 3-10m for the M6 vessel and 4 -10 m for the M8 vessel. In Figure 3.3.1 the waterway conditions and the ship dimensions are summarized.

Waterway conditions for Academic test case	Shallow $1.2 < h/T \leq 1.5$	Intermediate $1.5 < h/T \leq 3$	Deep $h/T > 3$
Narrow	X	X	X
Wide	X	X	X

Vessel types for Academic test case	M6 85·9,5·2	M8 110·11,4·2,7

Figure 3.3.1: Waterway conditions & ship dimensions for the Academic test case

The assessment of each method in the Academic test case will be based on three key criteria: recognition of the water depth and width variations and ship dimensions for a specific range of sailing speeds. Specifically, for each method, the total resistance and the propulsive power are plotted as a function of these parameters and the results analyzed to ensure that the method is able to effectively capture these effects. In order to select the most appropriate method, the results from each are compared against one another under different waterway conditions and for two motor vessel classes, which have been previously defined. By considering these criteria and analyzing the results, a method can be deemed valid if it is able to satisfactorily account the aforementioned criteria.

3.4 Real-world test case with evaluation criteria

In this section, it will be introduced the implementation of the real-world test case for the most promising methods, as determined from the initial round of testing - the Academic test case. The validation process of these methods in the real-world test case will be conducted from a practical perspective, using real power and fuel use data and evaluating according to the second and third criterion “Accurate results compared to real-world power and fuel use data considering the acceptable deviations rate that was determined to 20% & Practical applicability”. Through this assessment, the practical applicability of the selected methods from academic test case will be ensured. The real-world test case will involve two comparison processes, the delivered power and the fuel-consumption comparison processes. The former comparison process aims to examine what kind of power estimations can be derived from the selected methods within a deviation of 20% from the measurements. Regarding the latter comparison will be conducted in order to evaluate the performance of each method in the presence of current flows by considering the same deviation of 20%. The final selection of the best practice(s) will be based on the results from these two processes combined with the third evaluation criterion.

3.4.1. Real-world data introduction

On May 1st, 2015, the PROMINENT project (Promoting Innovation in the Inland Waterways Transport Sector) started. Co-funded through the Horizon 2020 Programme of the European Union, the project aims at

- Massive transition towards efficient and clean vessels by developing cost-effective solutions applicable to 70 % of the EU fleet and reduction of the corresponding implementation costs by 30 %
- Certification and monitoring of emission performance and development of innovative regimes
- Harmonization and modernization of professional qualifications and the stimulation of the further integration of IWT into sustainable transport chains

Following the above mentioned commitments, the fuel-consumption-reduction potential of a Danube vessel is evaluated. The under consideration vessel sails between Regensburg and Budapest on the Upper Danube. From this project important findings were derived and summarized next. The results comprise sailing time and fuel consumption derived for three different constant delivered power values representing the most significant power range the vessel is being operated, as well as 3 different speeds over ground when sailing downstream. They are evaluated for 15 characteristic sections of the Upper Danube when sailing upstream, as well as downstream. The aforementioned results are given for three different water levels: low, mean and highest water levels and they are combined to different sailing strategies comprising sailing with different constant brake powers upstream and speeds over ground downstream.

The vessel under consideration is the motor cargo vessel Herso 1, operated by Plimsoll Ltd. in Hungary. The MV Herso 1 is mostly operated together with the lighter SL Leonie on the Danube. The lighter SL Leonie is similar to the Europe II B lighter, commonly operated on the Danube but the main dimensions and the maximum deadweight are slightly smaller. The characteristic dimensions of both the motor vessel and the lighter are shown in (Appendix E, Table E-1). The configuration of the vessel in single or in longitudinal and coupled operation depends on the study of the power-speed relationship at specific water depths for the power evaluation and the current influence in the evaluation of the fuel consumption. Therefore, for the power evaluation the ship was considered in single operation while for the fuel evaluation longitudinal formation was selected for upstream trips and coupled for downstream trips.

The evaluation of the required power was based on the ship performance sailing in the fifteen stretches of the river with varying depths. Specifically, model tests were conducted to measure the delivered power as a function of the sailing speed for the MV Herso 1 in single operation and the results were illustrated by the delivered-power-speed diagram (Appendix E, Figure E-1) for the different water depths. For the evaluation of the fuel consumption the effect of currents was considered by converting the velocity over water to the velocity over the ground. This process was divided in upstream and downstream trips where the current effect is variable with increased consumption sailing against the currents. For upstream the fuel-use was computed for the most significant power range where the vessel is being operated (Appendix E, Table E-3) while for downstream the fuel was measured based on the maximum permitted sailing speed per river stretch (Appendix E, Table E-4).

3.4.2. Delivered power evaluation process

In the first process, it will be simulated the most promising methods to estimate the delivered power of a motor cargo vessel M6 class in a wide waterway under three different water depth conditions - shallow, intermediate, and deep. The power results will be plotted against the sailing speed and depth, and then compared with the corresponding power values obtained from the real-world data (Appendix E, Figure E-1). To ensure the accuracy of each method, the

evaluation criterion of a deviation rate of 20% from the actual values has been defined. In the following figure the waterway conditions for this test case are summarized.

Waterway conditions for Real world test case	Shallow $1.2 < h/T \leq 1.5$	Intermediate $1.5 < h/T \leq 3$	Deep $h/T > 3$
Wide	X	X	X

Figure 3.4.1: Waterway conditions for the Real-world test case

3.4.3. Fuel-use evaluation process

This subsection will handle the performance of the selected methods to the presence of a current flow. The calculations were realized as follows:

In the paper “Evaluation of the Fuel-consumption-reduction Potential of a Danube Vessel, n.d.) the fuel consumption was calculated. Originally, the upper Danube river is divided in fifteen stretches each of which has different current flows and water depths depending on the regime low, mean and high water level (Appendix E, Table E-2) The total length that is studied is 732.46km. For upstream trips a constant delivered power equal to 620kW(benchmark) is used for all the river sections while in downstream trips a maximum speed equal to 16km/h is used for all the stretches with an exception for the canal stretch that the maximum permitted speed is determined to 12km/h. Then taking into account the losses on the propeller shaft equal to 2%, the brake power is obtained. As a last step the selection of the specific fuel consumption (bsfc) is derived from (Appendix E, Table E-4) as function of the brake power. According to the previous methodology, the fuel use(consumption) in the report is derived.

Based on the forementioned process, a similar procedure also is applied to this dissertation for the calculation of the fuel consumption on the selected methods from the Academic test case. The calculations for the estimation of the fuel use will be performed for the medium water conditions and the corresponding current flow. Firstly, the input data for the upstream trip will be determined. Notably, the depth of each river section was chosen(Appendix E, Table E-2) and by using the power plot (Appendix E, Figure E-1) with a constant maximum delivered power equal to 620kW for all the different water depths in the river, the sailing speed over the water was determined (for each river stretch). This velocity will be used as input in the simulated methods in order to conduct the calculations and the brake power to be estimated. Following that, the calculation of the sailing over the ground will be achieved by using the Equation 3.1. Considering the velocity over the ground, the distance of each river section and by applying the Equation 3.3, the sailing time of each stretch will be derived. Then, the fuel use was computed for each section according to Equation 3.4 and the sum of all the fifteen fuel consumptions shows the total upstream fuel use. Secondly, the input data for a downstream trip will be determined. Specifically, for sailing downstream a velocity over the ground equal to 4.44m/s (16km/h) will be applied to all the river stretches whereas 3.33m/s (12km/s) will be used for the canal section. Based on these velocities and considering the current flow, the velocity over the water was computed and used as input speed in the three methods. Regarding the calculation of the fuel downstream is estimated by multiplying the sailing time downstream with estimated brake power and the specific fuel consumption through Equation 3.4. It is mentioned that the sum of the fuel use per river section gives the

total consumption for sailing downstream. Finally, the sum of the upstream and downstream fuel use indicated the amount of fuel that will be used for round trips.

$$V_{s,upstream} = V_{s,w} - |U_o| \left[\frac{m}{s} \right] \quad (3.3.1)$$

$$V_{s,downtream} = V_{s,w} + |U_o| \left[\frac{m}{s} \right] \quad (3.3.2)$$

$$t_{sailing} = \frac{\Delta x}{V_s} \text{ [hrs]} \quad (3.3.3)$$

$$\text{Fuel consumption} = P_{brake} \cdot SFC \cdot t_{sailing} \text{ [kg]} \quad (3.3.4)$$

III Results

4. Academic test case

In the literature study (Part I) five methods were presented that can predict the total resistance and the propulsive power as a function of the varying water depth and width and the sailing speed. These five power methods were developed in python notebooks, and they were simulated to produce the resistance and the power components for the inland vessels.

In this chapter, it will be presented the estimated total resistance and propulsive power results obtained through the five studied methods. The results will be visually represented through graphs, making it easier to interpret the values. To further analyze the results obtained, an in-depth analysis of each method in Sections 4.1 to 4.5 will be conducted. This analysis will provide a clear insight into the strengths and weaknesses of each approach. Following that, in section 4.6, the results obtained from all the methods will be plotted together, on graphs for shallow, intermediate, and deep water conditions for each ship type and channel width. By doing so, the most promising approaches that satisfy the criteria of varying depth and width, as well as different ship types will be derived.

4.1. Bolt method

- Narrow-M6

Figure 4.1.1 depicts the simulation of a motor vessel M6 navigating through a narrow waterway at three different depths, namely 3m, 5m and 10m. The pink line represents the most unfavorable scenario of a shallow and narrow waterway at a depth of 3m. At this depth, the maximum propulsive power is around 200kW, which is about one-fourth of its maximum installed power. It corresponds to a speed of 2.8 m/s, that is the highest speed that can be achieved in this water depth. As the depth increases to 5m and 10m, the ship maximum power and speed also increase. At a depth of 5m, the vessel needs 520kW to attain a speed of 4m/s, where this speed represents the limit speed(theoretical attainable velocity). In deep water conditions, the vessel is able to sail at its maximum installed power of 800kW when the speed is 5m/s. Regarding the resistance figure on the right, it is evident that the total resistance encountered by a vessel during sailing decreases with increasing water depth, by observing for a specific value of the speed. This is because the restrictions imposed from the canal reduced(larger depth) and as a consequence the magnitude of the shallow effects, such as the return flow and the water level depression reduced too. Both figures highlight the importance of recognizing the depth variation when sailing through a narrow waterway. This is because the curves for each depth do not coincide, especially in the preferred speed range of 2-4m/s, and the power demand decreases as the water depth increases, as evident in the comparison of the three power curves at a velocity of 2.5 m/s.

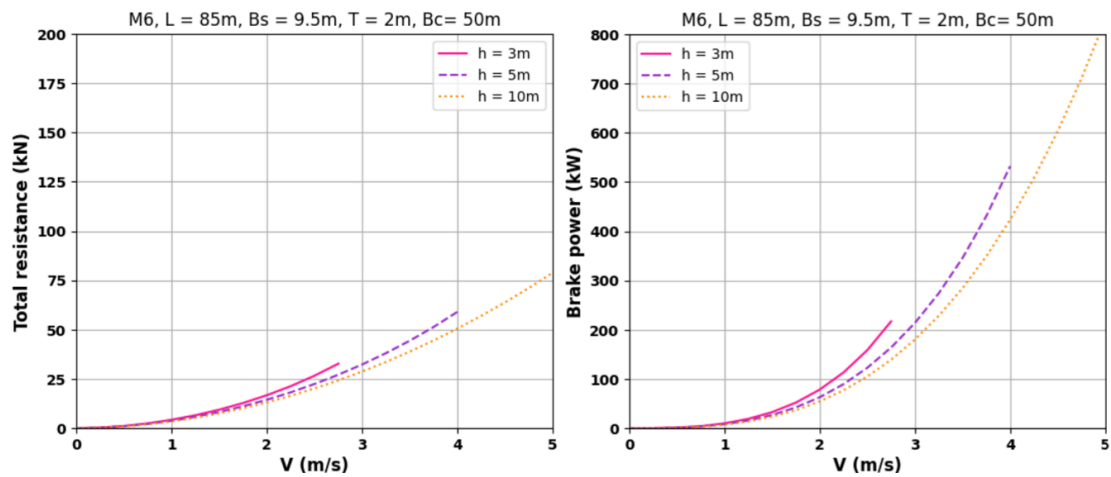


Figure 4.1.1: Total resistance & Brake power as a function of the vessel speed (M6-narrow), for different water depths

- *Wide-M6*

Figure 4.1.2 shows the simulation of motor vessel M6 in the case of a wide waterway and for three different water depths, 3m, 5m and 10m respectively. The maximum power output and corresponding sailing speed at a depth of 3m are approximately 400kW and 3.5 m/s, respectively. At 5m depth, the vessel achieves a maximum power output of 600kW, while at a depth of 10m, the vessel has not yet reached its maximum installed power of 800kW. Comparing the narrow (Figure 4.1.1) and wide cases for the same water depths and the same ship, it becomes evident that as the channel width increases, the vessel's resistance decreases. This reduction in resistance implies a decrease in the required power. For instance, at a water depth of 3 meters and a speed of 2.9 m/s, the required propulsion power is reduced by 20% in the wide case. Concerning the intermediate conditions at 4m/s the reduction amounted to 23% while for deep water, at the same speed (4m/s) the reduction amounts to 5%. These observations suggest that as the limitations of the channel, such as depth and width, decrease, the rate of power reduction diminishes abruptly. Overall, the Bolt (2003) method takes into account the variations in channel width, resulting in lower resistance and power values as the channel widens. However, the distinction between the curves is less prominent in the wide waterway compared to the narrow one, especially in deeper conditions. This indicates that there are critical combinations of ship and channel dimensions where exceeding these limits has little influence on the results.

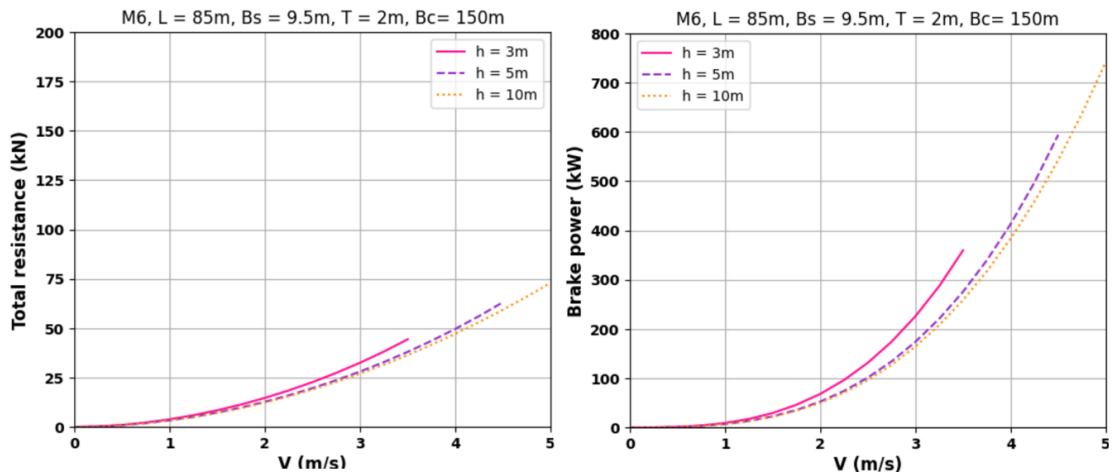


Figure 4.1.2: Total resistance & Brake power as a function of the vessel speed (M6-wide), for different water depths

- **Narrow-M8**

Figure 4.1.3 depicts the scenario of a motor vessel M8 navigating through a narrow channel with varying water depths of 4m, 5m, and 10m. It is noted that the 4m water illustrates the most challenging condition, which is a narrow and shallow channel. For this case, the maximum achievable power output is 750kW when sailing at a speed of 3m/s. As regards, the intermediate water depths, the power output increases significantly with a rate of 66%. and in deep water (10m) the maximum installed power can be achieved. In deeper water (10m), the vessel can achieve its maximum installed power output before reaching the maximum sailing speed of 5m/s. Notably, Bolt method captures the effect of varying depth, as there is a clear distinction between the three curves in the graph for the M8 vessel.

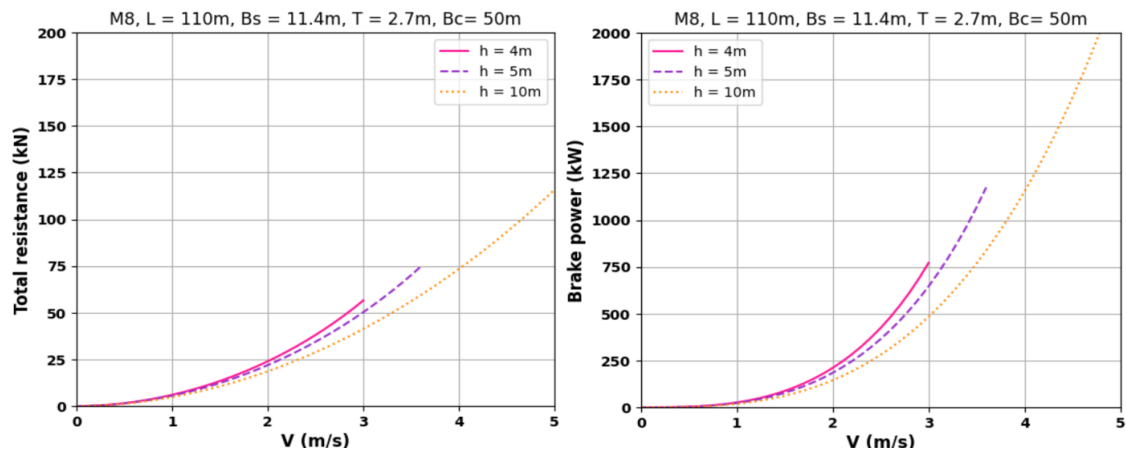


Figure 4.1.3: Total resistance & Brake power as a function of the vessel speed (M8-narrow), for different water depths

- **Wide-M8**

Figure 4.1.4 depicts a wide waterway for an M8 vessel at three different water depths. One observation is that a wider channel results in reduced total resistance encountered by the vessel. This is evident by comparing sailing in the narrow channel to sailing in the wider channel, both at a speed of 3 m/s. Moreover, it can be inferred that the reduction in resistance is more significant for shallower water depths than for deeper depths. This trend is reflected in the power figure as well, where lower required power is observed for the wider channels. As a result of the increased channel dimensions from narrow to wide, the limit speed also

increases. Specifically, the limit speed increases by 1m/s and 0.5 m/s for shallow-intermediate and deep water conditions, respectively.

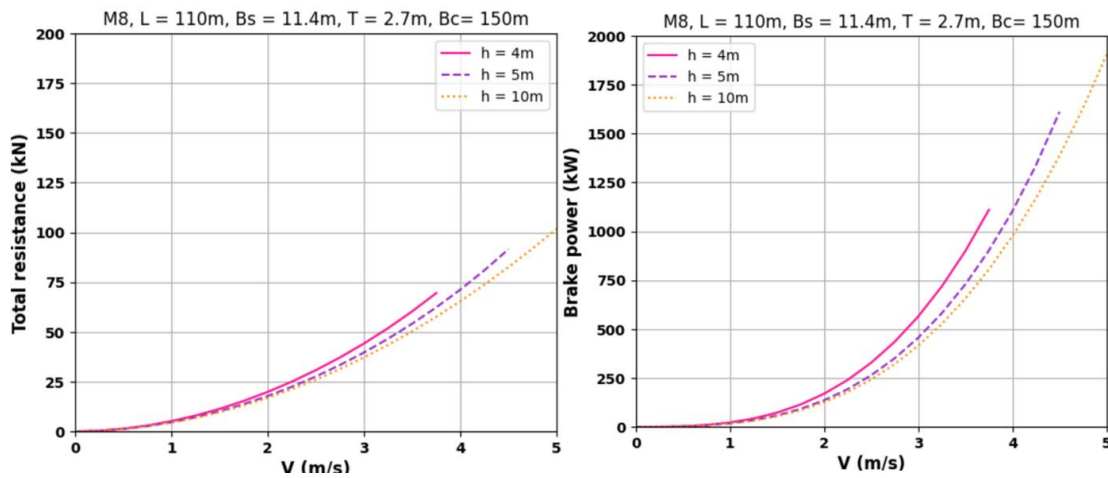


Figure 4.1.4: Total resistance & Brake power as a function of the vessel speed (M8-wide), for different water depths

4.2. Backer method

- *Narrow-M6*

Figure 4.2.1 shows the performance of the Backer (2019) method for M6 vessel, at a narrow channel and for three different water depths namely 3m, 5m and 10m. The left plot of the figure shows the total resistance encountered by the ship and the right plot the estimated brake power. From the resistance plot, it seems that at low sailing speeds, ranging from approximately 1m/s to 2.5m/s, the results obtained are almost identical for all three water depths with slightly higher values for 3m depth. However, as the sailing speed is getting higher, in case of the shallow water depth the limit speed is reached around to 2.8 m/s an event that indicate that the ship cannot sail with a larger velocity while the maximum resistance amount to 25kN. Also, in case of intermediate and deep water conditions, some variation between the purple and orange lines becomes noticeable, although the overall results are almost same with a deviation rate only 2.5%. Regarding the power results, the maximum power attainable for the three distinct water depths of 3m, 5m, and 10m is 100kW, 400kW, and 500kW, respectively. Furthermore, by comparing t the brake power at a sailing speed of 2.8m/s, it can be observed that the differences in the results are relatively small. However, the shallow case appears to be more distinct among the three cases as it approaches the maximum estimated power. In conclusion, it can be supposed that variations in depth are considered from the method in the case of a narrow waterway.

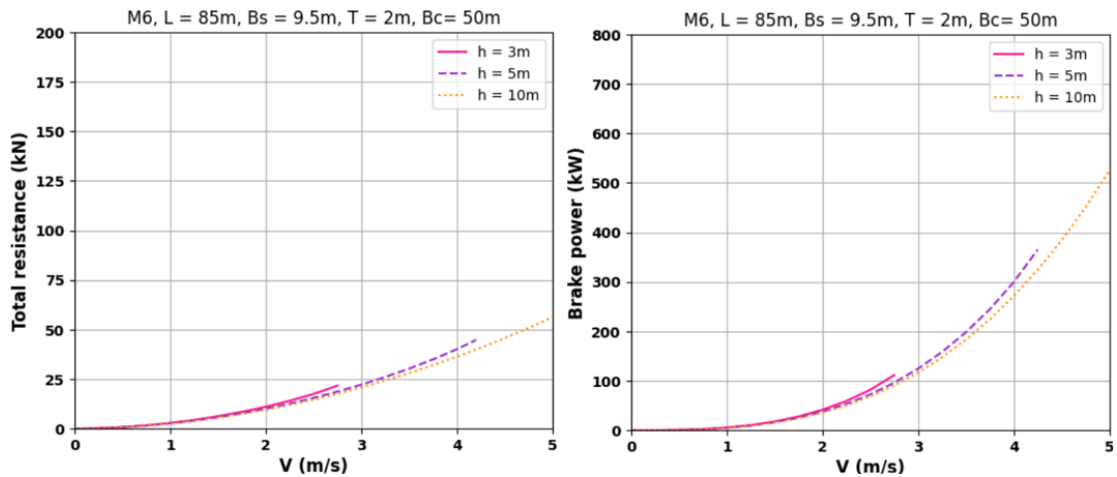


Figure 4.2.1: Total resistance & Brake power as a function of the vessel speed (M6- narrow), for different water depths

- **Wide-M6**

Figure 4.2.2 demonstrates the simulation of an M6 motor vessel in a wide waterway sailing in three different water depths 3m, 5m and 10m. The two plots in the figure display the resistance and the estimated brake power, respectively. Originally, it seems that the increase in channel width, resulted in increased limit speed. This effect is clear mainly in case of shallow water (pink line). However, by observing both plots it is concluded that the results either for the resistance or the brake power give similar values for the three distinct depths at each specific speed. Based on that, it seems that the depth variation does not consider in case of wide channels. Moreover, by comparing the results between the narrow case (above figure) and the present one, the width variation does not have a significant impact on the results (resistance & power) as the differences are minimal. Therefore, the varying width has little effect in the overall method.

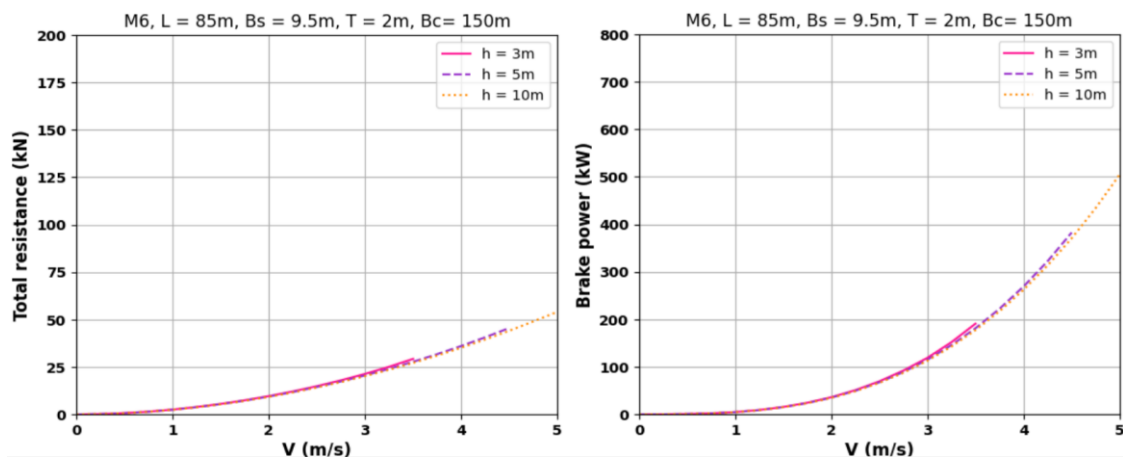


Figure 4.2.2: Total resistance & Brake power as a function of the vessel speed (M6- wide), for different water depths

- **Narrow-M8**

Figure 4.2.3 shows the Backer method for an M8 vessel at narrow conditions for three distinct depths 4m, 5m and 10m. On the left plot the estimated resistance is depicted while in the right one the results of the required power are illustrated. Sailing with low velocities both resistance and power estimations seem similar for all the depths. However, a variation in values among the water depths is obvious for sailing speeds ranging from 2.5m/s to 3.5m/s.

According to the results, it can be derived that Backer (2019) method is capable of detecting variations in depth when navigating through narrow waterways. It is mentioned that the trend observed in the case of M8 is also shown in M6 with the only difference lies in the different ships characteristics that lead to relatively higher results for M8 in contrast to M6.

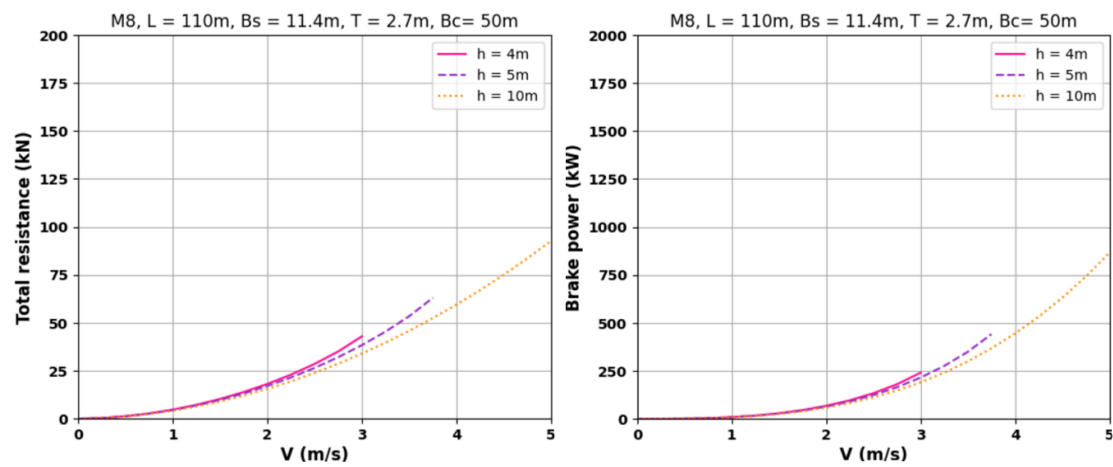


Figure 4.2.3: Total resistance & Brake power as a function of the vessel speed (M8-narrow), for different water depths

- **Wide-M8**

The next figure illustrates the results of an M8 motor vessel sailing in wide waterways with varying depths ranging from 4m to 10m. The total resistance that can be reached for each water distinct depth is approximately 50kN, 75kN and 80kN while the estimated power varies around 350kW, 600kW and 800kW respectively. Also, in this case the results either for the power or for the resistance at a specific speed across the different depths shows a deviation of the order of 1.5%. Based on that, it can be concluded that the depth variation in case of a wide channel does not consider from the method due to minimal deviations in the results. Subsequently, by comparing the effect of varying width between the narrow (Figure 4.2.3) and the wide channel the width variation has little influence in the method.

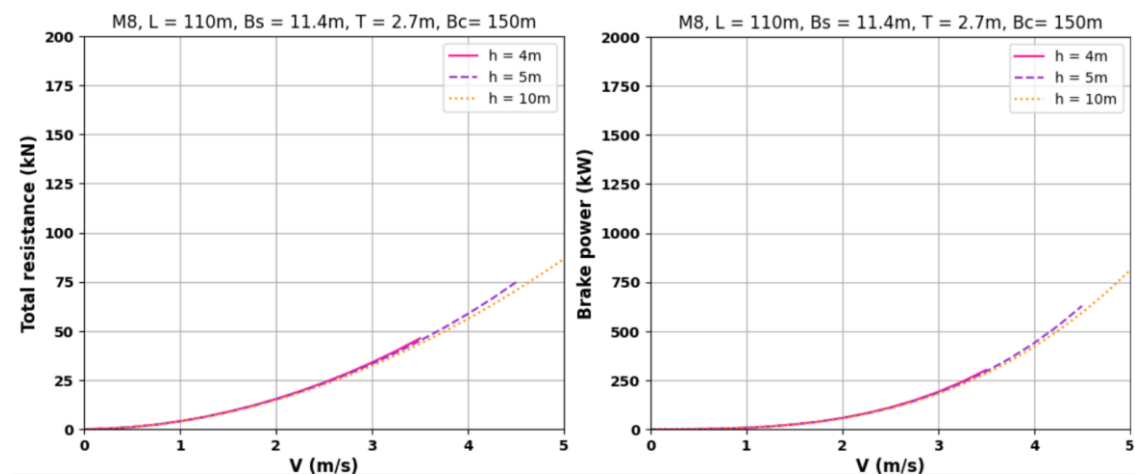


Figure 4.2.4: Total resistance & Brake power as a function of the vessel speed (M8-wide), for different water depths

4.3. Bolt method modified by Backer

- *Narrow-M6*

Figure 4.3.1 presents the performance of the Bolt theory modified by Backer for a narrow waterway and for three different water depths. Despite the modifications that were applied to the original theory, the final results are not optimistic for the resistance and the power calculation. More specifically, this approach does not consider the depth variations, since both resistance and power results have nearly the same values over the different water depths and provided a specific sailing speed.

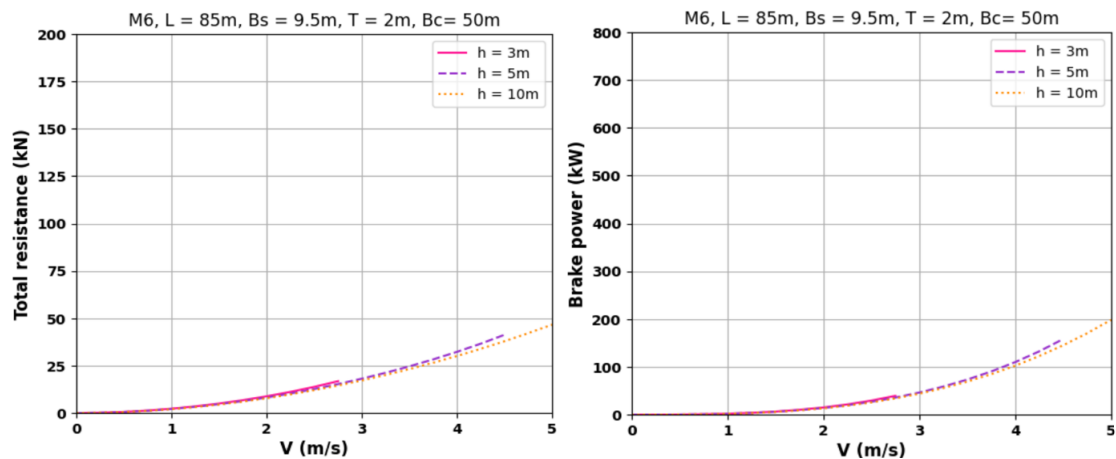


Figure 4.3.1: Total resistance & Brake power as a function of the vessel speed (M6-narrow), for different water depths

- *Wide-M6*

In Figure 4.3.2 the performance of modified Bolt theory is reflected but for a wide channel. Despite the modifications that were applied, it seems that the effect of width variation is not recognizable in this test case as the results of the resistance and the power are similar to the narrow case with imperceptible differences.

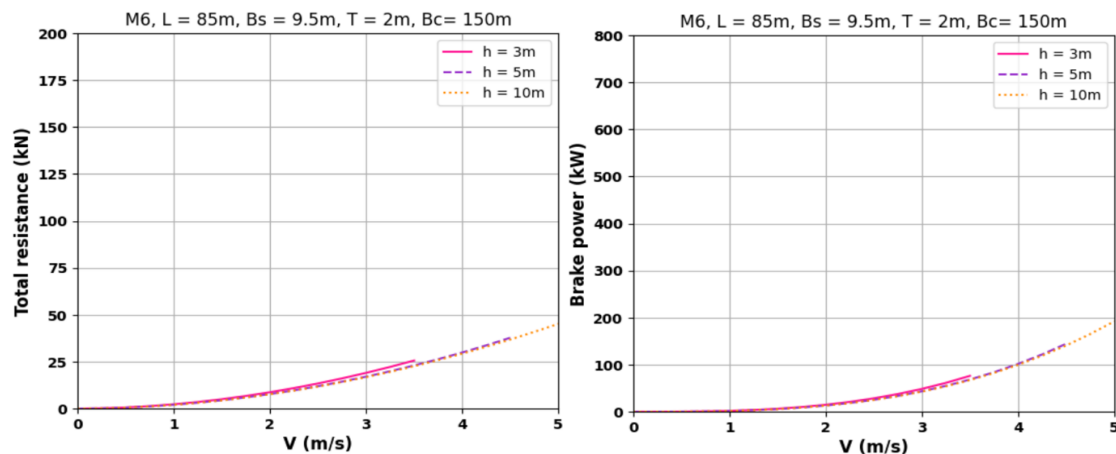


Figure 4.3.2: Total resistance & Brake power as a function of the vessel speed (M6-wide), for different water depths

- *Narrow-M8*

Figure 4.3.3 presents the situations of an M8 motor vessel, sailing in a narrow waterway and at three water depths namely 4m, 5m and 10m. It seems that at relatively low sailing speeds

2.8m/s to 3m/s the depth variation cannot be reflected as the resistance and mainly the power values across the different depths have minimal change.

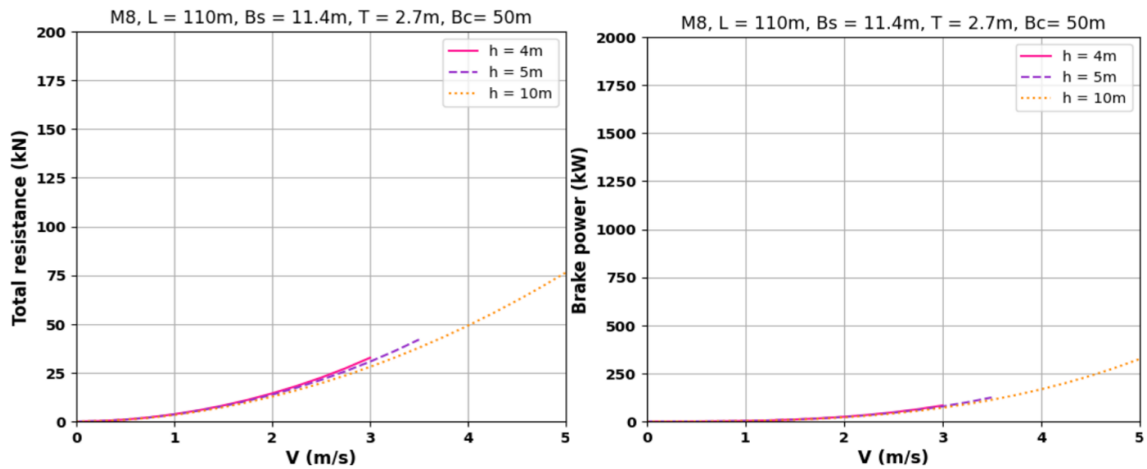


Figure 4.3.3: Total resistance & Brake power as a function of the vessel speed (M8-narrow), for different water depths

- **Wide-M8**

Figure 4.3.4 depicts the case of an M8 vessel sailing in a wide waterway for three different depths 4m, 5m, 10m. In this situation, method seems to take into account depth changes between shallow and deep water conditions for the prediction of the total resistance. To be specific the consideration of changing depth is obvious between velocities 2.9m/s and 3.7 m/s, nevertheless this effect is not illustrated in the power calculations.

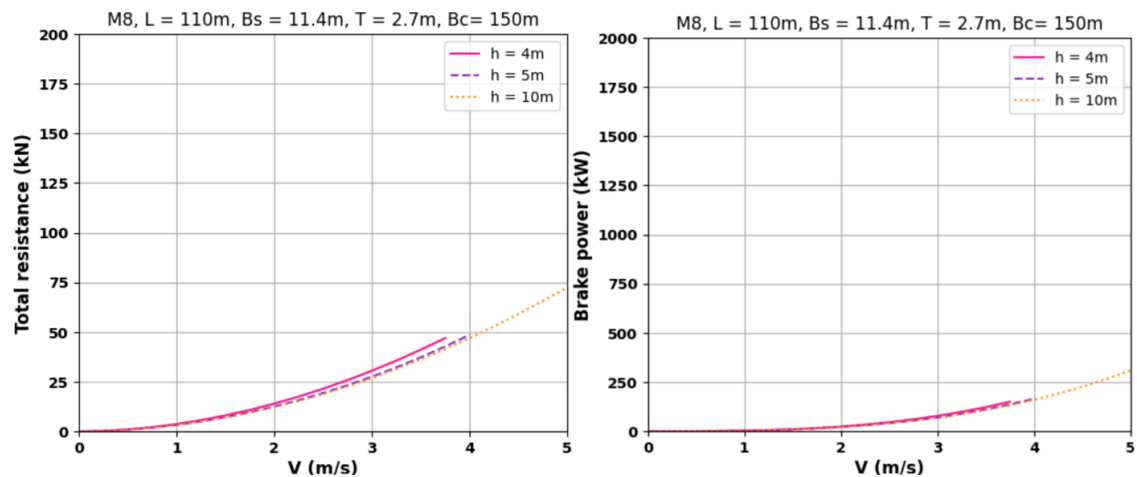


Figure 4.3.4: Total resistance & Brake power as a function of the vessel speed (M8-wide), for different water depths

4.4. Bolt method with speed correction for shallow water

- **Narrow-M6**

Figure 4.4.1 illustrates a narrow waterway with depth variation for a motor vessel, M6. The pink line represents the most unfavorable condition, which is a narrow and shallow channel with a depth of 3m. When comparing the power figure (on the right) for the 3m water depth condition to the larger depth conditions, we see that the maximum required power that can be achieved is 300kW at a sailing speed of 2.8 m/s. In contrast, for larger depths, the same required power is achieved at higher sailing speeds of 3.1m/s and 3.6m/s. Depth variations have a significant impact on the power output. In fact, for a depth of 5 meters, both the

resistance and maximum power are doubled compared to shallower depths. However, changes in speed do not appear to have as strong effect on power output as changes in depth. This behavior indicates that in confined waterways, the ship encounters larger resistance, which requires greater power to overcome. Instead, this effect becomes smaller when sailing in larger depths, where the ship encounters less resistance and requires less power to sail at the same speed.

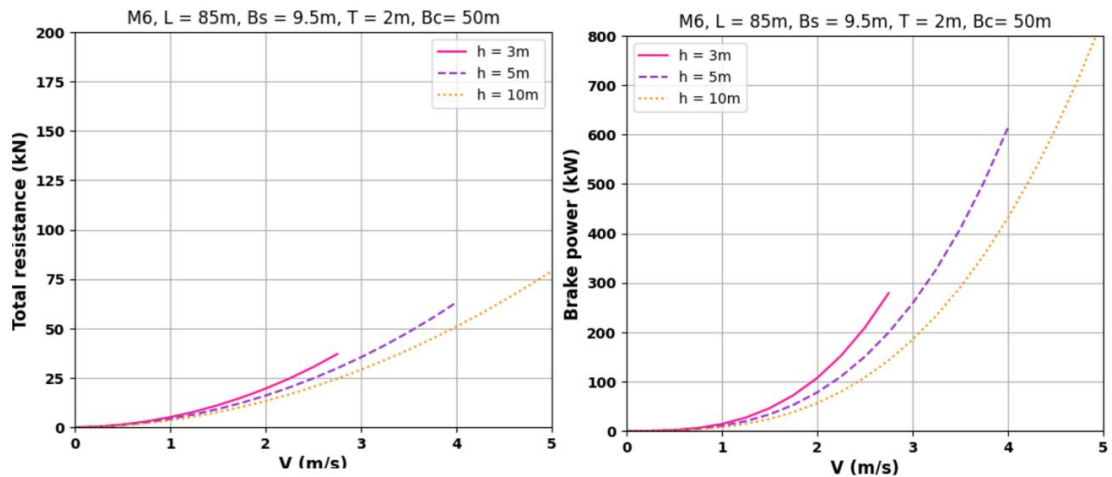


Figure 4.4.1: Total resistance & Brake power as a function of the vessel speed (M6-narrow), for different water depths

- *Wide-M6*

The following picture shows the simulation of M6 vessel in wide waterways for 3m , 5m and 10m depths. In contrast with the narrow case, wider channels permit relative higher sailing speeds, and it can be clear by comparing the shallow condition in both narrow and wide channels. By observing the Figure 4.4.2 the variation of the total resistance across the different water depths does not vary significant, however in power figure(left picture), it is obvious that either for 3m/s or 3.5m/s the power requirements for each water depth shows considerable differences.

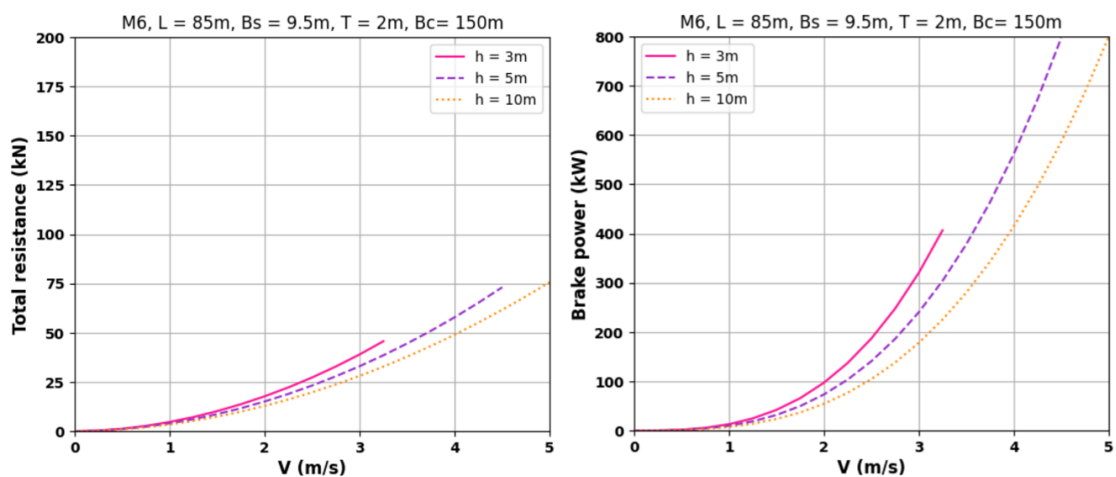


Figure 4.4.2: Total resistance & Brake power as a function of the vessel speed (M6-wide), for different water depths

- *Narrow-M8*

Figure 4.4.3 shows the simulation of an M8 in narrow waterways for 4m, 5m and 10m water depths. This method takes into account the depth variation as it seems from the changes both in ship resistance and propulsive by selecting a specific speed value and investigating the corresponding results at each water depth. Also, between 4m and 5m the results are quite similar due to 1m depth difference. This is particularly noticeable at low sailing speeds between 1m/s to 2m/s before the shallow water effects have fully developed. However, when considering the narrow case of the M6 motor, this trend does not hold for this speed range. This suggests that the dimensions of the ship have a significant impact on both resistance and power results, highlighting the importance of considering the specific characteristics of the vessel when analyzing its performance.

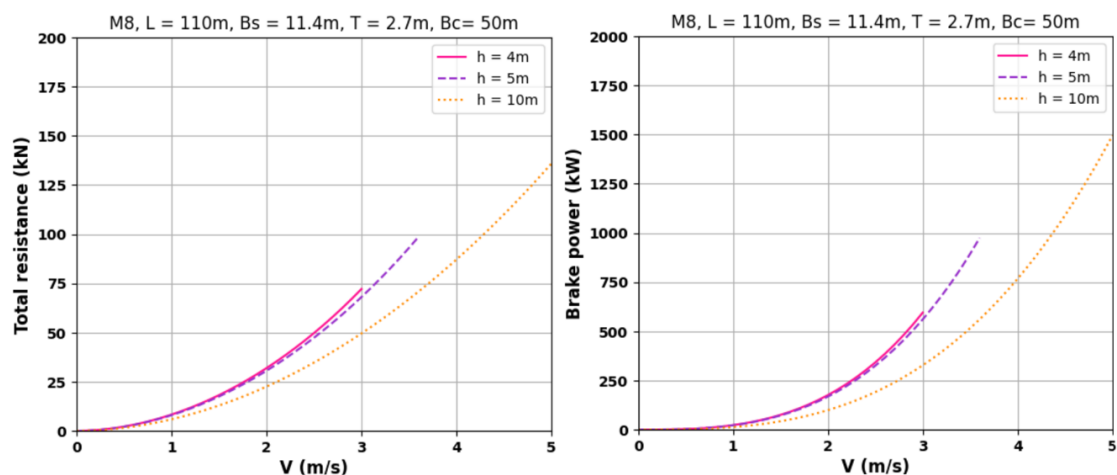


Figure 4.4.3: Total resistance & Brake power as a function of the vessel speed (M8-narrow), for different water depths

- *Wide-M8*

The simulation of an M8 motor vessel on wide waterways at three different depths shows that total resistance and propulsive power values are lower compared to the narrow case. For instance, total resistance equal to 75kN in shallow and wide channel attained at a speed of 3.4m/s while the same resistance which is the maximum for a narrow channel happened at a smaller speed of 3m/s. This example also shows the differences in the limit speed (maximum sailing speed) as a function of channel width and the ability of the method to recognize width variations. Regarding the power estimations, similar behavior has shown meaning lower values in wider channels compared to the narrower one. Additionally, the minimal variations for both parameters resistance and power from 4m to 5m are still obvious as the narrow case, despite the increase in channel width. This phenomenon can be explained by two factors. Firstly, the difference between a 4m and 5m ship is relatively small, making it difficult for the method to distinguish between the two depths accurately. Secondly, the interaction between ship dimensions and the channel can also have an impact on the accuracy of the method. This explanation is further supported by comparing the performance of the method when applied to M6 and M8 vessels in both narrow and wide channels. The M6 vessel shows a clear distinction in the curves, both in narrow and wide channels across the different depths indicating that the method is able to accurately distinguish between these width variations for the given ship type. However, in case of M8 vessels this distinction becomes less clear, by supporting the idea that channel and ship combinations can impact the method's reliability.

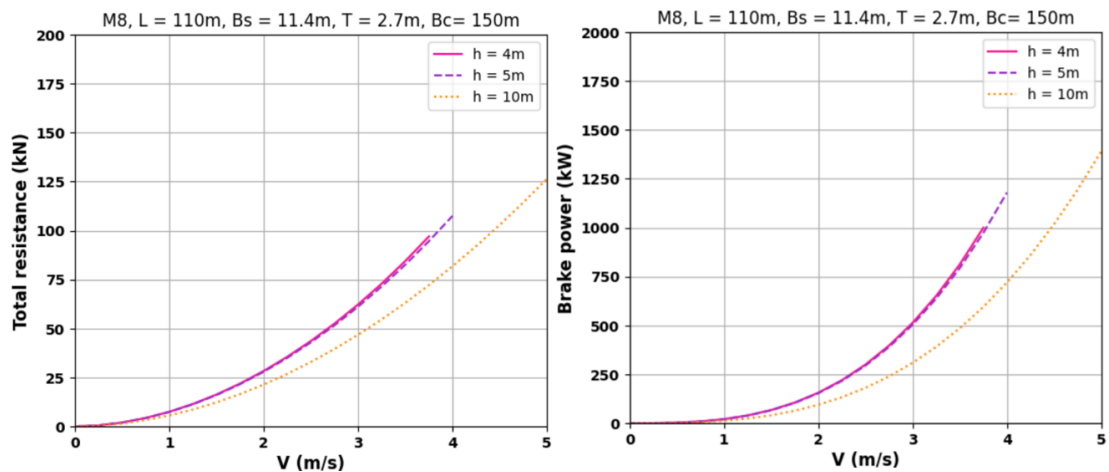


Figure 4.4.4: Total resistance & Brake power as a function of the vessel speed (M8-wide), for different water depths

4.5.TU Delft method

- *Narrow-M6*

Figure 4.5.1 shows the simulation of an M6 motor vessel, to sail into a narrow waterway for three different depths that correspond to 3m, 5m and 10m. The resistance figure(left) shows minimal changes in the estimated resistance values among the different water depths and focusing on a specific sailing speed. However, the power figure(right) shows three separate lines each of which reflect the different depths and for 3m depth the maximum power that can be achieved is 250kW while for 5m the brake power is almost doubled and for 10m the ship can sail with the maximum installed power.

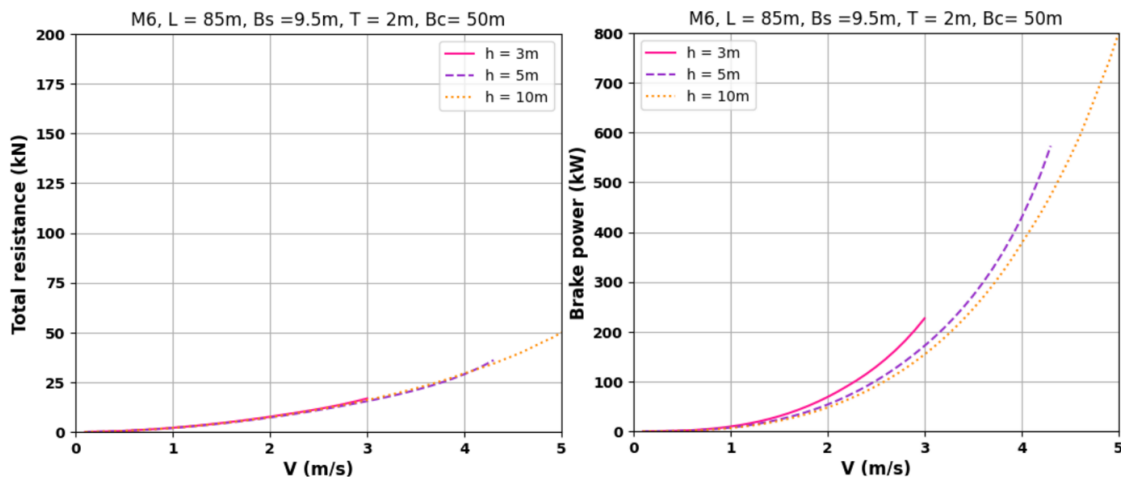


Figure 4.5.1: Total resistance & Brake power as a function of the vessel speed (M6-narrow), for different water depths

- *Wide-M6*

The figure illustrates the performance of the M6 vessel while sailing in wide channels with varying water depths of 3m, 5m, and 10m. The plot on the left side shows the resistance estimations for the vessel at different sailing speeds and depths. It can be observed that the results do not exhibit significant variations at low sailing speeds. On the right side, figure shows the estimated power as it is computed for the three different depths. The maximum

power that can be attained for sailing with 3.5m/s at a water depth of 3m is found to be 300kW, but for the same speed, the power result is halved for water depths of 5m and 10m. Additionally, by comparing the narrow and the wide channel cases for the brake power results, it can be seen that the latter shows a decreasing trend across the different water depths. This observation suggests that as the channel restrictions decrease and the channel is wider, the required power for sailing at a given speed, is actually reduced as opposed to the required power when sailing in a narrower channel.

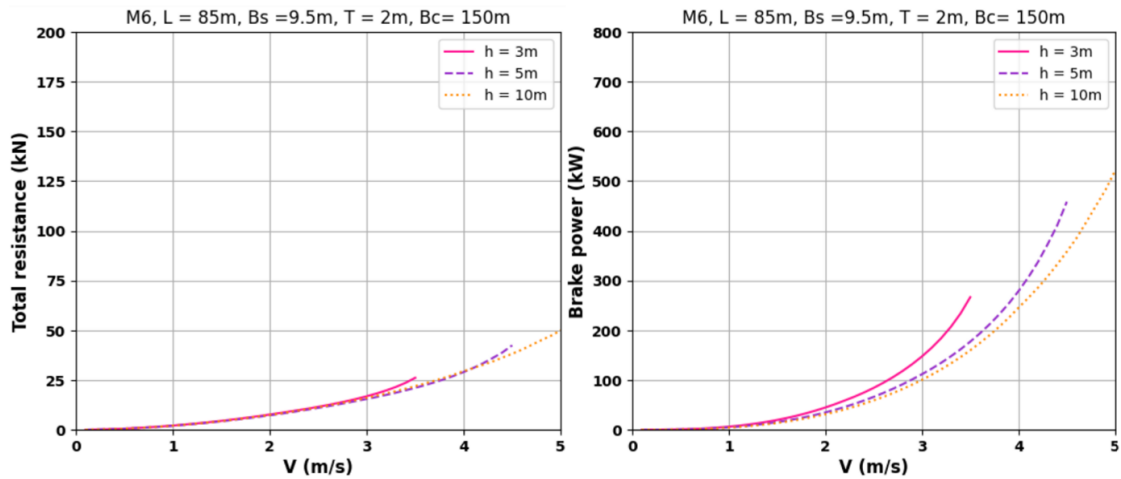


Figure 4.5.2: Total resistance & Brake power as a function of the vessel speed (M6-wide), for different water depths

- *Narrow-M8*

Figure 4.5.3 shows the simulations of a motor vessel M8 sailing in narrow water conditions for three different water depths. Originally, by observing the plot of the total resistance the differences in resistance calculations for the several depths at a given speed do not vary significantly. In contrast, power plot shows distinction across the different water depths at a specific sailing speed. It is mentioned that the distinction in both resistance and power results is pretty clear as the water depth is getting higher (purple & yellow line).

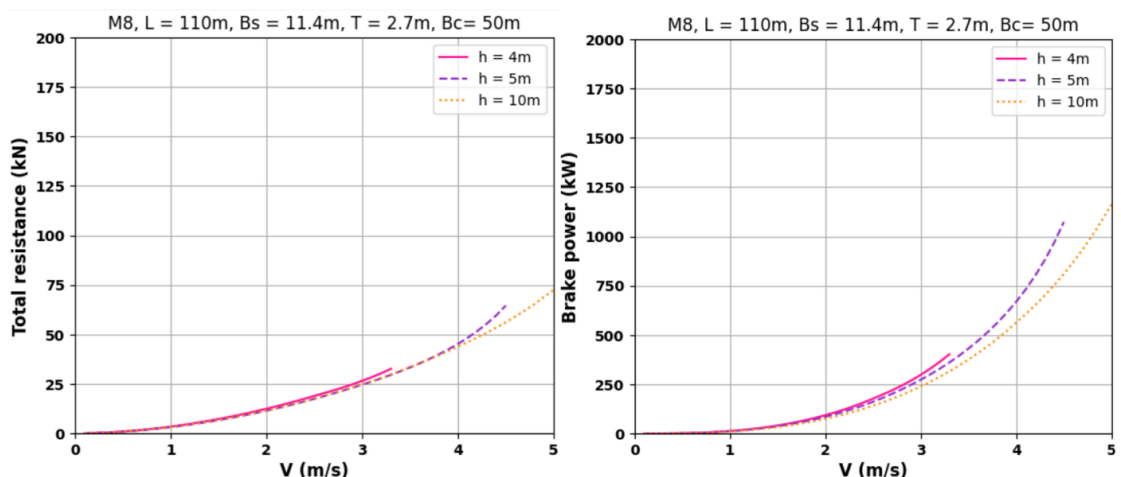


Figure 4.5.3: Total resistance & Brake power as a function of the vessel speed (M8-narrow), for different water depths

- *Wide-M8*

Figure 4.5.4 presents the simulation of an M8 motor vessel under sailing in wide channels of 150m and depths vary from 4m to 10m. Focusing on the power plot, it is obvious that the

maximum speed that can be achieved at 4m depths is around to 350kW while for 4m and 10m is almost doubled. Moreover, the differences in power demand between narrow(Figure 4.5.3) and wide case reflect that the latter required power will be decreased by 40%. Regarding the total resistance results of the wide case in relation to narrow one Figure 4.5.3), it seems that little change is reflected.

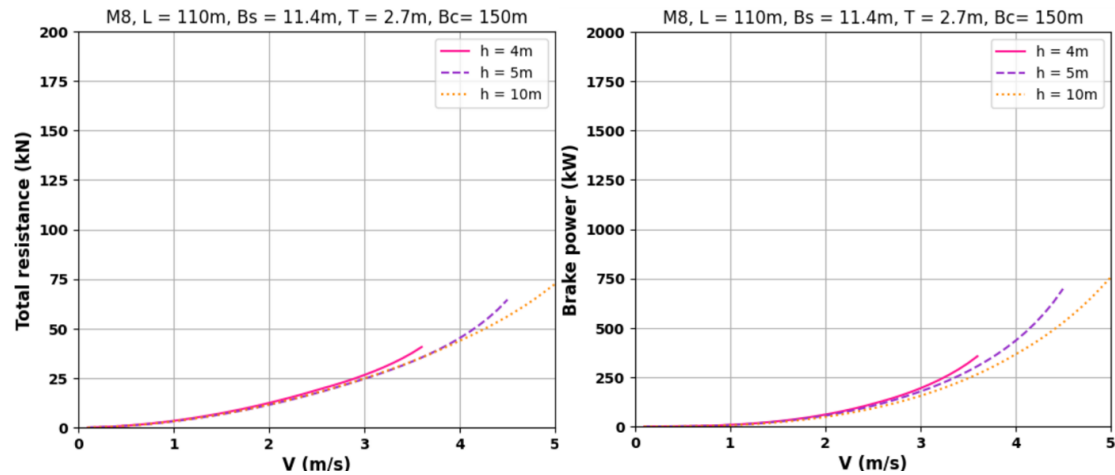


Figure 4.5.4: Total resistance & Brake power as a function of the vessel speed (M8-wide), for different water depths

4.6. Evaluation of the performance of the 5 studied method

In this section a comparison process will be conducted among the five studied methods for specific vessel types and channel dimensions . The power results for each method will be plotted together and the performance of each one will be reflected.

The Figure 4.6.1 shows the performance of the five power estimation methods in narrow channels and for shallow, intermediate and deep water conditions. As it can be seen, there are five lines each of which depicts the corresponding five methods. Bolt (2003) method and Bolt method with speed corrections have similar behavior in shallow and intermediate water depths as the difference in their results is 1.5%. The main difference between these two methods mainly is reflected in shallow depths, with Bolt method with speed correction to dominate because of the analytical return flow equations that included in the approach and make a clear break down between shallow and intermediate water depths. The TU Delft method's performance is illustrated by the purple line on the graphs. In shallow water scenarios, the power output grows as the velocity increases, until the velocity approaches its critical value. At that point, the power variation becomes restricted. This suggests that once the critical speed is attained, additional increases in power do not translate into higher velocities. This trend is clearly visible on the plot, as the purple line becomes nearly vertical beyond 3.8 m/s, until it reaches the maximum installed power of 800 kW. Explaining TU Delft method (Jiang, Baart & van Koningsveld, 2022) from a physical point of view, the use of Karpov's theory suggests an alternative criterion of how to define a limit in ship speed. According to this theory, maintaining the speed below the critical region characterized by the depth Froude number ($Fr=0.6-1$) can prevent ship grounding due to increased sinkage and trim. However, by comparing Bolt (2003) method and Bolt with speed correction with TU Delft method (Jiang, Baart & van Koningsveld, 2022), power results are varied significantly with the latter to give lower values. As far as Backer (2019) method, the performance looks same for all the depths with subtle changes in results. Bolt method modified by Backer, in shallow and

narrow conditions estimates extremely low propulsive power in relation to the other four methods and while in higher depths shows a relative increase, the overall performance is low.

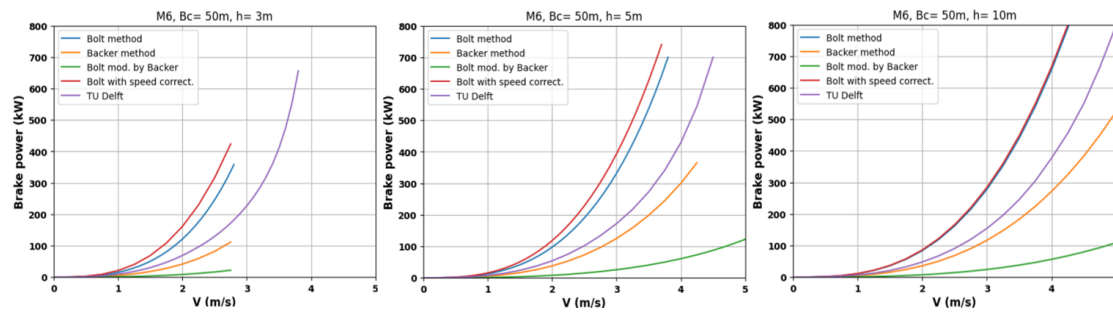


Figure 4.6.1: Performance of 5 methods in a narrow waterway for an M6 motor vessel

In the Figure 4.6.2 again an M6 motor vessel is simulated but in wide channels and for the same water depths as in the previous case. By comparing the wide and shallow case with the corresponding narrow and shallow, it is obvious that the width variations have great effect on power increase. More specifically, Bolt (2003) method and Bolt with speed corrections method reach the maximum installed in the wide case while it does not feasible in the narrow one. Moreover, similar behavior as the two previous methods, shows the TU Delft method (Jiang, Baart & van Koningsveld, 2022), but its power results in comparison to the other two methods are considerably lower. As regards, Backer (2019) method and Bolt method modified by Backer, power results are extremely low compared to the three forementioned methods while by comparing these two methods in case of narrow and in case wide channels, little change can be seen in power results across the different depths. It is mentioned that depth variation is not again recognizable from Backer and Bolt modified by Backer methods.

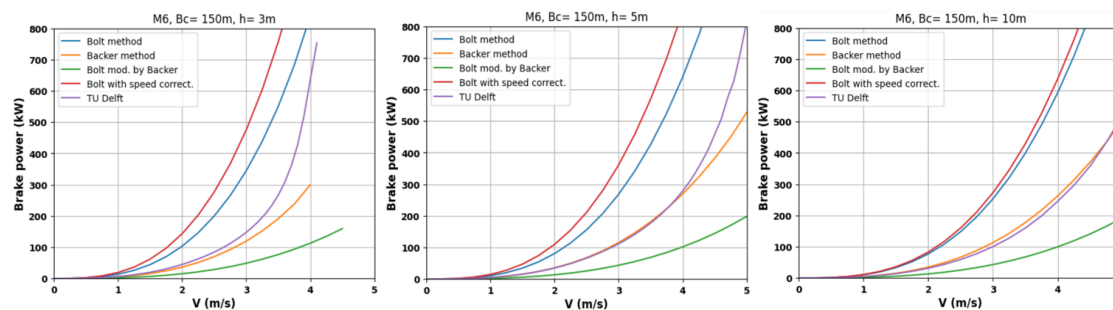


Figure 4.6.2: Performance of 5 methods in wide waterway for M6 vessel

Figure 4.6.3 depicts the performance of the five power methods in narrow conditions for a motor vessel M8 and for three different water depths. In case of shallow water (1st figure) Bolt method with speed corrections shows significantly different behavior compared to the other four methods. This is clearly illustrated for sailing speeds between 2m/s to 3m/s. For sailing speeds higher than 3m/s, Bolt (2003) method, Bolt method speed corrections and Bolt method modified by Backer estimates constant power values as the limit speed is reached and cannot sail with a higher velocity. As regards Backer (2019) method, a similar behavior as the previous discussed methods is observed but the maximum power is approximately 500kW and is realized when the sailing speed is reached. In contrast to forementioned methods, TU Delft method (Jiang, Baart & van Koningsveld, 2022) can estimate brake power for sailing speeds higher than 4m/s, as the effect of the limit speed does not consider in its calculation process. Additionally, by observing Backer (2019) method and Bolt method modified by Backer, the depth variation seems not be taking into account like to the previous two test cases. In terms

the Bolt method modified by Backer, still estimate extremely low power values among the five methods.

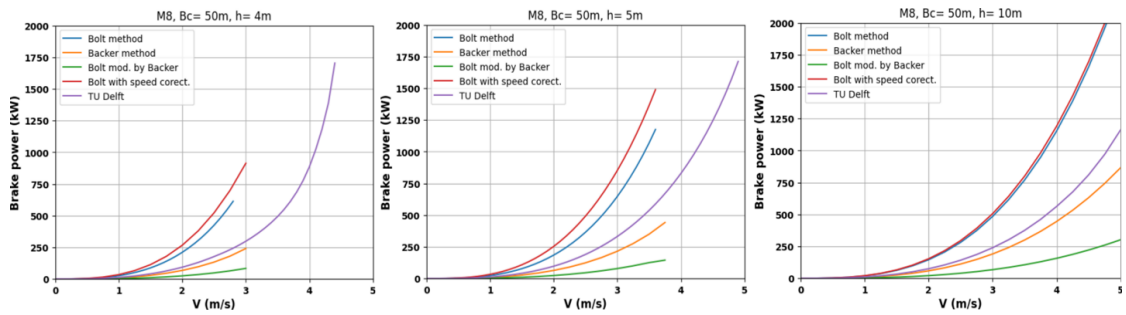


Figure 4.6.3: Performance of 5 methods in narrow & shallow waterways for M8

Lastly, the results of the five methods in wide channels and for shallow, intermediate and deep water conditions presented in Figure 4.6.4. Bolt (2003) method and Bolt method with speed corrections present similar results for all the different water depths while this effect is distinguished in 10m depth. The explanation of this behavior is related to the small difference in depths, from 4m to 5m water depth, but still the variation in power results is relatively obvious. According to Backer (2019) method the power results across the different water depths are almost identical. In this test case is clear that TU Delft method (Jiang, Baart & van Koningsveld, 2022) takes into account depth variation and in shallow water. Brake power goes up vertically when the sailing speed reaches up to 4.4m/s. Finally, Bolt method modified by Backer performs uniformly for all the water conditions and the results are very low in contrast to the other four methods.

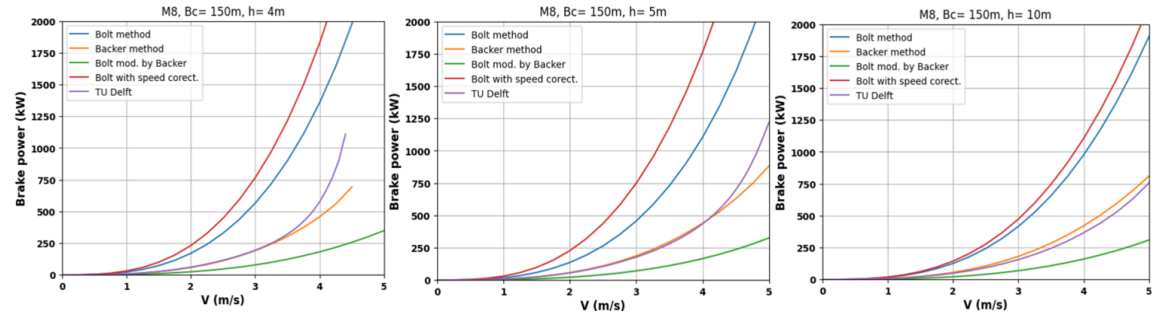


Figure 4.6.4: Performance of 5 methods in wide & shallow waterways for M8

4.7. Selection of the three most promising methods

In the previous section, the performance of five methods for brake power estimations is examined. Originally these methods compute brake power, and the results are presented in figures. The simulations were conducted for two types of ships, in both narrow and wide channels, and for three different water depths shallow, intermediate, and deep.

After evaluating five different methods, only three have been found to meet the first criterion "Accurate representation of important theoretical concepts". These methods have been identified as being the most promising for accurately calculating power. Specifically, they recognize the effects of changing depth, width, and speed. As a result, the Bolt (2003) method, Bolt method with speed correction, and TU Delft method (Jiang, Baart & van Koningsveld, 2022) have been selected for further analysis. Moving forward, the next step for these selected methods is to undergo a validation process using real-world data, which will be

discussed in chapter 5. This process will help to ensure that these methods are not only theoretically sound but also practical and effective in real-world conditions.

5. Real-world test case

This chapter will present the results from the simulations in the real-world test case, for the three most promising methods as they were derived from the previous chapter. Firstly, the effectiveness of Bolt (2003) method, Bolt method with speed correction and TU Delft method (Jiang, Baart & van Koningsveld, 2022) will be validated with real delivered power measurements in order to assess the power-speed relationship. Secondly, these three methods will be tested in the presence of currents to examine the current influence in power-use. The implementation was achieved by computing the fuel consumption for upstream and downstream sailing and was validated with real fuel-use data. For the power test (1st round) a motor vessel M6 was used while for the current influence test (2nd round) a pushed and a coupled convoy were simulated.

In Section 5.1 the results of the comparison process between measured and real power for the three selected methods will be shown. Moving on Section 5.2, the fuel consumption results will be used in order to test how the three methods perform in case of the presence of current flows. Concluding with section 5.3 the best practice(s) validated in two ways, will be introduced.

5.1. Three methods tested by real power-speed data of a single barge

This section will be handled the power estimation results as they were computed from Bolt, Bolt with speed correction and TU Delft methods. The following three subsections will illustrate the comparison process between the estimations the measurements through plots while the tables will present the results for the speed range of 1.5-5 m/s.

5.1.1. Bolt method

In this section, the Bolt (2003) method is used to compute the delivered power of an M6 motor vessel in a narrow waterway for three distinct water depths, namely 3m, 5m, and 10m. The acceptable deviation rate was determined equal to 20% due to several uncertainties that are included in the method (main engine & propeller characteristics). The delivered power results obtained from the Bolt (2003) method are presented in Figure 5.1.1 (left), whereas the corresponding results acquired from real-world data are displayed in the right figure.

The results presented initially in the study indicate the shallow water condition, which is highlighted with a pink line in both graphs. To evaluate the accuracy of the estimated delivered power results, the differences between the estimated and real-world data were calculated and summarized in Table 5.1. The last line of the table represents the deviation rate. The analysis is focused on sailing speeds of 2.5m/s, 3m/s, and 3.5m/s, which are considered the most indicative for sailing in shallow water. The results obtained from the comparison show a good correlation between the estimated and real delivered power results for these sailing speeds indicating acceptable deviation rate within 20%.

The second scenario depicted in the figure corresponds to intermediate water conditions, where the delivered power decreases as the water depth increases. This trend is evident in both estimated and actual values, as can be seen by the purple lines. The results of this scenario are presented in Table 5.2, showing a relatively high deviation rate, with differences amounting to approximately 25%-50%. An exception is shown for sailing speeds of 2.5m/s as

the deviated rate is around to 3% but cannot prove the reliability of the method for this water depth.

The last case that is studied corresponds to deep water conditions and is illustrated with the dark red line. The trend of reduced delivered with increasing water depth is still obvious and in 10m. This reveals that Bolt (2003) method considers the sensitivity in depth variation. Also, the real power data indicate the same dropping trend as the previous two cases, and this could be a first indicator for the accuracy of the method. For that case the results are summarized in Table 5.3 with higher deviations rates compared to intermediate and shallow case, which are reach up to 60%. This 60% is out of the upper limit of 20% a fact shows that the reliability of the method in deep water conditions drops.

Considering the analysis for each water depth, the Bolt (2003) method is capable of predicting the delivered power of vessels in shallow water conditions and between a specific speed range from 2.5m/s up to 3.5m/s. For higher water depths the accuracy of the method reduced significantly as it was proved from the measured or real values.

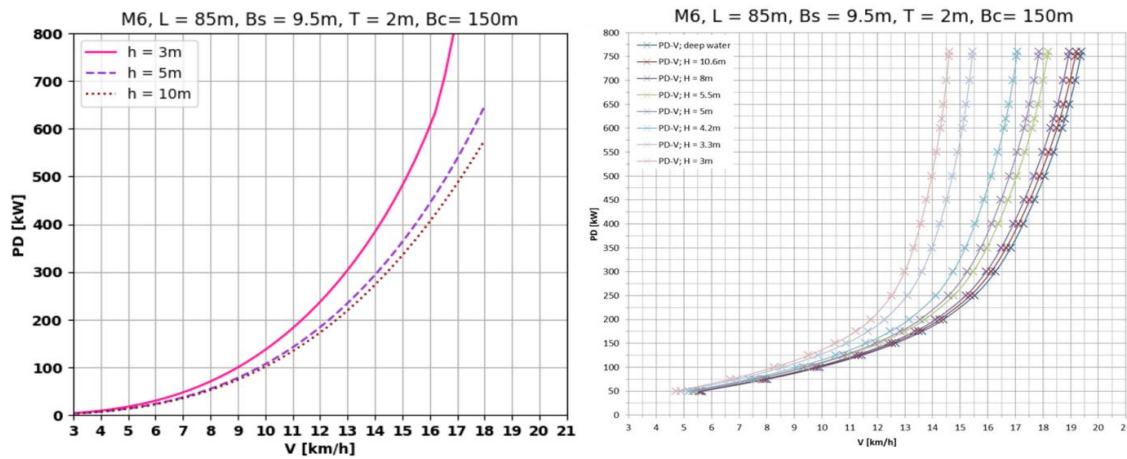


Figure 5.1.1: Comparison between estimated delivered power (Bolt method) & measured power data (Simic & Radojic, 2013; MoVe IT!2014)

Delivered Power h=3m Bc=150m [kW]	V=1.5 [m/s]	V=2 [m/s]	V=2.5 [m/s]	V=3 [m/s]	V=3.5 [m/s]	V=4 [m/s]
Real Power	60	82	112	160	255	675
Estimated Power	26.6	61	119	192	305.5	379.9
ΔP_d [%]	55.6%	25.6%	6.25%	20%	19.8%	43.7%

Table 5.1: Comparison between $P_{estimated}$ & P_{real} for ($h=3m, B_c=150m$)

Delivered Power h=5m Bc=150m [kW]	V=1.5 [m/s]	V=2 [m/s]	V=2.5 [m/s]	V=3 [m/s]	V=3.5 [m/s]	V=4 [m/s]	V=4.5 [m/s]
Real Power	55	70	95	125	165	248	405

Estimated Power	20.44	47.6	91.97	157.97	250.52	375.4	540.3
ΔP_d [%]	63.6%	32%	3.2%	26.4%	51.8%	51.2%	33.3%

Table 5.2: Comparison between $P_{estimated}$ & P_{real} for ($h=5m$, $B_c=150m$)

Delivered Power h=10m $B_c=150m$ [kW]	V=1.5 [m/s]	V=2 [m/s]	V=2.5 [m/s]	V=3 [m/s]	V=3.5 [m/s]	V=4 [m/s]	V=4.5 [m/s]	V=5 [m/s]
Real Power	50	65	85	115	148	220	300	513
Estimated Power	19.56	45.43	87.4	149.3	235.1	348.6	493.83	675.12
ΔP_d [%]	60%	30.7%	2.8%	29.8%	58.8%	58.4%	64.6%	31.6%

Table 5.3: Comparison between $P_{estimated}$ & P_{real} for ($h=10m$, $B_c=150m$)

5.1.2. Bolt method with speed correction

In this section Bolt method with speed corrections is used to calculate the delivered power of a M6 motor vessel sailing in wide waterway of 150m and for three different depths namely, 3m, 5m and 10m. It is mentioned that the acceptable deviation rate was determined equal to 20% due to several uncertainties that are included in the method (main engine & propeller characteristics).

In Figure 5.2.1 the left plot shows the results as they are obtained from the power method, while the right one shows the actual values. In both plots, the pink line represents the shallow situation, and Table 5.4 summarizes the corresponding power results. Comparing the estimated and actual values for the shallow case, the deviation rate varies significantly among the different velocities. Also, in specific sailing speeds a 40% rank difference is appeared.

Moving on to the intermediate case with a water depth of 5m, the results are depicted with a purple line in Figure 5.2.2. It is clear from the plot that when the water depth increases, the delivered power decreases compared to the shallow case. Then by comparing the estimated and actual power values, it is observed that the deviations are significant, with the deviation rate reaching approximately 70% for specific sailing speeds.

Lastly, the deep scenario is also simulated, the results of which are shown with the dark red line. Similar to the previous two scenarios the deviations are still high between measurements and real values. At 10m depth and for sailing speeds of 2.5m/ 3m/s the deviation seems to be within the acceptable 20%. However, this cannot prove the accuracy of the methods since the overall performance varies randomly across the different water depths.

Bolt method with speed corrections and Bolt (2003) method have the same calculation process for the total resistance and the power. The main difference between these two lies in the equations of the return flow velocity. The modified version applies two different equations depending on the ratio of the depth over the draft, one for the shallow case and one for the intermediate and deeper depths. Therefore, this calculation process is more analytical and the relevant return flow results gives higher values. This the reason that, these two methods while the follow the same methodology, when they are compared with the actual values conclude to significant differences.

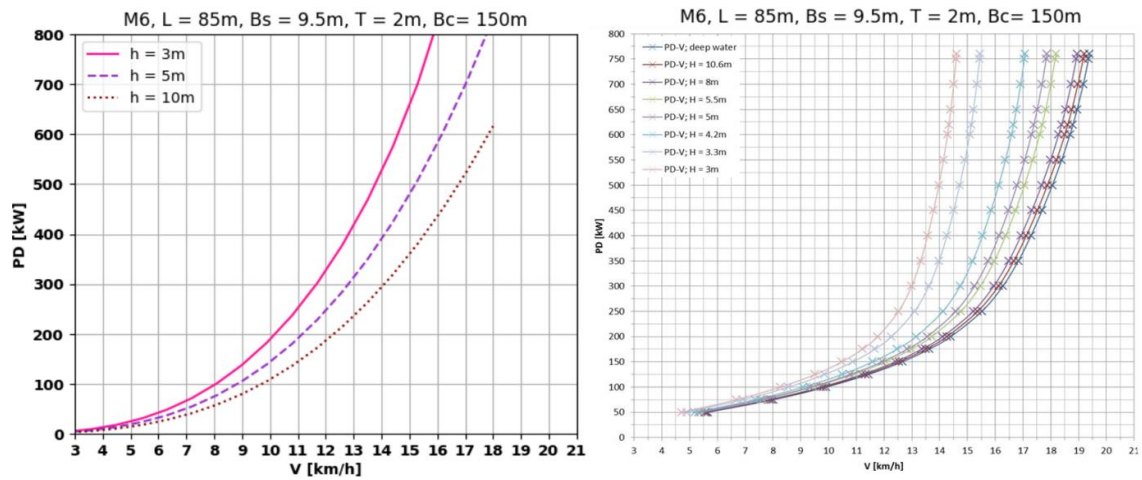


Figure 5.1.2: Comparison between estimated delivered power (Bolt method with speed corrections) & measured power data (Simic & Radojic, 2013; MoVe IT!2014)

Delivered Power[kW] h=3m Bc=150m	V=1.5 [m/s]	V=2 [m/s]	V=2.5 [m/s]	V=3 [m/s]	V=3.5 [m/s]	V=4 [m/s]
Real Power	60	82	112	160	255	675
Estimated Power	30.69	71.44	138	237.5	378.49	574.47
ΔP_d [%]	48.85%	12.87%	23.2%	48.43%	48.43%	14.89%

Table 5.4: Comparison between $P_{estimated}$ & P_{real} for (h=3m, Bc=150m)

Delivered Power[kW] h=5m Bc=150m	V=1.5 [m/s]	V=2 [m/s]	V=2.5 [m/s]	V=3 [m/s]	V=3.5 [m/s]	V=4 [m/s]	V=4.5 [m/s]
Real Power	55	70	95	125	165	248	405
Estimated Power	23.53	36.97	105.46	180.5	284.84	423.8	603.65
ΔP_d [%]	57.22%	47.18%	11%	44.4%	72.66%	70.88%	49.05%

Table 5.5: Comparison between $P_{estimated}$ & P_{real} for (h=5m, Bc=150m)

Delivered Power[kW] h=10m Bc=150m	V=1.5 [m/s]	V=2 [m/s]	V=2.5 [m/s]	V=3 [m/s]	V=3.5 [m/s]	V=4 [m/s]	V=4.5 [m/s]	V=5 [m/s]
Real Power	50	65	85	115	148	220	300	513
Estimated Power	17.77	41.38	79.75	136.4	214.8	318.55	451.14	616.24
ΔP_d [%]	64.46%	36.33%	6.17%	18.6%	45.13%	44.79%	50.3%	20.12%

Table 5.6: Comparison between $P_{estimated}$ & P_{real} for (h=10m, Bc=150m)

5.1.3. TU Delft method

The last method that is tested with the real power values is the TU Delft method (Jiang, Baart & van Koningsveld, 2022). The acceptable deviation rate was determined equal to 20% due to several uncertainties that are included in the method (main engine & propeller characteristics). Figure 5.3.1 on the left plot illustrates the delivered power results as were computed from the method and on the right plot the actual power values as were given.

The first scenario that is analyzed is the shallow water case which is depicted in the pink line. Table 5.7 provides a summary of the power values obtained from both the proposed method and actual measurements, with corresponding deviation rates computed. Especially, it is observed that the divergence of this method at sailing speeds of 2.5m/s, 3m/s, 3.5m/s and 4m/s is significantly low, an event that can lead to increased accuracy of the proposed approach.

The second scenario that is presented in Figure 5.3.1 is the intermediate water depth case. The results for that case are highlighted with the purple line in both plots. Table 5.8 comprehensively shows the power values as they are derived from the TU Delft method (Jiang, Baart & van Koningsveld, 2022) and from the real data. By observing this table, the difference between the measured and the real value falling as the sailing speed increases. It is mentioned that among the three methods, TU Delft method (Jiang, Baart & van Koningsveld, 2022) is the only one that seems to converge relatively well with the actual values in the case of 5m water depth.

Finally, the case of 10m water depth is presented in the next figure, the values of which are indicated with the dark red line. As it is derived from the results in Table 5.9, the deviation between the measurements and the real data is relatively small at high sailing speeds, indicating good agreement between the two. Moreover, comparing TU Delft method (Jiang, Baart & van Koningsveld, 2022) and Bolt (2003) method in deep water, the former performs better at high speeds while that latter at lower velocities.

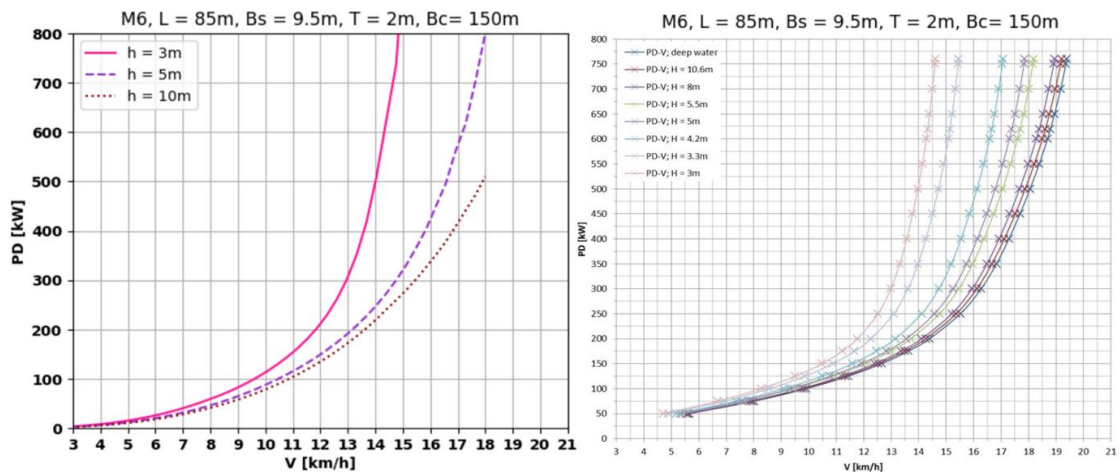


Figure 5.1.3: Comparison between estimated delivered power (TU Delft method) & measured power data (Simic & Radojicic, 2013; MoVe IT!2014)

Delivered Power h=3m	V=1.5 [m/s]	V=2 [m/s]	V=2.5 [m/s]	V=3 [m/s]	V=3.5 [m/s]	V=4 [m/s]

Bc=150m [kW]							
Real Power	60	82	112	160	255	675	
Estimated Power	35	50	91	150	265	635	
ΔP_d [%]	41.6%	39%	18.75%	6.2%	3.9%	5.9%	

Table 5.7: Comparison between $P_{measured}$ & P_{real} for ($h=3m$, $B_c=150m$)

Delivered Power h=5m Bc=150m [kW]	V=1.5 [m/s]	V=2 [m/s]	V=2.5 [m/s]	V=3 [m/s]	V=3.5 [m/s]	V=4 [m/s]	V=4.5 [m/s]
Real Power	55	70	95	125	165	248	405
Estimated Power	30	43	78	110	175	272	445
ΔP_d [%]	45.5%	38.5%	17.8%	12%	6%	9.7%	10%

Table 5.8: Comparison between $P_{measured}$ & P_{real} for ($h=5m$, $B_c=150m$)

Delivered Power h=10m Bc=150m [kW]	V=1.5 [m/s]	V=2 [m/s]	V=2.5 [m/s]	V=3 [m/s]	V=3.5 [m/s]	V=4 [m/s]	V=4.5 [m/s]	V=5 [m/s]
Real Power	50	65	85	115	148	220	300	513
Estimated Power	23	40	68	100	160	240.53	345	507
ΔP_d [%]	54%	38.5%	20%	13%	8.1%	9.3%	15%	1.15%

Table 5.9: Comparison between $P_{measured}$ & P_{real} for ($h=10m$, $B_c=150m$)

5.2. Three methods tested by fuel report with current influence and vessel type variation

This section will handle the performance of the three selected methods to the presence of a current flow. It is mentioned that in the previous comparison process with the real power data the effect of flows is absent.

The results of the simulation of a motor vessel M6 (single operation) are presented in Table 5.10. By comparing the three methods with the real power consumption, only the TU Delft method (Jiang, Baart & van Koningsveld, 2022) shows a better fit. More specifically, in case of an upstream trip the difference in fuel use between TU Delft method (Jiang, Baart & van Koningsveld, 2022) and real value is 62kg, while the difference between Bolt (2003) method and Bolt method with speed correction and the real consumption is amounted to 1643kg. Regarding the downstream trip, the deviation rate between TU Delft method (Jiang, Baart & van Koningsveld, 2022) and the real value is approximately 1.5% in contrast to Bolt (2003) method and Bolt method with speed correction that is approximately 311%.

Based on the fuel use data analysis, it can be concluded that only TU Delft method (Jiang, Baart & van Koningsveld, 2022) is stand out among the other two methods in the presence of a

current flow. Therefore, the TU Delft method(Jiang, Baart & van Koningsveld, 2022) can be regarded as the most reliable and accurate option for predicting the fuel use in case of current flows and for motor cargo vessels.

Methods	Trips	Fuel use [kg]	Real-fuel use [kg]	Δ Fuel use [%]
			M6	
Bolt method	Upstream	7970.8	6609	20.6%
	Downstream	7289.68	1773	311%
	Roundtrip	15260.48	8382	82%
Bolt method with speed correction	Upstream	7970.8	6609	20.6%
	Downstream	7289.68	1773	311%
	Roundtrip	15260.48	8382	82%
TU Delft method	Upstream	6547.44	6609	0.93%
	Downstream	1797.27	1773	1.36%
	Roundtrip	8344.71	8382	0.45%

Table 5.10: Comparison of the fuel consumption of each method with the real fuel used for a motor vessel M6

Based on the analysis of fuel use data for both a pushed convoy during an upstream trip and a coupled convoy during a downstream trip, the results are displayed in Table 5.11. According to the analysis, the variance between the estimated and measured fuel use exceeded the acceptable deviation rate of 20% for Bolt and Bolt with speed correction methods for downstream and round trips. However, the Bolt (2003) method and Bolt method with speed correction showed better fuel prediction for upstream trips but still the deviation rate is higher than 20%. Despite this, after evaluating the performance of all three methods, it is clear that TU Delft method (Jiang, Baart & van Koningsveld, 2022) can be recommended as the most reliable practice in the case of a pushed or coupled convoy.

Methods	Trips	Fuel use [kg]	Real-fuel use [kg]	Δ Fuel use [%]
			Pushed & Coupled convoys	
Bolt method	Upstream	11072.2	8226	35.6%
	Downstream	7659.58	4205	82%
	Roundtrip	18731.78	12431	33.6%

Bolt method with speed correction	Upstream	11072.2	8226	35.6%
	Downstream	7659.58	4205	82%
	Roundtrip	18731.78	12431	33.6%
TU Delft method	Upstream	8550.68	8226	3.9%
	Downstream	4125.46	4205	1.89%
	Roundtrip	12676.15	12431	1.97%

Table 5.11: Comparison of the fuel consumption of each method with the real fuel used for pushed & coupled convoy

Through a comparison of the performance of the three methods in simulating a motor vessel versus a pushed or coupled convoy, important findings were derived. The Bolt (2003) method and Bolt method with speed correction demonstrate a decrease in variance either sailing upstream or downstream in case of simulating pushed or couples convoys. Meanwhile, TU Delft method (Jiang, Baart & van Koningsveld, 2022) shows excellent agreement with the measured data for all the types of inland vessels. Therefore, the performance of Bolt (2003) method and Bolt method with speed correction in the presence of a current flow combined with the different vessel types (single motor barge, pushed/coupled convoys) requires further investigation while TU Delft method (Jiang, Baart & van Koningsveld, 2022) can be applied.

5.3. Selection of the best practice(s)

The aim of this section is to determine the best power estimation method by analyzing the results of two rounds of tests. Three tables have been structured, each representing a different depth condition, to summarize the power results of each method along with their corresponding measurements. These tables provide a comprehensive overview of which method is suitable for power calculation, with a 20% deviation rate from the actual values. Additionally, the fuel-use tests have been taken into consideration to ensure an objective selection process.

5.3.1. Selection based on power-speed results

In Table 5.12 the case of shallow water conditions is presented. In shallow water depths, the shallow phenomena such return flow, ship waves and water level depression are dominant and more intensive. Taking into account the magnitude of these effects, it is recommendable to sail at relative low speeds i.e., 2.5m/s to 4m/s and as it is obvious Bolt (2003) method and TU Delft method (Jiang, Baart & van Koningsveld, 2022) outperform the Bolt method with speed corrections because they show acceptable deviation rate within the 20%(upper limit). There is a considerable variance between the estimated and real power values, particularly at low speeds ranging from 1.5m/s to 2m/s. In actual operating conditions, a ship has a minimum power engine setting that is dependent on the engine characteristics. As a result, when the ship is sailing at very low speeds or when it is moored, the shaft still rotates at a certain designed speed and power is generated accordingly, which is not considered by the power estimation methods that rely on parameters such as sailing speed and water depth. Consequently, the significant deviation observed between the estimated and actual values at

low speeds partially can be justified. However, it is a phenomenon that requires detailed investigation.

ΔP_d [%] h=3m	V=1.5 [m/s]	V=2 [m/s]	V=2.5 [m/s]	V=3 [m/s]	V=3.5 [m/s]	V=4 [m/s]
Bolt method	55.6%	25.6%	6.25%	20%	19.8%	43.7%
Bolt method with speed corrections	48.8%	12.87%	23.2%	48.43%	48.43%	14.89%
TU Delft method	41.6%	39%	18.7%	6.2%	3.9%	5.9%

Table 5.12: Delivered power difference of each method for shallow water conditions

Table 5.13 depicts the deviation rate of three methods together for the delivered power in intermediate water depths. The Bolt and Bolt with speed corrections methods show a significant deviation from the actual power results. The Bolt method with speed corrections presents approximately double difference deviation rate compared to the Bolt (2003) method at sailing speeds between 3m/s and 4.5m/s. This difference is attributed to the return flow equations used in each method. The Bolt method with speed corrections estimates larger return currents than the Bolt (2003) method, resulting in a considerable difference. On the other hand, the TU Delft method (Jiang, Baart & van Koningsveld, 2022) provides an acceptable deviation rate of approximately 15%, especially for sailing speeds between 2.5m/s and 5m/s, which is considered the preferable sailing range in intermediate water depths. In conclusion, TU Delft method (Jiang, Baart & van Koningsveld, 2022) is recommended for the calculation of the power in intermediate water depths.

ΔP_d [%] h=5m	V=1.5 [m/s]	V=2 [m/s]	V=2.5 [m/s]	V=3 [m/s]	V=3.5 [m/s]	V=4 [m/s]	V=4.5 [m/s]
Bolt method	63.6%	32%	3.2%	26.4%	51.8%	51.2%	33.3%
Bolt method with speed corrections	57.2%	47.18%	11%	44.4%	72.66%	70.88%	49.05%
TU Delft method	45.5%	38.5%	17.89%	12%	6%	9.7%	17%

Table 5.13: Delivered power difference of each method for intermediate water conditions.

The Table 5.14 shows the differences in the delivered power for deep water conditions. Based on the results the TU Delft method (Jiang, Baart & van Koningsveld, 2022) presents the lower deviation from the real values, almost for the whole range of the sailing speeds. In deep water higher sailing speeds are preferred, so TU Delft method (Jiang, Baart & van Koningsveld, 2022) could be suggested as the most suitable in deep water depths.

ΔP_d [%] h=10m	V=1.5 [m/s]	V=2 [m/s]	V=2.5 [m/s]	V=3 [m/s]	V=3.5 [m/s]	V=4 [m/s]	V=4.5 [m/s]	V=5 [m/s]
Bolt method	60%	30.7%	2.8%	29.8%	58.8%	58.4%	64.6%	31.6%
Bolt method with speed corrections	64.5%	36.33%	6.17%	18.6%	45.13%	44.79%	50.3%	20.12%
TU Delft method	54%	38.5%	20%	13%	8.1%	9.3%	15%	1.15%

Table 5.14: Delivered power difference of each method for deep water conditions

Table 5.12 summarizes the final results for the three most promising methods for shallow water, excluding current flow effect. The Bolt (2003) method and the TU Delft method (Jiang, Baart & van Koningsveld, 2022) both show an acceptable percentage of deviation, making them suitable for calculating required power. The Bolt (2003) method is less complex than the TU Delft method (Jiang, Baart & van Koningsveld, 2022), requiring fewer input data and equations, and is therefore recommended for quick power calculations. However, in cases where high accuracy is essential, using both methods may be beneficial.

The Tables 5.13 and 5.14 provide the results for the three methods used to estimate power in intermediate and deep water depths. These methods were compared based on their variances from the real data. After analyzing the data presented in the tables, it was concluded that the TU Delft method (Jiang, Baart & van Koningsveld, 2022) had the lowest variance and thus was the most accurate method for power estimation in these water depths. This means that the estimates produced by the TU Delft method (Jiang, Baart & van Koningsveld, 2022) were closer to the actual values than the other two methods.

5.3.2. Selection based on fuel-use results

Observing the fuel consumption estimations in Section 5.2, TU Delft method appears to be the most appropriate approach for estimating fuel-use in the presence of current flow. This method is suitable for motor cargo vessels as well as pushed or coupled convoys. Nonetheless, it's essential to note that the Bolt and Bolt with speed correction methods demonstrated significant discrepancies in simulating motor vessels and pushed/coupled convoys. The observed deviations between the estimated and measured values for the different vessel types imply that additional fuel use data is necessary for further investigation.

5.4. Summary

The purpose of the aforementioned analysis results focusing on the selection of the best practice(s). Starting with Section 5.1 the power estimations as they were derived from each method presented and analyzed while in Section 5.3.1 the best practice according to power data was selected. Therefore, for shallow water conditions and in the absence of currents both Bolt method and TU Delft method are suggested. In case of intermediate and deep water conditions only TU Delft method (Jiang, Baart & van Koningsveld, 2022) can be proposed since the variance from the real values is lower than 20%. The analysis in Section 5.2 focused on the effect of current flows on sailing into inland channels. The results indicated that only the TU Delft method (Jiang, Baart & van Koningsveld, 2022) is recommended for power and fuel-use

calculations when accounting for currents. This is because the TU Delft method (Jiang, Baart & van Koningsveld, 2022) demonstrates significantly lower deviation from the real fuel use compared to other methods.

III Discussion, conclusions & recommendations

6. Discussion Part A: Application of the best practice(s) in shallow water depth

In this section, the Bolt (2003) method and the TU Delft method (Jiang, Baart & van Koningsveld, 2022) that were suggested as the best practices for shallow water will be applied to two motor vessel types, an M6 and an M8. It is mentioned that both methods are suggested for shallow water application without current flows while only TU Delft method is suggested in case of flows. In this chapter only an analysis of the different estimated results will be presented without currents. More specifically these two methods will be used to calculate the resistance and the power in shallow water depth, both in narrow and wide waterways. In Sections 6.1 and 6.2 the results for the motor vessels M6 and M8 will be presented respectively.

6.1. Resistance and Power results for a motor vessel M6 (CEMT IVa)

In this paragraph, it will be discussed the resistance and power estimates obtained using the Bolt (2003) method and the TU Delft method (Jiang, Baart & van Koningsveld, 2022). Both methods showed acceptable performance according to "Real-world test case", but they differ in their approach to calculate total resistance and estimating brake power. Consequently, while both methods yield reasonable calculations, there are deviations between the total resistance results and the estimated brake power results.

Tables 6.1 and 6.2 illustrate the results of an M6 motor vessel in a narrow waterway according to Bolt (2003) method and TU Delft method (Jiang, Baart & van Koningsveld, 2022) respectively. Based on the results only friction resistance, total resistance and the different power components can be compared as they are the only common parameters between the two methods. Originally by observing the friction resistance, in Bolt (2003) method (Table 6.1) the maximum value that can be reached is approximately 17kN while in TU Delft method (Table 6.2) the maximum value is around to 10kN. Based on the simulation results, it was observed that the Bolt (2003) method predicts a significantly higher total resistance than the TU Delft method (Jiang, Baart & van Koningsveld, 2022) for sailing speeds between 1.5 and 3 m/s. This difference was found to be almost double in magnitude. It is important to note that for the specific ship type considered and shallow water conditions, speeds exceeding 2.8 m/s cannot be attained according to Bolt (2003) method. The Bolt (2003) method incorporates a limit speed, which indicates the maximum sailing speed that can be achieved with the corresponding power. Beyond this limit speed, any further increase in speed does not result an increase in power requirements. On the other hand, the TU Delft method (Jiang, Baart & van Koningsveld, 2022) uses a depth Froude number criterion to determine the maximum attainable velocity, ensuring that the velocity remains in the subcritical region. Interestingly, the simulation results show that the TU Delft method (Jiang, Baart & van Koningsveld, 2022) permits a higher limit speed of around 3.5 m/s compared to the Bolt (2003) method. The difference between the two methods can be attributed to the different speed theories utilized in the simulations. Nevertheless, it is important to acknowledge that, when considering a mathematical perspective, the TU Delft method is capable of computing power and resistance for a velocity of 3.5m/s. However, it is crucial to recognize that this theoretical feasibility does

not align with practical reality. This discrepancy becomes evident through the outcomes of simulations, as illustrated in Figure 4.5.1, where the graphical representations exhibit irregularities and inconsistencies, deviating from a consistent pattern and therefore results reached up to 3m/s. The same behavior with the resistance is obvious in the brake power results. According to Bolt (2003) method the maximum propulsive power is 230kW while with TU Delft method (Jiang, Baart & van Koningsveld, 2022) the power amounted to 220kW.

h/T [-]	1.5	1.5	1.5	1.5
V [m/s]	1.5	2	2.5	3(2.8)
Rf [kN]	4.83	8.42	13.16	16.79
Rp [kN]	3.2	5.7	8.9	11.24
Rz[kN]	1.36	2.61	4.55	6.27
Rtot[k]	9.39	16.73	26.62	34.3
Pb[kW]	32.66	78.4	158.6	232.95

Table 6.1: Resistance and Power results in narrow waterway(M6, Bc=50m) - Bolt method

h/T [-]	1.5	1.5	1.5	1.5	1.5
V [m/s]	1.5	2	2.5	3	3.5
Rf [kN]	2.66	4.48	6.72	9.35	12.36
R_{viscous} [kN]	3.27	5.5	8.25	11.5	15.18
R_{APP} [kN]	0.33	0.56	0.84	1.17	1.54
R_w [kN]	0	0	0	0.15	1.93
R_{res}[kN]	0.88	1.59	2.44	4.1	7.47
Rtot[kN]	4.48	7.66	11.54	16.85	26.12
Pb[kW]	30.2	68.7	129.4	226.7	410.2

Table 6.2: Resistance and Power results in narrow waterway(Bc=50m) – TU Delft method

Tables 6.3 and 6.4 present the results of the Bolt (2003) method and TU Delft method (Jiang, Baart & van Koningsveld, 2022) calculations for a motor vessel class M6 operating in a wide waterway. Specifically, the friction resistance in the Bolt (2003) method shows a decrease when compared to the narrow waterway case, while the TU Delft method yields the same friction resistance results for both narrow and wide waterways. This difference is due to the use of limit speed, which accounts for changes in width in the Bolt (2003) method but not in the TU Delft method (Jiang, Baart & van Koningsveld, 2022) that works with Karpov's correction theory. The resistance components in TU Delft approach, like friction resistance, exhibit similar estimations across the different width conditions in the waterways. It should be noted that the resistance calculations in this theory do not consider the impact of channel width on the results. However, the width effect is incorporated in the power estimations by using a hydrodynamic coefficient that depends on the depth, width, and sailing speed. However, the accuracy of the TU Delft method (Jiang, Baart & van Koningsveld, 2022) is not compromised, as it uses Karpov's correction theory to calculate velocities in shallow waters and this theory does not consider the width variation for velocity determination. Also, as it has already mentioned in the narrow case for the TU Delft method (Jiang, Baart & van Koningsveld, 2022), the mathematical approach results in velocities up to 4m/s in this condition, but in reality, the maximum velocity is 3.5 m/s. Regarding the estimated brake power, the results are varying in each method, with Bolt method to predict higher power.

h/T [-]	1.5	1.5	1.5	1.5	1.5
V [m/s]	1.5	2	2.5	3	3.5
Rf [kN]	4.8	8.22	12.45	17.5	23.32
Rp [kN]	3.2	5.7	8.9	11.24	11.24
Rz[kN]	0.4	0.78	1.35	2.21	3.63
Rtot[kN]	8.42	14.69	22.7	32.53	44.4
Pb[kW]	29.23	67.98	131.26	225.73	326.8

Table 6.3: Resistance and Power results in wide waterway(M6, Bc=150m) - Bolt method

h/T [-]	1.5	1.5	1.5	1.5	1.5	1.5
V [m/s]	1.5	2	2.5	3	3.5	4
Rf [kN]	2.66	4.48	6.72	9.35	12.36	15.75
R_{viscous} [kN]	3.27	5.5	8.25	11.5	15.18	19.34
R_{APP} [kN]	0.33	0.56	0.84	1.17	1.54	1.97
R_w [kN]	0	0	0	0.15	1.93	19.65
R_{res}[kN]	0.88	1.59	2.44	4.1	7.47	13.68
Rtot[kN]	4.48	7.66	11.54	16.85	26.12	54.6
Pb[kW]	19.61	44.68	84.1	147.4	266.6	637.1

Table 6.4: Resistance and Power results in wide waterway(Bc=150m) – TU Delft method

6.2. Resistance and Power results for a motor vessel M8 (CEMT Va)

In Tables 6.5 and 6.6 a motor vessel M8 operating in shallow and narrow waterways is presented. Friction resistance according to Bolt (2003) method predicts higher and, in some cases double values compared to TU Delft method while it gives constant friction when the limit speed is reached. Regarding the total resistance calculations, the deviations are significant between the two methods due to different components that considered from each method. Notably, Bolt (2003) method developed according to classical resistance approach where the total resistance was split to three main components in contrast to TU Delft method (Jiang, Baart & van Koningsveld, 2022) that followed the analytical approach. It is highlighted that the same behavior in calculations of the total resistance is shown also in the corresponding calculations of the motor vessel M6. The main difference in the narrow waterway between the two types of motor cargo vessels, lies in the variations in the maximum attainable velocity. Specifically, for an M6 the velocity is around to 2.8m/s while for M8 the value amounted to 3 m/s. These variations attributed to the ship dimensions and the water depths that were considered in the limit speed equation and in turn in the calculations. The brake power estimations differ for two reasons. Firstly, the power efficiencies used in each method are different, with TU Delft method (Jiang, Baart & van Koningsveld, 2022) to use appropriate shallow water efficiencies. Secondly, variations in the total resistance further amplify these discrepancies.

h/T [-]	1.5	1.5	1.5	1.5
V [m/s]	1.5	2	2.5	3
Rf [kN]	7.9	13.8	21.53	31.45
Rp [kN]	5.19	9.23	14.43	20.77
Rz[kN]	2.7	5.09	8.62	13.8

Rtot[kN]	15.84	28.15	44.57	66.05
Pb[kW]	56.79	135.89	272.83	495.2

Table 6.5: Resistance and Power results in narrow waterway(M8, Bc=50m) – Bolt method

h/T [-]	1.5	1.5	1.5	1.5	1.5
V [m/s]	1.5	2	2.5	3(3.25)	3.5
Rf [kN]	4.11	6.95	10.4	14.5	19.2
R_{viscous} [kN]	5	8.4	12.6	17.6	23.3
R_{APP} [kN]	0.51	0.87	1.3	1.82	2.4
R_w [kN]	0	0	0	0.08	0.87
R_{res}[kN]	1.75	3.15	4.9	7	11.06
Rtot[kN]	7.3	12.44	18.9	26.55	37.7
Pb[kW]	40.74	93	176.9	297.8	492.9

Table 6.6: Resistance and Power results in narrow waterway(M8, Bc=50m) – TU Delft method

In the next Tables 6.7 and 6.8 the resistance and power results from a motor vessel M8 in a wide and shallow water waterway according to Bolt and TU Delft methods are presented respectively. Comparing the friction and total resistance Bolt (2003) method estimates higher values compared to the corresponding values from TU Delft method (Jiang, Baart & van Koningsveld, 2022) but lower between narrow and wide channels. The deviations in the friction results attributed to the different sailing speeds and friction coefficients that were used from each method. Specifically, TU Delft method (Jiang, Baart & van Koningsveld, 2022) based on friction coefficient that takes into account shallow water effects while Bolt method simulates with classic formula according to ITTC57. Finally, by observing the brake power results between the two methods, significant variation seems in the values. One noticeable distinction is that the Bolt method can achieve the maximum speed limit in wide channels with more power compared to the TU Delft method (Jiang, Baart & van Koningsveld, 2022) for a particular ship and channel.

h/T [-]	1.5	1.5	1.5	1.5	1.5
V [m/s]	1.5	2	2.5	3	3.5(3.65)
Rf [kN]	7.64	13.06	19.8	27.8	37.13
Rp [kN]	5.19	9.23	14.43	20.77	28.28
Rz[kN]	0.79	1.49	2.5	3.95	6.07
Rtot[kN]	13.63	23.78	36.73	52.56	71.49
Pb[kW]	47.88	111.34	215.01	369.22	585.82

Table 6.7: Resistance and Power results in wide waterway(M8, Bc=150m) – Bolt method

h/T [-]	1.5	1.5	1.5	1.5	1.5	1.5
V [m/s]	1.5	2	2.5	3	3.5(3.8)	4
Rf [kN]	4.11	6.95	10.4	14.5	19.2	25.5
R_{viscous} [kN]	5	8.4	12.6	17.6	23.3	29.75
R_{APP} [kN]	0.51	0.87	1.3	1.82	2.4	3.06
R_w [kN]	0	0	0	0.08	0.87	8

R_{res}[kN]	1.75	3.15	4.9	7	11.06	18.4
R_{tot}[kN]	7.3	12.44	18.9	26.55	37.7	59.2
P_b[kW]	26.47	60.46	114.9	193.5	320.4	575.3

Table 6.8: Resistance and Power results in wide waterway(Bc=150m) – TU Delft method

7. Discussion Part B

The comparison process used a limited amount of real power and fuel data, which meant that a deviation rate of 20% was defined as acceptable. While this deviation may initially seem significant for a reliable selection of a power method in inland shipping, it was based on two key factors: the limited amount of real data available and the uncertainties inherent in resistance-power methods. On one hand, the limited real data permitted an evaluation process that enabled us to draw conclusions regarding the most suitable power estimation method for inland shipping. However, on the other hand, if more data were become available in the future, these deviation rate could be refined, and the conclusions that would be drawn may need to be updated accordingly. Furthermore, a number of variables such as the type and year of construction of the main engines, the propeller characteristics, the geometry, and the real-wetted surface area can strongly influence the reliability of resistance predictions and hence power estimation. Therefore, while a 20% deviation rate may seem large, it was considered a logical choice, given the limitations we had to contend with.

The selection of an appropriate representative and logical deviation rate for evaluating the accuracy of power estimation methods is dependent on the intended use of the methods. There is no fixed formula or guideline specifying an ideal value such as 20%, 5%, or 200%. Rather, the acceptable deviation rate is determined by the specific case being investigated, its constraints and limitations, as well as the studied period. For a general annual estimate, a deviation of 20% or more may be acceptable. However, for a more precise calculation of the propulsive power, it is advisable to employ specific strategies and aim for a smaller deviation rate. By doing so, we can increase the accuracy of our estimation and obtain more reliable results. Therefore, it's important to consider the intended use of the estimate and apply the appropriate selection and methodology accordingly.

Ships require power for two main purposes: hotel systems and propulsion. Hotel electric power (HEP) refers to the electricity needed to operate systems on board a ship other than propulsion, such as lighting, refrigeration, and climate control. The hotel electric power is also present when the ship is moored, or it is in stationary mode or slow at extremely low speeds. In general, the HEP required for inland ships is relatively low due to their smaller scale and the fewer activities taking place on board. However, as ships become larger, the HEP component becomes more significant, and its percentage in the total power consumption needs to be carefully considered. For the purpose of this report, we did not analyze the HEP component, as it is generally not a significant factor in inland shipping. Our focus was instead on the power required for propulsion, which is crucial for the movement of the ship through water. Therefore, when comparing measured and simulated values of delivered power at low sailing speeds, there can be significant deviations due to the difference in focus between the measurements, which include both propulsive and hotel power, and the simulations, which focus only on propulsive power. These deviations are particularly more pronounced at low speeds, as the propulsive power needed is lower in contrast to higher speeds where the propulsive load is a more significant portion of the total power consumption, leading to a larger difference between measured and simulated values in low speeds.

The first round of testing, the "Academic test case" was conducted to assess the performance of five different methods. The selection of the most promising methods was primarily based on the evaluation of the brake power. The reason behind this choice lies in the fact that brake power provides a comprehensive measure as it takes into account transmission efficiency (shaft losses) and gearing efficiency. Since the five methods that were examined have varying

values of these power efficiency coefficients, the differences in power efficiencies among them lead to variations in their brake power results. Therefore, brake power can be considered an objective and reliable indicator to assess the performance of each method. By utilizing brake power as the primary indicator, the evaluation process can account for the differences in power efficiencies and provide a relative accurate comparison of the methods' performances.

The simulations in the "Real-world test case (1st part: Delivered power comparison)" focused on evaluating the accuracy of the different methods for estimating delivered power, using real data available for a specific type of vessel. The available data, which were based on full-scale measurements, provided information on the performance of a motor cargo vessel, the MV Herso, that operates on the route between Budapest and Regensburg on the Upper Danube River. Due the available power data, the simulations were conducted solely on motor vessels of class IVa (M6) and were limited to evaluating the performance of the methods on how accurate predict the delivered power compared with measurements. This selection of the vessel type and the delivered power was made in order to ensure that the simulations were as realistic and representative as possible, given the available data.

The real world power-speed relation data in the diagram (Appendix E, Figure E-1) starts at the minimum power of 50 kW with sailing speeds of around 5 km/h. This kind of limitation consequently lead the comparison process in the "Real-world test case" to be conducted for a specific range of velocities and not smaller than 5 km/h. Therefore, the velocity range has as follows:

- Shallow water depth, comparison from 1.5m/s to 4m/s
- Intermediate water depth, comparison from 1.5m/s to 4.5m/s
- Deep water depth, comparison from 1.5m/s to 5m/s

The second part of the "Real-world test case" evaluate the performance of each of the three methods in the presence of an ambient flow (current flow). To achieve this comparison the fuel-use report was used. This report includes the fuel consumption both for a motor cargo vessel (single operation) and for a pushed/coupled convoy (motor vessel & lighter). The simulations were conducted using the average water level as it can be considered the most representative level for the waterways. It is mentioned that the performance of each method in terms of pushed/coupled convoys was conducted only through the fuel use, as they were the only available real data.

The three selected methods as they were derived from the "Academic test case" also evaluated in terms of the presence of current flows. For this evaluation process, fuel-use data were used. The fuel report indicated differences in fuel consumption between upstream and downstream trips. Specifically, the upstream fuel consumption was associated with a delivered power of 620 kW. This delivered power value corresponds to 81.5% of the nominal brake power at Maximum Continuous Rating (MCR, 780 kW), which the ship-owner reported to be the engine's most economic operating range in terms of specific fuel consumption. According to that statement, both M6 vessel(single operation) and the pushed convoy (M6 & lighter) were compared only for this power value in case of downstream trips and for the corresponding speed of 16 km/h for all river stretches except for the Gabcikovo canal where the speed is 12 km/h for downstream trips.

8. Conclusions & Recommendations

8.1. Conclusions

Looking back on the research questions defined in Chapter 1, it will be addressed how these questions are answered. Specifically, the thesis focused on the main research question:

“What resistance and power related estimation methods are available in literature, how can objectively evaluate how these methods perform and how can these evaluation results be used to provide Rijkswaterstaat with the best practices?”

To address the main research question, five sub-questions formulated that we wanted to answer when defining the main objectives of this thesis. These five questions will be dealt with to draw the most important conclusions resulting from this research study.

“Sub-question 1: What methods are available in literature for the estimation of the total resistance and the propulsive power and how these resistance methods consider the resistance components?”

To answer this question a comprehensive analysis was on the available literature methods and how they determine their resistance components was conducted. According to that, it was derived that the friction-viscous resistance and the wave resistance are the main components for the inland ships that constitute the total resistance. Following that, three approaches were developed to explain how the total resistance is divided into different components and the literature methods were classified accordingly. It was found that most of the methods, such as the Karpov theory (van Terwisga, 1989), Gulddammer (1974) method and Bolt (2003) method, accounted for the main resistance components, use the first approach where the viscosity effect did not consider separately from the water friction. In the second approach, where the viscosity effect was treated as a factor multiplied by the friction coefficient, the ITTC theory (Morrall, 1970) was based. In the third approach the Holtrop and Mennen (1982) method and TU Delft method (Jiang, Baart & van Koningsveld, 2022) are included, that consider the multiply resistance components and the viscosity effect separately. By comparing the 2nd and the 3rd approaches, it was concluded that the TU Delft method was selected to further investigated since it covers the viscosity effect and simultaneously considers the multiply resistance terms in contrast to the other approaches. The purpose of this analysis and classification was to evaluate whether the inclusion of the main resistance components (1st & 2nd approaches) or the use of several resistances (3rd approach) leads to improved reliability and greater accuracy of the results. Indeed, it was found from the simulations the results of which were analytically described in Sub-questions 4 and 5, that the distinction of the total resistance into more components such as transom or appendage resistance, is one factor among others that improves method's reliability.

“Sub-question 2: What are Backer van Ommeren recommendations to improve Bolt method, and to what extent these recommendations will indeed improve Bolt method?”

After proposed equations for estimating return flow, water level drop, waterway characterization, and substitution of coefficients, a literature study was conducted based on Backer suggestions and comments. Two methods were derived, the first one is "Backer method" while the second is "Bolt method modified by Backer". By means of the literature study, the first method "Backer method" was analyzed. The method demonstrated accurate prediction of both resistance and brake power for the narrow case across the three different water depths. More specifically, by considering a specific sailing speed, both parameters

(resistance and power) exhibited a decrease with increasing water depth. In contrast, when considering a wide waterway and holding the water depth constant, the accuracy of the method was reduced as the method does not account for the effect of width. Consequently, the estimated values for resistance and brake power were very similar, even when comparing for a specific sailing speed. Our analysis showed that the method performed equally well in both M6 and M8 vessels, regardless of the different ship dimensions and water depths. However, the accuracy of the method was reduced moving from narrow to wide channels, a fact that was verified by both ship simulations. Therefore, "Backer method" is not widely applicable for resistance and power estimations due to its width limitation and cannot be suggested for further use by Rijkswaterstaat.

The Backer method was developed in python notebook, and it includes a formula that needs iterations to compute the return flow (Schijf, 1949). The Newton Raphson method was used in order to perform the calculations. During the simulations of an M6 and an M8 motor vessel, it was observed that for specific values of the depth, the width and for sailing speeds ranging within 0m/s-5m/s, the return flow can be computed. Specifically, when the limit speed is reached the equation of the return flow cannot converge, indicating that the maximum return flow is computed and simultaneously the algorithm stop running. So, for an M6 vessel in narrow waterways the maximum sailing speed was found equal to 2.8m/s while for wide waterways the corresponding value amounted to 3.5m/s. Regarding, an M8 vessel sailing in narrow channels the maximum permitted sailing velocity is 3m/s while for wider waterways the sailing speed is 3.5m/s. The aforementioned speed values, indicate the maximum attainable velocities per ship type and per waterway conditions and simultaneously present that if the velocity is larger, the return flow equation does not converge anymore. It is mentioned that the limit speed depends on ship and channel dimensions, so variations in these parameters directly change the result (different limit speed between M6 & M8). Therefore, it is recommended to conduct a preliminary investigation to determine the appropriate speed and depth range as well as the channel, given the ship type in order to compute the limit speed and the return flow velocity. Therefore, this method involves some trial and error until the optimal values are identified and the simulations are conducted. Additionally, it is obvious that the maximum sailing velocity at a wide channel for both types of motor cargo vessels is the same, an evident that indicates the weakness of the method in resistance and power estimations in wide waterways.

According to the literature study on the Backer comments, a second method "Bolt method modified by Backer" was developed. Variations in width and depth were considered, as they impact the encountered resistance and required propulsive power differently. However, the performance of the method presented reduced accuracy in estimating resistance as the values were nearly identical across all three water depths when a specific sailing speed was considered. The same trend was evident and more pronounced in the results for the brake power. The method's limitations lie in its inability to accurately account for variations in both width and depth, making it unsuitable for determining power measurements in inland waterways. Therefore, it is not recommended for use in inland shipping where variations in width and depth are common. It is mentioned that Backer van Ommeren's proposed equations have been found to exhibit poor accuracy compared to the original theory, suggesting that they do not result in a substantial improvement.

"Sub-question 3: What are the available options to improve the current power method in terms of resistance and propulsive power estimation for inland ships?"

The calculation of the resistance and the propulsive power of inland ships can be considered a complex process due to the challenges in accurately predicting the impact of shallow water phenomena on the sailing inland ships. According to seven Backer van Ommeren comment "use of alternative formulations or application of another method for the power estimation", two additional methods were investigated.

First the "Bolt method with speed correction" was developed. As it has already mentioned, two return flow equations were used, one that predict the return flow in shallow water depths and a second one for the intermediate and the deeper water depths. The results in terms of total resistance and required power were higher compared to the original Bolt (2003) method. Nevertheless, the width and the depth variations were considered from the method since the estimated values(resistance and power) are varying across the water depths and from narrow to wide waterways. Overall, from a theoretical perspective, the Bolt method with speed correction presented acceptable performance, as it takes into account the various factors that affect a ship's resistance and power requirements.

The second method that was selected to study from the literature is the TU Delft method (Jiang, Baart & van Koningsveld, 2022). It is an entirely different method in terms of the calculation of the shallow velocity and the resistance components. Regarding the performance of the method in estimating resistance and power, it showed to effectively recognize variations in both width and depth. Notably, the values indicate a decreasing trend in resistance and power estimations as the depth or width of the waterway increases, for a given sailing speed.

The validity of these aforementioned methods combined with the Bolt (2003) method, the Backer method and the Bolt method modified by Backer is examined in two rounds of tests, the Academic test case and the Real world test. The simulation and the results were presented in the follow question.

“Sub-question 4: How can the performance of these methods best be compared and what criteria should be applied to enable the objective selection of the most promising methods?”

The performance of the five studied methods that already mentioned was examined and compared in two stages. To accurate evaluate the practical use of these methods three criteria were defined and important findings were derived.

1. Accurate representation of important theoretical concepts
2. Accurate results compared to real-world power and fuel use data considering the acceptable deviations rate that was determined to 20%
3. Practical applicability

The five methods were observed for their performance in recognizing the variation in water depth for a narrow fairway. All methods showed a decrease in required brake power with increasing depth. To further test depth variation, simulations were conducted in a wider channel. Results showed that only the Bolt method, Bolt method with speed corrections, and TU Delft method recognized the different depths in wider channels, as their power values were lower compared to the narrow channel.

The performance of the methods was also tested in terms of varying width. Comparing the brake power results between a narrow and wide waterway for shallow water depths and a

specific sailing speed, Backer method and Bolt method modified by Backer showed little difference in power results with the former to perform slightly better results. However, Bolt (2003) method, Bolt method with speed corrections, and TU Delft method (Jiang, Baart & van Koningsveld, 2022) appeared to clearly consider the width variation. The academic tests for an M8 vessel showed similar performance results to an M6 vessel, confirming the selection of these three methods.

The real-world test case was divided into two parts, where simulations were conducted for a wide waterway with varying water depths - shallow, intermediate, and deep. In the first part of the test, a motor vessel M6 was simulated, while in the second part, both an M6 vessel and a pushed/coupled convoys were considered. The selection of vessel types for each case was based on the available data and is explained in Chapter 7, which discusses the limitations of the real data. In the first part, the performance of the three selected methods was validated using the delivered-power data set available. The three methods were examined to determine their accuracy in predicting the required power. In the second part of the Real-world test case, the performance of the three methods was evaluated in the presence of an ambient flow. The validation was carried out using fuel-use data.

The results indicate that the Bolt and TU Delft methods are effective in accurately predicting the required brake power for inland ships operating in shallow water conditions. Despite this, for resistance and power estimations at intermediate and deeper depths, only the TU Delft method (Jiang, Baart & van Koningsveld, 2022) is recommended as its variance is lower than 20% for speed ranges 2.5-4.5m/s and 2.5-5m/s respectively. In shallow water conditions, both methods showed acceptable deviations from the measurements, with a maximum deviation rate of 20% for sailing speeds ranging from 2.5m/s to 4m/s. However, at lower sailing speeds of 1.5m/s to 2m/s, the deviation rate was observed to be higher than 20%. This can be attributed to two factors. Firstly, there is increased interaction between the sailing vessel and the boundary layer, which requires further investigation. Secondly, the minimum engine power setting that each vessel includes was not taken into account by the methods. Further analysis could be conducted on this phenomenon in shallow water if additional power data sets were made available.

Based on the performance of the three methods in the presence of a current flow and simulating a motor cargo vessel, a pushed and a couple convoy, it was observed that only the TU Delft method provided an acceptable deviation rate in predicting fuel use. In contrast, both the Bolt and Bolt with speed correction methods demonstrated a significant deviation from the actual fuel use, indicating a lower level of accuracy in predicting power when a current flow is considered. Therefore, TU Delft method can be suggested as a best practice in power estimations considering the current flow effect.

The last criterion that was used to evaluate the performance of the promising methods is related with the level of applicability (easy use) of the method and the required input data for the simulations. A method that uses fewer equations to accurately predict brake power is preferable to one that requires solving more equations for achieving the same level of accuracy. Moreover, a method that based on algebraically formulas and simultaneously yields accurate results is favored. Finally, it is important to use simple input data for conducting simulations, as the use of complex parameters such as propeller characteristics or engine RPM may enhance the accuracy of a method, but obtaining such data can be very challenging. Considering the aforementioned information, it has been observed that although the Bolt method uses simple equations and a relatively small set of input data, its effectiveness is

uncertain, as the spectrum of applicability in real conditions with currents is limited. In contrast TU Delft method seems to meet these requirements along with the acceptable performance from the Academic and the Real-world test cases could be considered an accurate power predicting method.

“Sub-question 5: Based on these criteria what can be recommended as a best practice moving forward for the Rijkswaterstaat?”

The three criteria that were addressed in the previous sub question were combined with the results derived from the Real-world test case to prove the best practice.

Based on the first criterion, both the Bolt (2003) method and the TU Delft method (Jiang, Baart & van Koningsveld, 2022) are capable of providing accurate power estimations in shallow water and especially in real shallow conditions where the ratio of the water depth to ship draft is equal to 1.5. The Bolt (2003) method shows an acceptable deviation rate for sailing speeds ranging between 2.5m/s to 3.5m/s, while the TU Delft method (Jiang, Baart & van Koningsveld, 2022) performs well for sailing speeds from 2.5m/s to 4m/s. Additionally, the TU Delft method (Jiang, Baart & van Koningsveld, 2022) provides favorable power results in intermediate and deeper depths, making it a widely used method in various water conditions.

According to the second criterion, the TU Delft method (Jiang, Baart & van Koningsveld, 2022) can provide accurate estimations of the real delivered power (no current flow consideration) and fuel use data. Specifically, this method predicts fuel use for both upstream and downstream trips, as well as round trips, with a deviation rate of less than 1.5%. This level of accuracy validates that the TU Delft method (Jiang, Baart & van Koningsveld, 2022) can effectively consider the effect of current flows and provide precise results in case of motor cargo vessels and pushed or coupled convoys. In contrast, the Bolt (2003) method has been found to provide satisfactory results for delivered power only in shallow water depths. Nevertheless, when current flows are taken into account, the deviations between the estimated and actual values vary considerably. Although the results are relatively encouraging for pushed and coupled convoys(smaller deviations), but further investigation is required to establish their accuracy due to the significant discrepancies observed.

The practical applicability of a method was the final criterion used to determine the best practice for estimating the required power. In this regard, the Bolt (2003) method outperform the TU Delft method (Jiang, Baart & van Koningsveld, 2022). This is because the Bolt (2003) method involves fewer equations and requires less complex input data for accurately predicting the power. As a result, the Bolt (2003) method is deemed more practical and efficient for estimating power requirements.

Both the Bolt (2003) method and the TU Delft method (Jiang, Baart & van Koningsveld, 2022) meet the three criteria, which makes it difficult to choose one as best practice. Furthermore, both methods are valid approaches to power estimation, the simple approach used by the Bolt (2003) method makes it more practical for some applications, while the TU Delft method (Jiang, Baart & van Koningsveld, 2022) may be more suitable for situations where a more detailed analysis is required. The TU Delft method (Jiang, Baart & van Koningsveld, 2022) has an advantage over the Bolt (2003) method in that it can be applied regardless of whether there is current flow or not. Ultimately, both methods are valid choices for shallow water without currents, and it is suggested the selection of the most suitable method by considering its limitations and the specific requirements of the studied case.

In summary, the comments and recommendations provided by Backer van Ommeren have yielded significant findings and improvements in the field of power prediction. One notable outcome is the enhanced validity of the Bolt (2003) method, which was achieved through the validation of real data. This validation process has strengthened the method's credibility and reliability. Furthermore, the implementation of the "Bolt method with speed correction" shows promise for application by Rijkswaterstaat, particularly in shallow water scenarios where it takes into account the phenomena associated with such conditions. However, it is important to note that further validation is required before its adoption can be recommended with confidence. Moreover, the investigation into an alternative power method has yielded the TU Delft method (Jiang, Baart & van Koningsveld, 2022), in particular, demonstrates accurate behavior in shallow water conditions while effectively capturing current effects and providing reliable estimations even in deeper depths. In conclusion, Backer van Ommeren comments and recommendations have led to significant advancements.

8.2. Recommendations

Although the results of the current study are promising, they also highlight the need for further improvement of the proposed methods and future research. Based on the discussion and conclusions drawn from the study, the following recommendations can be derived.

- **Validation of the methods, based on alternative friction formula and power efficiency coefficients.**

It is proposed the substitution of the friction coefficient in Bolt (2003) method and "Bolt method with speed correction", which is typically predicted by the ITTC57 formula, with the modified friction coefficient for shallow water conditions. This modified friction coefficient accounts for the effects of shallow water (Zeng et al., 2018). This substitution is recommended to be applied to both the Bolt (2003) method and Bolt method with speed correction and tested firstly in combination with the relative velocity and secondly by using the sailing speed instead of this shallow water velocity.

The substitution of the power efficiency coefficients for the calculation of the delivered power in shallow water is suggested. This recommendation related to Bolt (2003) method and Bolt method with speed correction. Specifically, the product of the open water efficiency, the hull efficiency and the relative rotative efficiency that are used in the delivered power is also expressed as the hydrodynamic efficiency, influenced by water depth among others. (Bilen & Zerjal, 1999; Simic & Radojicic, 2013; MoVe IT! 2014; Marin, 2020; Radojicic et al., 2021).

- **Acquisition of additional real data for the validation of the methods.**

In Chapter 5, Sections 5.1.1 to 5.1.3 the three selected methods, as they were derived from the Academic test case, they were evaluated by real world inland vessel delivered-power data. From this comparison, it was observed that the three methods vary significantly in shallow water depths during sailing with very low speeds ranging from 1.5-2m/s. Specifically, all the three methods estimated lower delivered power in contrast to the measurements. Therefore, it is suggested to investigate this phenomenon and the validation with additional real-power data for same and for different types of vessels.

In the Real-world test case, the three selected methods were simulated for the mean water level. However, it is recommended that the fuel consumption be tested for both minimum and high water levels. By conducting these tests would provide additional

insight into the vessel's fuel consumption behavior under varying water level conditions, allowing for more comprehensive analysis and optimization of the method's performance.

Finally, to objectively validate the suitability of the Bolt (2003) method and TU Delft method (Jiang, Baart & van Koningsveld, 2022) for predicting power in shallow water conditions, it is recommended to compare these methods with a more extensive power dataset. Currently, the available real-power data are limited, and therefore a more comprehensive dataset is needed for a robust validation.

- **Conduction of laboratory test considering the current flow effect.**

The current effects on ship power use can be significant. Thus, it is recommended to conduct further research (e.g., model tests) that considers the presence of currents for power-speed relationship. This would provide a more comprehensive understanding of the current influence in the real world operating conditions. Furthermore, when additional fuel-use data become available, it is also suggested Bolt method, Bolt method with speed correction, and TU Delft method (Jiang, Baart & van Koningsveld, 2022) be re-evaluated to enhance the findings that were derived from the present study.

List of figures

Figure 1.2.1: Inland waterway transport performance in Europe by region & quarter (CCNR., 2022).....	17
Figure 1.2.2: Modal split of freight transport in 2019 data (Sipotra, 2021).....	18
Figure 1.2.3: Percentage of freight transport by modality in the Netherlands (Percentage Goederentransport per Modaliteit in Nederland, Binnenvaartcijfers, 2023b)	19
Figure 1.7.1: Flow of the outline of the Master Thesis	25
Figure 2.1.1: Frictional and pressure resistance and their direction (Van Koningsveld, Verheij, Taneja & De Vriend, 2021)	29
Figure 2.1.2: Wave interference of an actual ship hull. V and λ denote the velocity and the wavelength (Du, Ouahsine, Sergent, & Hu, 2020).....	29
Figure 2.1.3: Components of Hull resistance (The United States Naval Academy, 2001)	30
Figure 2.1.4: Schematization of a ship to illustrate different power components and efficiencies (Seger, 2021)	33
Figure 2.4.1: Comparison between simplified and iteratively calculations for return flow & power (Backer Van Ommeren, 2019).....	38
Figure 2.4.2: Effect of maximum depth and width in return flow and required power calculations (Backer Van Ommeren, 2019)	39
Figure 2.4.3: Left picture M8 at 5m, Right picture M8 at 7.5m (Backer Van Ommeren, 2019).....	40
Figure 2.4.4: Comparison between (Tuck, 1966; Pacurarum & Domnisoru, 2017)	42
Figure 3.2.1: Resistance & power calculation process	49
Figure 3.3.1: Waterway conditions & ship dimensions for the Academic test case	50
Figure 3.4.1: Waterway conditions for the Real-world test case.....	52
Figure 4.1.1: Total resistance & Brake power as a function of the vessel speed (M6-narrow), for different water depths.....	56
Figure 4.1.2: Total resistance & Brake power as a function of the vessel speed (M6-wide), for different water depths	57
Figure 4.1.3: Total resistance & Brake power as a function of the vessel speed (M8-narrow), for different water depths.....	57
Figure 4.1.4: Total resistance & Brake power as a function of the vessel speed (M8-wide), for different water depths	58
Figure 4.2.1: Total resistance & Brake power as a function of the vessel speed (M6- narrow), for different water depths.....	59
Figure 4.2.2: Total resistance & Brake power as a function of the vessel speed (M6- wide), for different water depths	59
Figure 4.2.3: Total resistance & Brake power as a function of the vessel speed (M8-narrow), for different water depths.....	60
Figure 4.2.4: Total resistance & Brake power as a function of the vessel speed (M8-wide), for different water depths	60
Figure 4.3.1: Total resistance & Brake power as a function of the vessel speed (M6-narrow), for different water depths.....	61
Figure 4.3.2: Total resistance & Brake power as a function of the vessel speed (M6-wide), for different water depths	61
Figure 4.3.3: Total resistance & Brake power as a function of the vessel speed (M8-narrow), for different water depths.....	62

Figure 4.3.4: Total resistance & Brake power as a function of the vessel speed (M8-wide), for different water depths	62
Figure 4.4.1: Total resistance & Brake power as a function of the vessel speed (M6-narrow), for different water depths.....	63
Figure 4.4.2: Total resistance & Brake power as a function of the vessel speed (M6-wide), for different water depths	63
Figure 4.4.3: Total resistance & Brake power as a function of the vessel speed (M8-narrow), for different water depths.....	64
Figure 4.4.4: Total resistance & Brake power as a function of the vessel speed (M8-wide), for different water depths	65
Figure 4.5.1: Total resistance & Brake power as a function of the vessel speed (M6-narrow), for different water depths.....	65
Figure 4.5.2: Total resistance & Brake power as a function of the vessel speed (M6-wide), for different water depths	66
Figure 4.5.3: Total resistance & Brake power as a function of the vessel speed (M8-narrow), for different water depths.....	66
Figure 4.5.4: Total resistance & Brake power as a function of the vessel speed (M8-wide), for different water depths	67
Figure 4.6.1: Performance of 5 methods in a narrow waterway for an M6 motor vessel.....	68
Figure 4.6.2: Performance of 5 methods in wide waterway for M6 vessel	68
Figure 4.6.3: Performance of 5 methods in narrow & shallow waterways for M8.....	69
Figure 4.6.4: Performance of 5 methods in wide & shallow waterways for M8.....	69
Figure 5.1.1: Comparison between estimated delivered power (Bolt method) & measured power data (Simic & Radojic, 2013; MoVe IT!2014).....	72
Figure 5.1.2: Comparison between estimated delivered power (Bolt method with speed corrections) & measured power data (Simic & Radojic, 2013; MoVe IT!2014)	74
Figure 5.1.3: Comparison between estimated delivered power (TU Delft method) & measured power data (Simic & Radojic, 2013; MoVe IT!2014).....	75

List of tables

Table 5.1: Comparison between $P_{\text{estimated}}$ & P_{real} for (h=3m, $B_c=150\text{m}$)	72
Table 5.2: Comparison between $P_{\text{estimated}}$ & P_{real} for (h=5m, $B_c=150\text{m}$)	73
Table 5.3: Comparison between $P_{\text{estimated}}$ & P_{real} for (h=10m, $B_c=150\text{m}$)	73
Table 5.4: Comparison between $P_{\text{estimated}}$ & P_{real} for (h=3m, $B_c=150\text{m}$)	74
Table 5.5: Comparison between $P_{\text{estimated}}$ & P_{real} for (h=5m, $B_c=150\text{m}$)	74
Table 5.6: Comparison between $P_{\text{estimated}}$ & P_{real} for (h=10m, $B_c=150\text{m}$)	74
Table 5.7: Comparison between P_{measured} & P_{real} for (h=3m, $B_c=150\text{m}$)	76
Table 5.8: Comparison between P_{measured} & P_{real} for (h=5m, $B_c=150\text{m}$)	76
Table 5.9: Comparison between P_{measured} & P_{real} for (h=10m, $B_c=150\text{m}$)	76
Table 5.10: Comparison of the fuel consumption of each method with the real fuel used for a motor vessel M6	77
Table 5.11: Comparison of the fuel consumption of each method with the real fuel used for pushed & coupled convoy	78
Table 5.12: Delivered power difference of each method for shallow water conditions	79
Table 5.13: Delivered power difference of each method for intermediate water conditions.	79
Table 5.14: Delivered power difference of each method for deep water conditions.....	80
Table 6.1: Resistance and Power results in narrow waterway(M6, $B_c=50\text{m}$) - Bolt method.	84
Table 6.2: Resistance and Power results in narrow waterway($B_c=50\text{m}$) – TU Delft method	84
Table 6.3: Resistance and Power results in wide waterway(M6, $B_c=150\text{m}$) - Bolt method ..	85
Table 6.4: Resistance and Power results in wide waterway($B_c=150\text{m}$) – TU Delft method ..	85
Table 6.5: Resistance and Power results in narrow waterway(M8, $B_c=50\text{m}$) – Bolt method	86
Table 6.6: Resistance and Power results in narrow waterway(M8, $B_c=50\text{m}$) – TU Delft method	86
Table 6.7: Resistance and Power results in wide waterway(M8, $B_c=150\text{m}$) – Bolt method..	86
Table 6.8: Resistance and Power results in wide waterway($B_c=150\text{m}$) – TU Delft method ..	87
Table A- 1: RWS classification of Dutch inland waterways based on the minimum waterway profile for straight sections.	109
Table A- 2: Waterway & Ship dimensions according to Bolt simulations	110
Table A- 3: Waterway & Ship dimensions according to Backer simulations.....	110
Table B-1: RWS classification of inland ships in the Netherlands	111
Table D- 1: Comparison between power from survey data and estimated power.....	115
Table E- 1: Main characteristics of motor vessel Herso 1 & the SL Leonie lighter	116
Table E- 2: Navigation conditions used for the round trip calculations performed (Regensburg – Budapest).....	116
Table E- 3: Sailing time and fuel consumption for upstream trip	116
Table E- 4: Sailing time and fuel consumption for downstream trip	117
Table E- 5: Brake specific fuel consumption bsfc on the propeller curve used in the performance calculations. P_b is the brake power of the main engine	117

Table F- 1: Estimated fuel use for a motor cargo vessel M6 sailing upstream.....	118
Table F- 2: Estimated fuel use for a motor cargo vessel M6 sailing downstream.....	118
Table F- 3: Estimated fuel use for a pushed convoy sailing upstream	119
Table F- 4: Estimated fuel use for a coupled convoy sailing downstream	119

Bibliography

- Backer Van Ommeren, E. (2019). Rekenmodel brandstof verbruik binnevaartschepen. TU Delft, TNO, RWS.
- Baldasso, E., Elg, M., Haglind, F., & Baldi, F. (2019, November 8). Comparative Analysis of Linear and Non-Linear Programming Techniques for the Optimization of Ship-Machinery Systems. *Journal of Marine Science and Engineering*; MDPI. <https://doi.org/10.3390/jmse7110403>
- Blaauw, H. (1983). Prediction of squat of ships sailing in restricted water. TU Delft Repositories. <http://resolver.tudelft.nl/uuid:6239de7f-46d9-48f5-acea-75e7cc1e421f>
- Blaauw, H. G., & Knaap, F. M. C. (1985). Deterioration of cross sections in waterways prediction of water level drop.
- Bolt, E. (2003). Schatting energieverbruik binnenvaartschepen versie 3. Adviesdienst Verkeer En Vervoer afdeling Scheepvaart.
- Bouwmeester, J. (1986). Scheepssnelheden op beperkt water met gegeven motorvermogen. TU Delft Repositories. <http://resolver.tudelft.nl/uuid:8f6fac3b-9ec8-4b88-9bfa-4eae3cdf42>
- Bundesanstalt für Wasserbau Federal Waterways Engineering and Research Institute. (2016). *Driving Dynamics of Inland Vessels : Vessel Behaviour on European Inland Waterways and Waterway Infrastructure with Special Respect to German Waterways (BAW Karlsruhe, Trans.)*.
- Bureau Voorlichting Binnenvaart. (2023, February 16). Bureau Voorlichting Binnenvaart. <https://bureauvoorlichtingbinnenvaart.nl/>
- CCNR. (2022, April 28). 1. FREIGHT AND PASSENGER TRANSPORT ON INLAND WATERWAYS - CCNR - Observation Du Marché. CCNR - Observation Du Marché. <https://inland-navigation-market.org/chapitre/1-freight-and-passenger-transport-on-inland-waterways/?lang=en>
- Climate change mitigation: reducing emissions. (2023, April 27). European Environment Agency. <https://www.eea.europa.eu/en/topics/in-depth/climate-change-mitigation-reducing-emissions>
- Du, P., Ouahsine, A., Sergent, P., & Hu, H. (2020, August 15). Resistance and wave characterizations of inland vessels in the fully confined waterway. *Ocean Engineering*; Elsevier BV. <https://doi.org/10.1016/j.oceaneng.2020.107580>
- EU achieves 20-20-20 climate targets, 55 % emissions cut by 2030 reachable with more efforts and policies. (n.d.). European Environment Agency. <https://www.eea.europa.eu/highlights/eu-achieves-20-20-20>
- European Environment Agency's home page. (n.d.). <https://www.eea.europa.eu/>
- Eurostat. (n.d.). Eurostat. <https://ec.europa.eu/eurostat/>
- Evaluation of the fuel-consumption-reduction potential of a Danube vessel. (n.d.). <https://doi.org/10.5281/zenodo.1451695>

Freight transport statistics: Modal split [PDF file]. (2021). <https://www.sipotra.it/wp-content/uploads/2021/10/Freight-transport-statistics-modal-split.pdf>.

Fumuso, A. (2021, July 25). European Commission released a follow up plan on its EU Green Deal-inland waterway transport. <https://www.inlandwaterwaytransport.eu/eu-commission-released-follow-up-plan-on-its-eu-green-deal/>

Green Deal Zeevaart, Binnenvaart en Havens | Greendeals. (2019). <https://www.greendeals.nl/green-deals/green-deal-zeevaart-binnenvaart-en-havens>

Groenveld, R. (1999). Capacities of Inland Waterways: Ports, waterways, and inland navigation. <http://resolver.tudelft.nl/uuid:8954ca91-eb56-483b-ac5a-7819f5adb2e5>

Guldhammer, H. (1974). SHIP RESISTANCE - Effect of form and principal dimensions. (Revised). TU Delft Repositories. <http://resolver.tudelft.nl/uuid:4a6f2694-a3ab-4a90-beac-7f38c41d4e40>

Holtrop, J. (1978). A statistical power prediction method. TU Delft Repositories. <http://resolver.tudelft.nl/uuid:62c40df8-18cc-4225-a65a-54ff5c1609fb>

Holtrop, J. (1982). An approximate power prediction method. TU Delft Repositories. <http://resolver.tudelft.nl/uuid:ee370fed-4b4f-4a70-af77-e14c3e692fd4>

Identify typical fleet families and operational profiles on European inland waterways and canals – Prominent-IWT. (n.d.). <https://www.prominent-iwt.eu/attachments-waterways-and-canal/>

Inland waterways. (n.d.). Mobility and Transport. https://transport.ec.europa.eu/transport-modes/inland-waterways_en

Inland waterways: Overview of Inland Waterway shipping in Europe. (n.d.). European Alternative Fuels Observatory. Retrieved January 20, 2023, from <https://alternative-fuels-observatory.ec.europa.eu/transport-mode/inland-waterways>

Janssen, P. (1953). The relation between the form of cross section the cross section, the method of revetment and the distribution of the water velocities in a waterway. TU Delft Repositories. <http://resolver.tudelft.nl/uuid:bd05357f-2235-47bc-88bc-30ae7764a0f2>

Koedijk, O. C. (2020). Richtlijnen Vaarwegen 2020.

MAN Energy Solutions. (n.d.). MAN Energy Solutions. <https://www.man-es.com/>

Maynard, S. T. (1990). Velocities induced by commercial navigation, Department of the Army Corps, Technical report HL-90-15, Louisville, USA of Engineers.

Ministerie van Infrastructuur en Waterstaat. (2021a, June 22). Inland Shipping. Freight Transport | Government.nl. <https://www.government.nl/topics/freight-transportation/inland-shipping>

Ministerie van Infrastructuur en Waterstaat. (2021b, June 22). Inland Shipping. Freight Transport | Government.nl. <https://www.government.nl/topics/freight-transportation/inland-shipping>

- Mobility and transport. (2023, March 28). Mobility and Transport. https://transport.ec.europa.eu/index_en
- Morrall, A. (1970). 1957 ITTC model ship correlation line values of frictional resistance coefficient. TU Delft Repositories. <http://resolver.tudelft.nl/uuid:16d77473-7043-4099-a8c6-bf58f555e2e7>
- Pacuraru, F., & Domnisoru, L. (2017). Numerical investigation of shallow water effect on a barge ship resistance. IOP Conference Series, 227, 012088. <https://doi.org/10.1088/1757-899x/227/1/012088>
- Percentage goederentransport per modaliteit in Nederland – Binnenvaartcijfers. (n.d.-a). <https://binnenvaartcijfers.nl/percentage-goederentransport-per-modaliteit-in-nederland/>
- Percentage goederentransport per modaliteit in Nederland – Binnenvaartcijfers. (n.d.-b). Retrieved January 20, 2023, from <https://binnenvaartcijfers.nl/percentage-goederentransport-per-modaliteit-in-nederland/>
- Pompée, P. – J. (2015). About modelling inland vessels resistance and propulsion and interaction vessel – waterway. Smart Rivers.
- Radmilovic, Z., & Maras, V. (2011). Role of Danube inland navigation in Europe. International Journal for Traffic and Transport Engineering, 1(1). <https://trid.trb.org/view/1116389>
- Radojčić, D., Simić, A., Momčilović, N., Motok, M., & Friedhoff, B. (2021a). Waterborne Transport—Representative Ship Types. Springer eBooks, 45–68. https://doi.org/10.1007/978-3-030-77325-0_4
- Radojčić, D., Simić, A., Momčilović, N., Motok, M., & Friedhoff, B. (2021b). Design of Contemporary Inland Waterway Vessels: The Case of the Danube River. Springer Nature.
- Robijns, T. (2014). Flow beneath inland navigation vessels. TU Delft Repositories. <http://resolver.tudelft.nl/uuid:380ca986-dccd-469b-94f6-7e57940ced4f>
- Schijf, J. (1949). Protection of embankments and bed in inland and maritime waters, and in overflows or weirs. TU Delft Repositories. <http://resolver.tudelft.nl/uuid:e0a52ec1-b6d3-475d-b50c-80e6c6e2fe0e>
- Segers, L. (2021). Mapping inland shipping emissions in time and space for the benefit of emission policy development: A case study on the Rotterdam-Antwerp corridor. <http://resolver.tudelft.nl/uuid:a260bc48-c6ce-4f7c-b14a-e681d2e528e3>
- Stolker, C., & Verheij, H. J. (2006). Ship-induced water motions beneath the ship's hull, 31th International Navigation Congress PIANC, Estoril, Portugal.
- The United States Naval Academy. (2001, March 2). <https://www.usna.edu/>
- Tuck, E. O. (1966). Shallow water flows past slender bodies. TU Delft Repositories. <http://resolver.tudelft.nl/uuid:a5d2f839-584e-43c3-b5b7-ada1ec7711d5>
- Van Koningsveld, M., Verheij, H., Taneja, P., & De Vriend, H. (2021). Ports and Waterways: Navigating the changing world. <https://doi.org/10.5074/t.2021.004>
- Waterway Guidelines 2020 | TU Delft Repositories. (2020). <http://resolver.tudelft.nl/uuid:d05c053e-e2d9-426e-891e-c4ca31793d2f>

Watson, D. (1998). *Practical Ship Design*. Elsevier.

Zeng, Q., Thill, C., Hekkenberg, R., & Rotteveel, E. (2019). A modification of the ITTC57 correlation line for shallow water. *Journal of Marine Science and Technology*, 24(2), 642–657. <https://doi.org/10.1007/s00773-018-0578-7>

Appendix A: Waterway classification

In the following table the Dutch classification of waterways is shown, and the following dimensions are related with the Waterway Guidelines, TU Delft Repositories (2020). In the second column the minimum water depth is presented based on the maximum draft according to the CVB Guidelines (1996). However, today inland navigation vessels often have a slightly deeper draft, a fact that led to increase the minimum water in the most popular waterways. In conclusion, it is suggested, when new waterways are built or existing ones upgraded, the waterway management authority should select the second value.

class	minimum waterway profile (m)				
	depth D ¹	width W _t W _d		side wind increment Δw inland zone coastal zone	
normal profile					
I	3.1 - 3.5	20.4	10.2	2	4
II	3.5 - 3.6	26.4	13.2	3	6
III	3.5 - 3.8	32.8	16.4	4	8
IV	3.9 - 4.2	38.0	19.0	5	11
Va	4.9	45.6	22.8	7	14
Vb	5.6	45.6	22.8	9	18
VIa/M12 ²	5.6	68.0	34.0	7	14
VIa/BII-2b	5.6	91.2	45.6	6	14
VIb	5.6	91.2	45.6	9	19
VIc	5.6	91.2	45.6	13	27
narrow profile ³					
I	2.9 - 3.3	15.3	10.2	3	5
II	3.3 - 3.4	19.8	13.2	4	7
III	3.3 - 3.5	24.6	16.4	5	10
IV	3.6 - 3.9	28.5	19.0	7	15
Va	4.6	34.2	22.8	9	19
Vb	5.2	34.2	22.8	12	24
single-lane profile ³					
I	2.9 - 3.3	10.2	5.1	to be determined	to be determined
II	3.3 - 3.4	13.2	6.6		
III	3.3 - 3.5	16.4	8.2		
IV	3.6 - 3.9	19.0	9.5		
Va	4.6	22.8	11.4		
Vb	5.2	22.8	11.4		

Table A- 1: RWS classification of Dutch inland waterways based on the minimum waterway profile for straight sections.

scheepsklasse	CEMT	richting	lading	b	t	doorsn	v	L	B	T
M6	II	beide	leeg	49,86667	3,5	82,86667	7	85	9,5	0,8
M6	III	beide	leeg	52,84444	3,5	112,0667	8	85	9,5	0,8
M6	IV	beide	leeg	69,66667	3,9	150,1	17	85	9,5	0,8
M6	Va	beide	leeg	79,14286	4,9	196,2343	17	85	9,5	0,8
M6	Vb	beide	leeg	75	5,6	232,08	17	85	9,5	0,8
M6	VI	beide	leeg	100	6	500	17	85	9,5	0,8
M6	Ijssel	beide	leeg	100	3,2	320	16	85	9,5	0,8
M6	Lek	beide	leeg	150	5	750	18	85	9,5	0,8
M6	Waal	beide	leeg	250	7	1750	18	85	9,5	0,8
M6	Ijssel	op	leeg	100	3,2	320	18	85	9,5	0,8
M6	Lek	op	leeg	150	5	750	18	85	9,5	0,8
M6	Waal	op	leeg	250	7	1750	18	85	9,5	0,8
M6	Ijssel	af	leeg	100	3,2	320	15	85	9,5	0,8
M6	Lek	af	leeg	150	5	750	18	85	9,5	0,8
M6	Waal	af	leeg	250	7	1750	18	85	9,5	0,8

Table A- 2: Waterway & Ship dimensions according to Bolt simulations

Kanaal	Breedte schip Bs [m]	Diepgang schip beladen Ts (= T) [m]	Diepgang schip leeg max Tsl (= Tb) [m]	Diepte kanaal op as vaarweg h (= D) h / Ts	Wind toeslag 'toeslag' (= Δ _w) [m]	Bruto oppervlak excl. toeslag [m ²]	Oppervak verlies door taluut [m ²]	Oppervlak toeslag [m ²]	Netto oppervlak plus toeslag (afgerond) [m ²]	Breedte kanaal (afgerond) [m]	Gemiddelde diepte kanaal (afgerond) [m]	
CEMT I	5.05	2.50	1.20	3.10	124%	2	62.6	-3.0	3.7	63	22	2.86
CEMT II	6.60	2.60	1.40	3.50	135%	3	92.4	-5.9	6.0	92	29	3.17
CEMT III	8.20	2.70	1.50	3.50	130%	4	114.8	-6.6	8.4	117	37	3.16
CEMT IV	9.50	2.90	1.60	3.90	134%	5	148.2	-9.5	11.3	150	43	3.49
CEMT Va	11.40	3.00	1.60	4.90	163%	7	223.4	-21.7	16.1	218	53	4.11
CEMT Vb	11.40	3.50	0.80	5.60	160%	9	255.4	-23.9	19.4	251	55	4.56
CEMT Vla ¹⁾	17.00	4.00	2.00	5.60	140%	7	380.8	-27.2	21.0	375	75	5.00
CEMT Vla ²⁾	22.80	4.00	0.80	5.60	140%	6	510.7	-36.5	14.4	489	97	5.04
CEMT Vlb	22.80	4.00	0.80	5.60	140%	6	510.7	-36.5	14.4	489	97	5.04
CEMT Vlc	22.80	4.00	0.80	5.60	140%	9	510.7	-36.5	21.6	496	100	4.96
ARK (oud)	25.00	4.00	n.v.t.	6.00	150%	0	600.0	-46.1	0.00	554	100	5.54
ARK (nu)	25.00	4.00	n.v.t.	6.00	150%	0	600.0	0.00	0.00	600	100	6.00

Table A- 3: Waterway & Ship dimensions according to Backer simulations

Appendix B:RWS vessel classification

Motor vessels									
Classification		Characteristics						Loading rate	
CEMT	RWS	B [m]	L [m]	Tunloaded [m]	Tloaded [m]	Weight class	Pinstalled [kW]	loaded condition	% loaded km
II	M1	5,05	38,5	1,2	2,5	L1	175	75%	70%
III	M2	6,6	52,5	1,4	2,6	L1	300	75%	70%
III	M3	7,2	62,5	1,5	2,6	L1	640	75%	70%
III	M4	8,2	67	1,5	2,7	L1	640	75%	70%
III	M5	8,2	82,5	1,5	2,7	L2	640	75%	70%
IVa	M6	9,5	82,5	1,6	2,9	L2	1070	75%	70%
IVa	M7	9,5	105	1,6	3,0	L2	1070	75%	70%
Va	M8	11,4	110	1,8	3,5	L3	1750	65%	85%
Va	M9	11,4	135	1,8	3,5	L3	2200	65%	85%
Via	M10	13,5	110	2,0	4,0	L3	2400	65%	85%
Via	M11	14,2	135	2,0	4,0	L3	2400	65%	85%
Via	M12	17	135	2,0	4,0	L3	3000	65%	85%
Barges									
Classification		Characteristics						Loading rate	
CEMT	RWS	B [m]	L [m]	Tunloaded [m]	Tloaded [m]	Weight class	Pinstalled [kW]	loaded condition	% loaded km
I	B01	5,2	55	1	1,9	L1	175	75%	70%
II	B02	6,6	65	1,4	2,6	L1	300	75%	70%
III	B03	7,5	80	1,4	2,6	L1	300	75%	70%
III	B04	8,2	85	1,4	2,7	L1	640	75%	70%
IVa	B1	9,5	95	1,6	3	L2	1070	75%	70%
Va	BII-1	11,4	102,5	1,8	3,5	L2	1750	65%	85%
Vb	BII-2l	11,4	180	2	3,8	L3	1750	65%	85%
Via	BII-2b	22,8	120	2	3,9	L3	2400	65%	85%
Vib	BII-4	22,8	190	2	3,8	L3	3000	65%	85%
Vic	BII-6l	22,8	270	2	3,8	L3	4000	65%	85%
VIIa	BII-6b	34,2	195	2	3,8	L3	4000	65%	85%
Convoys									
Classification		Characteristics						Loading rate	
CEMT	RWS	B [m]	L [m]	Tunloaded [m]	Tloaded [m]	Weight class	Pinstalled [kW]	loaded condition	% loaded km
I	C1l	5,05	79	1,3	2,5	L1	175	75%	70%
I	C1b	10,1	38,5	1,3	2,5	L1	175	75%	70%
IVb	C2l	9,5	177,5	1,6	3	L2	1070	75%	70%
Vb	C3l	11,4	180	2	3,8	L3	1750	65%	85%
Via	C2b	19	95	1,6	3	L2	1070	75%	70%
Via	C3b	22,8	102,5	2	3,8	L3	2400	65%	85%
Vib	C4	22,8	185	2	3,8	L3	3000	65%	85%

Table B-1: RWS classification of inland ships in the Netherlands

Appendix C: Backer method-2nd approach

Backer van Ommeren tested different equations for the calculation of the return flow and the water level depression. He aimed to find the most accurate and suitable for the determination of these two important parameters that have significant influence in the total ship resistance and the required power. Therefore, he investigated the performance of Equation 1 to determine the return flow and the use of Equations 2.15 and 2.16 to compute the water level depression.

$$U_r = \sqrt{2 \cdot g \cdot z + V_s^2} - V_s^2 \left[\frac{m}{s} \right] \quad (0.1)$$

The figures provided depict the total resistance and brake power of two types of motor cargo vessels, namely M6 (Figure C-1) and M8 (Figure C-2). However, when compared with the Backer method, this approach exhibits insufficient performance in estimating both the total resistance and brake power. Specifically, it seems that does not consider the depth and the width variation as the estimated results indicate similar values.

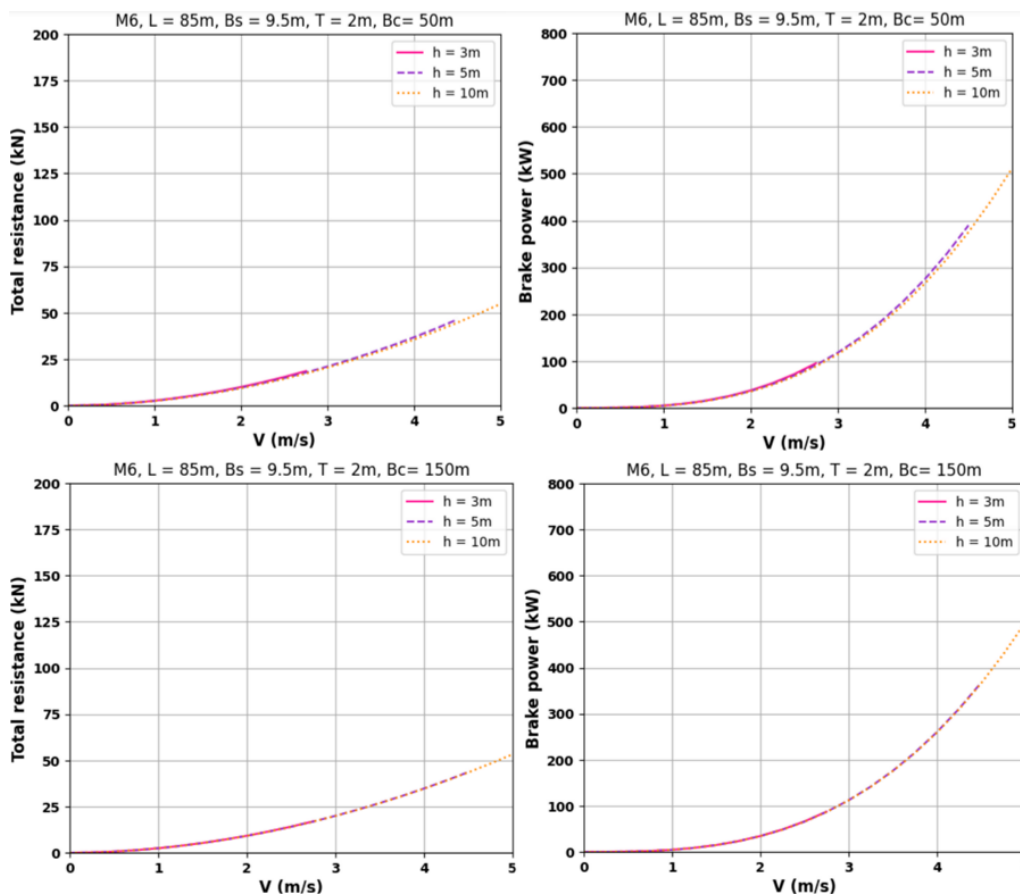


Figure C-1: Total resistance & Brake power as a function of the vessel speed & water depth for an M6 vessel at narrow (top figure) and wide (bottom figure) waterways

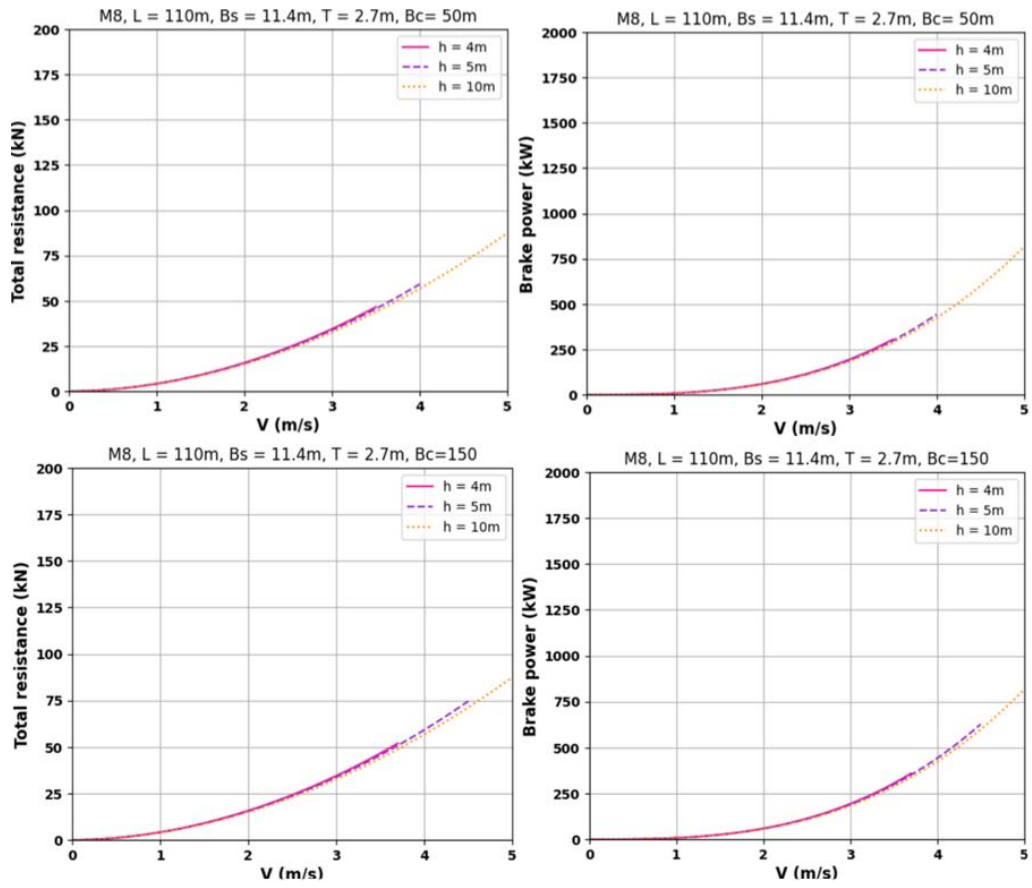


Figure C- 2: Total resistance & Brake power as a function of the vessel speed & water depth for an M8 vessel at narrow (top figure) and wide (bottom figure) waterways

Appendix D: Comparison between power from survey data & estimated power according to Bolt method

In Table D-1 the two red frames depict the installed power as it was given from the skippers and the measured brake power as it was derived from the method. In case of loaded vessels, the results of the calculated power are smaller compared to the values from the survey but in high classes the measurements could be considered quite similar to the installed power in contrast to the smaller ship class. The reason of this divergence between survey and measurements in small ship classes is that smaller ships have been designed to use only a part of the installed power while the larger ship have a well-designed propeller that use almost 90% of the installed power.

Another indication to assess the differences between measurements and real-world data is the value of actual power given specific fuel consumption. For a consumption of 200g/kWh which can be considered a minimum value, and a specific gravity of 0.85, it appears that the calculated power only comes to about 75% of the installed. It is attributed the specified consumption that belongs to an economical speed and do not to the indicated/preferred speed.

Nevertheless, by focusing on the second part of the table where the calculated values by using the Bolt theory are presented the brake power of an empty is larger compared to a loaded one. This strange result indicates that there are errors in the Bolt model.

AVV class	M1	M2	M3	M4	M5	M6	M7	M8
survey								
number of ships	24	19	9	10	9	21	1	17
L (m)	38.85	53.65	59.84	70.95	80.35	86.99	84.84	106.95
B (m)	5.31	6.63	7.06	8.33	8.20	9.39	9.50	11.25
T (m)	2.42	2.42	2.54	2.61	2.69	2.86	3.20	3.35
load power (t)	353	546	700	963	1181	1475	1800	2711
Pb (kW)	185	278	311	451	646	881	746	1267
V loaded (km/h)	11.4	13.6	13.9	14.7	15.8	15.6	13.5	16.5
n_gel (rpm)	1490	1612	1394	1189	1279	1393	1250	982
burn_gel (l/h)	28.6	50.9	58.1	83.3	115.0	154.0	75.0	189.3
use power at 200g/kwh	122	216	247	354	489	655	319	805
deployed perc	66%	78%	79%	79%	76%	74%	43%	64%
V empty (km/h)	15.2	17.3	16.9	17.2	19.1	18.3	18.0	18.5
n_empty (rpm)	1560	1612	1361	1132	1261	1280	1200	883
burn_empty (l/h)	26.4	47.9	55.6	77.8	95.6	118.1	75.0	145.4
use power at 200g/kwh	112	204	236	331	406	502	319	618
deployed perc	61%	73%	76%	73%	63%	57%	43%	49%
vgel m/s	3.17	3.79	3.87	4.08	4.38	4.34	3.75	4.59
flow m/s	4.22	4.80	4.69	4.78	5.29	5.08	5.00	5.14
use empty/full	92%	94%	96%	93%	83%	77%	100%	77%
power estimate								
Loaded								
h/T	2,500	2,500	2,500	2,500	2,500	2,500	2,000	2,000
swf	1.005	1.005	1.005	1.005	1.005	1.005	1.038	1.038
Ve _{eff} (m/s)	3.182	3.810	3.893	4.104	4.405	4.360	3.891	4.767
R _f (kN)	5.7	11.9	14.4	20.5	26.2	30.6	25.5	51.4
R _p (kN)	9.7	17.5	20.4	27.5	32.2	38.3	46.0	85.7
R _t (kN)	15.4	29.4	34.8	48.0	58.3	68.9	71.5	137.1
Pb (kW)	98	223	270	392	511	598	536	1260
Empty								
T _{gem}	60	70	70	70	70	80	80	80
T _{max}	110	130	130	130	130	140	140	140
R _f (kN)	6.2	12.8	14.2	19.6	26.1	29.6	28.4	42.3
R _p (kN)	7.8	14.9	15.1	18.5	22.4	25.4	33.3	41.6
R _t (kN)	14.0	27.6	29.3	38.1	48.5	55.0	61.7	83.9
Pb (kW)	118	265	275	364	513	558	617	863

Table D- 1: Comparison between power from survey data and estimated power

Appendix E: Data for the evaluation of the fuel consumption

	MV Herso 1	SL Leonie
Year of construction	1961	
Length overall, L _{OA}	84.95 m	70.75 m
Breadth moulded, B	9.50 m	10.44 m
Maximum draught, T _{MAX}	2.70 m	2.47 m
Deadweight at T _{MAX}	1382 t	1427 t
Main engine: Deutz RBV 8M 545	780 kW (MCR)	
Auxiliary engines: 2 x Deutz 912	appr. 30 kW each	
Bow thruster engine: DAF 1160	212 kW	
Fixed pitch propeller (FPP), directly driven	5 blades	
Propeller diameter, D	1.55 m	

Table E-1: Main characteristics of motor vessel Herso 1 & the SL Leonie lighter

	River kilometre [km]	H _{LNWL} [m]	H _{MWL} [m]	H _{HNWL} [m]	V _{LNWL} [km/h]	V _{MWL} [km/h]	V _{HNWL} [km/h]	Reference gauge
	2376.00-2327.72	7.50	7.50	7.50	0.80	2.24	4.70	Pfelling
Free flow	2327.72-2281.70	3.00	4.18	6.20	2.40	3.40	5.10	Pfelling
Free flow	2281.70-2249.47	3.00	4.18	6.20	3.68	4.93	7.06	Pfelling
	2249.47-2230.60	7.50	7.83	8.40	1.00	2.59	5.30	Pfelling
	2230.60-2203.20	7.50	7.50	7.50	1.50	3.26	7.10	Kienstock
	2203.20-2184.00	6.50	6.50	6.50	1.90	3.85	8.10	Kienstock
	2184.00-2147.00	10.60	10.60	10.60	0.80	1.87	4.20	Kienstock
	2147.00-2132.00	5.60	6.45	8.30	0.70	1.08	1.90	Kienstock
	2132.00-2038.00	7.50	8.04	9.20	1.60	2.83	5.50	Kienstock
Free flow	2038.00-2008.00	4.20	5.65	8.80	3.70	4.99	7.80	Kienstock
	2008.00-1921.00	8.30	8.87	10.10	1.50	2.89	5.90	Kienstock
Free flow	1921.00-1873.00	3.30	4.93	7.90	4.80	6.40	9.30	Wildungsmauer
	1873.00-1852.00	7.70	7.70	7.70	1.40	3.42	7.10	Wildungsmauer
Canal	(1852.00-1811.00)							
Gabcikovo	37.56 – 0.00	9.80	9.80	9.80	1.00	1.64	2.80	Wildungsmauer
Free flow	1811.00-1640.00	3.80	5.45	8.90	3.10	4.10	6.20	Budapest

Table E-2: Navigation conditions used for the round trip calculations performed (Regensburg – Budapest)

MV Herso1	Unit	620 kW	500 kW	400 kW	Δ 500 kW	[%]	Δ 400 kW	[%]
Time sailed at LNWL	[h]	51.46	53.43	55.74	1.97	3.8	4.28	8.3
Time sailed at MWL	[h]	51.78	54.17	56.97	2.39	4.6	5.19	10.0
Time sailed at HNWL	[h]	60.16	63.79	68.13	3.63	6.0	7.97	13.2
Fuel used at LNWL	[kg]	6531	5530	4697	-1001	-15.3	-1834	-28.1
Fuel used at MWL	[kg]	6609	5643	4836	-966	-14.6	-1773	-26.8
Fuel used at HNWL	[kg]	7735	6694	5826	-1041	-13.5	-1909	-24.7

Table E-3: Sailing time and fuel consumption for upstream trip

MV Herso 1 + SL Leonie	Unit	16 km/h	15 km/h	14 km/h	Δ 15 km/h	[%]	Δ 14 km/h	[%]
Time sailed at LNWL	[h]	48.43	49.48	52.77	1.05	2.2	4.34	9.0
Time sailed at MWL	[h]	46.75	49.46	52.77	2.71	5.8	6.02	12.9
Time sailed at HNWL	[h]	46.57	49.26	52.18	2.69	5.8	5.61	12.0
Fuel used at LNWL	[kg]	5898	5489	4148	-409	-6.9	-1750	-29.7
Fuel used at MWL	[kg]	4205	3322	2580	-883	-21.0	-1625	-38.6
Fuel used at HNWL	[kg]	1902	1490	1195	-412	-21.7	-707	-37.2

Table E- 4: Sailing time and fuel consumption for downstream trip

P_B	bsfc	Remark
[kW]	[kg/kWh]	
50	0.28	Caterpillar 3508B 783 kW
100	0.24	Caterpillar 3508B 783 kW
195	0.225	VOLVO Penta D34A MT 701kW
390	0.212	VOLVO Penta D34A MT 701kW
575	0.208	VOLVO Penta D34A MT 701kW
735	0.21	Ship owner (Plimsoll Ltd.)

Table E- 5: Brake specific fuel consumption bsfc on the propeller curve used in the performance calculations. P_b is the brake power of the main engine

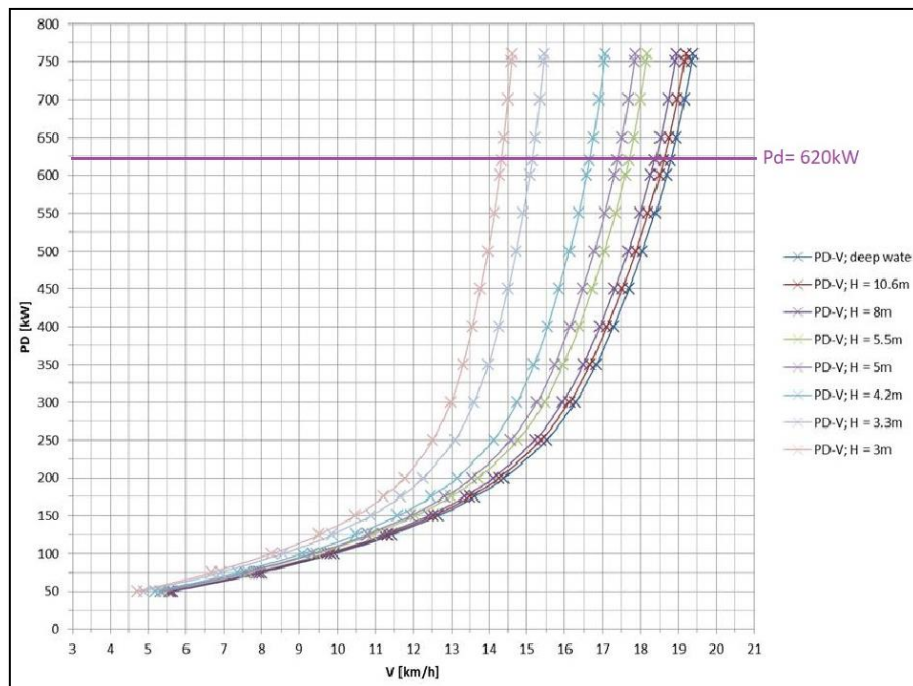


Figure E- 1: Power-speed diagram of the Herso 1 in single operation, given for different water depths

Appendix F: Fuel consumption

Δx [m]	H_{MWL} [m]	$U_{o,MWL}$ [m/s]	$V_{s,ow}$ [m/s]	$V_{s,up,g}$ [m/s]	$t_{s,up}$ [s]	SF [-]	P_b [kW]	Fuel use [kg]
49000	7.5	0.6222222	5.06	4.4353	11047.73	0.21	792.04	510.4309
45300	4.18	0.9444444	4.5	3.5918	12612.06	0.21	630	463.4932
32130	4.18	1.3694444	4.5	3.1668	10145.89	0.21	630	372.8614
18870	7.83	0.7194444	5.1	4.3971	4291.465	0.21	800	200.2684
27400	7.5	0.9055556	5.1	4.1951	6531.43	0.21	800	304.8
19200	6.5	1.0694444	4.9	3.8699	4961.369	0.21	734	212.4293
370000	10.6	0.5194444	4.9	4.4597	8296.522	0.21	696.5	337.0808
150000	6.45	0.3	4.7	4.4652	3359.312	0.21	647	126.786
940000	8.04	0.7861111	5.1	4.3537	21590.83	0.21	800	1007.572
300000	5.65	1.3861111	4.95	3.5721	8398.421	0.21	778	381.1483
870000	8.87	0.8027778	5.16	4.3668	19923.06	0.21	800	929.7426
480000	4.93	1.7777778	4.79	3.0182	15903.52	0.21	727	674.4417
21000	7.7	0.95	5.1	4.16	5048.077	0.21	800	235.5769
37560	9.8	0.4555556	4.02	3.5708	10518.65	0.21	390	239.2993
171000	5.45	1.1388889	4.85	3.7176	45997.42	0.21	736	1974.822
732460								7970.8

Table F- 1: Estimated fuel use for a motor cargo vessel M6 sailing upstream

Δx [m]	H_{MWL} [m]	$U_{o,MWL}$ [m/s]	$V_{s,ow}$ [m/s]	$V_{s,dn,og}$ [m/s]	$t_{s,dn}$ [s]	SF [-]	P_b [kW]	Fuel use [kg]
49000	7.5	0.6222222	5.062	4.444	11026.10261	0.21	790	514.551455
45300	4.18	0.9444444	5.384	4.444	10193.51935	0.21	652.4	475.69757
32130	4.18	1.3694444	5.809	4.444	7229.972997	0.21	652.4	337.39874
18870	7.83	0.7194444	5.159	4.444	4246.174617	0.21	800	198.154815
27400	7.5	0.9055556	5.34	4.444	6165.616562	0.21	800	287.728773
19200	6.5	1.0694444	5.509	4.444	4320.432043	0.21	800	201.620162
370000	10.6	0.5194444	4.959	4.444	8325.832583	0.21	721.68	388.538854
150000	6.45	0.3	4.73	4.444	3375.337534	0.21	660	157.515752
940000	8.04	0.7861111	5.226	4.444	21152.11521	0.21	800	987.09871
300000	5.65	1.3861111	5.826	4.444	6750.675068	0.21	800	315.031503
870000	8.87	0.8027778	5.16	4.444	19576.9577	0.21	800	913.591359
480000	4.93	1.7777778	5.24	4.444	10801.08011	0.21	800	504.050405
21000	7.7	0.95	5.39	4.444	4725.472547	0.21	800	220.522052
37560	9.8	0.4555556	3.785	3.33	11279.27928	0.21	326.1	331.610811
171000	5.45	1.1388889	5.578	4.444	38478.84788	0.21	800	1795.67957
732460								7289.68

Table F- 2: Estimated fuel use for a motor cargo vessel M6 sailing downstream

Δx [m]	H_{MWL} [m]	$U_{o,MWL}$ [m/s]	$V_{s,ow}$ [m/s]	$V_{S,up,og}$ [m/s]	$t_{s,up}$ [s]	SF [-]	P_b [kW]	Fuel use [kg]
49000	7.5	0.6222222	5.06	4.4353	11047.73	0.21	800	515.5608
45300	4.18	0.9444444	4.5	3.5918	12612.06	0.21	800	588.5628
32130	4.18	1.3694444	4.5	3.1668	10145.89	0.21	800	473.4748
18870	7.83	0.7194444	5.1	4.3971	4291.465	0.21	800	200.2684
27400	7.5	0.9055556	5.1	4.1951	6531.43	0.21	800	304.8
19200	6.5	1.0694444	4.9	3.8699	4961.369	0.21	800	231.5305
370000	10.6	0.5194444	4.9	4.4597	8296.522	0.21	800	387.171
150000	6.45	0.3	4.7	4.4652	3359.312	0.21	800	156.7679
940000	8.04	0.7861111	5.1	4.3537	21590.83	0.21	800	1007.572
300000	5.65	1.3861111	4.95	3.5721	8398.421	0.21	800	391.9263
870000	8.87	0.8027778	5.16	4.3668	19923.06	0.21	800	929.7426
480000	4.93	1.7777778	4.79	3.0182	15903.52	0.21	800	742.1642
21000	7.7	0.95	5.1	4.16	5048.077	0.21	800	235.5769
37560	9.8	0.4555556	4.02	3.5708	10518.65	0.21	571.7	490.8704
171000	5.45	1.1388889	4.85	3.7176	45997.42	0.21	800	2146.546
732460								11072.2

Table F- 3: Estimated fuel use for a pushed convoy sailing upstream

Δx [m]	H_{MWL} [m]	$U_{o,MWL}$ [m/s]	$V_{s,ow}$ [m/s]	$V_{S,dn,og}$ [m/s]	$t_{s,dn}$ [s]	SF [-]	P_b [kW]	Fuel use [kg]
49000	7.5	0.6222222	5.062	4.444	11026.10261	0.21	800	514.5515
45300	4.18	0.9444444	5.384	4.444	10193.51935	0.21	800	475.6976
32130	4.18	1.3694444	5.809	4.444	7229.972997	0.21	800	337.3987
18870	7.83	0.7194444	5.159	4.444	4246.174617	0.21	800	198.1548
27400	7.5	0.9055556	5.34	4.444	6165.616562	0.21	800	287.7288
19200	6.5	1.0694444	5.509	4.444	4320.432043	0.21	800	201.6202
370000	10.6	0.5194444	4.959	4.444	8325.832583	0.21	800	388.5389
150000	6.45	0.3	4.73	4.444	3375.337534	0.21	800	157.5158
940000	8.04	0.7861111	5.226	4.444	21152.11521	0.21	800	987.0987
300000	5.65	1.3861111	5.826	4.444	6750.675068	0.21	800	315.0315
870000	8.87	0.8027778	5.16	4.444	19576.9577	0.21	800	913.5914
480000	4.93	1.7777778	5.24	4.444	10801.08011	0.21	800	504.0504
21000	7.7	0.95	5.39	4.444	4725.472547	0.21	800	220.5221
37560	9.8	0.4555556	3.785	3.33	11279.27928	0.21	550.8	526.3664
171000	5.45	1.1388889	5.578	4.444	38478.84788	0.21	800	1795.68
732460								7659.58

Table F- 4: Estimated fuel use for a coupled convoy sailing downstream

Appendix G: Background physics

Theories for confined waterways

This section deals with the significance of the water movement around the ship and its impact on the vessel and the principles that were applied for the development of resistance estimation models. It should be clear, that water motion interacting with ship hull, resist on the ship motion and ultimately influences the amount of power required.

1. Principle of preservation of energy
2. Bernoulli's principle
3. Schijf energy method
4. Bouwmeester theory

- Primary water motion

As a ship sails in a waterway, either narrow or wide, induces water motions. In this thesis the so-called primary water motion is analyzed, as it is the basis for the Bolt theory.

What does it mean primary water motion? The primary water motion consists of the displacement of the water that is caused by the sailing ship, resulting in the return current and the water level depression. Worded differently, primary water motion can be seen as a large wave system.

- Energy conservation

Originally, the primary water motion was explained from Bernoulli's theorem and the equation of continuity. So, Bernoulli equation between two cross sections of a fairway considering the total head:

$$H = h_0 + \frac{V_s^2}{2g} [m]$$
$$h_I - h_{II} = z$$

In Schijf(1949) and Janssen (1953) theories rearrange the previous equation in terms of energy conservation, so the water level drop was arisen. Specifically, two cross sections were selected, one in the undisturbed channel where the water sails with velocity equal to the ship speed but in the opposite direction and the second cross section at the ship that the water sails alongside and under the ship with velocity equal to sailing speed plus the return flow velocity. In Figure G-1 the two cross sections that were used along with the Bernoulli's theorem for the estimation of the water level drop is shown. Also, the continuity equation was rewritten, and the discharge was derived.

$$z = \frac{(V_0 + U_r)^2}{2g} - \frac{V_0^2}{2g} [m]$$
$$Q = (V_0 + U_r) \cdot (A_c - A_s - B_s \cdot z) \left[\frac{m^3}{s} \right]$$

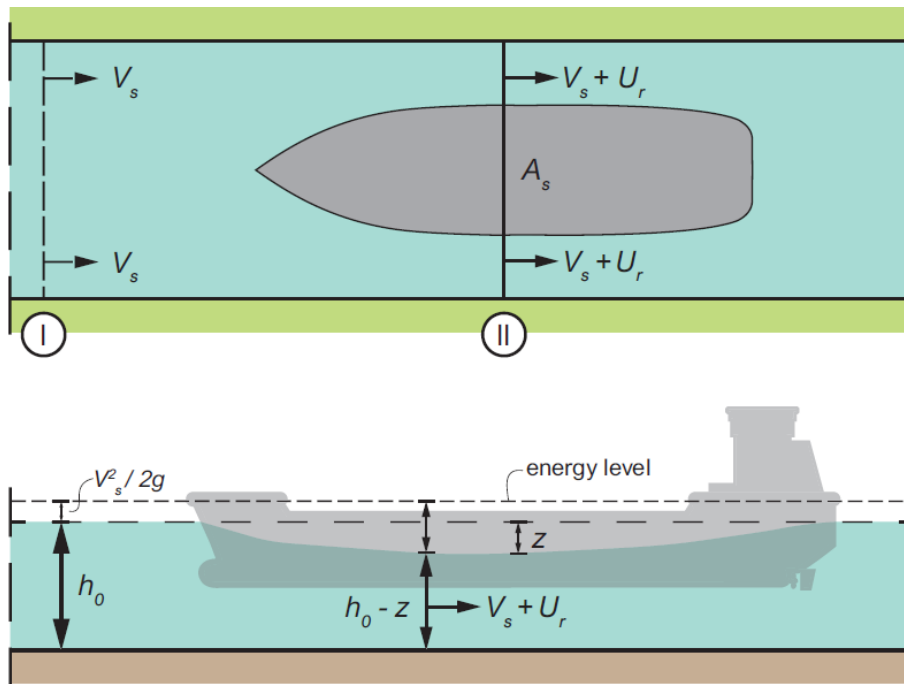


Figure G- 1: Relative water motion in a ship-fixed coordinate system (Van Koningsveld, Verheij, Taneja & De Vriend, 2021)

○ (Schijf, 1949)

Schijf developed the natural limit that is dependent on the depth and width restrictions. Limit velocity is the maximum possible sailing velocity that a ship can reach, given certain vessel classes and waterway dimensions. This velocity can be reached when the return flow is so large that in turn cause higher water level drop alongside the ship's hull and the depth is equal to critical depth. In this case all the water is concentrated at the bow of the ship (cannot travel at the stern to fulfill) where a motor vessel cannot overcome this accumulation.

Method of Schijf assumed rectangular cross section and applicability to motor vessels only. The combination of water level drop equation and discharge equation, that contain two unknowns U_r and z and eliminating one of them, the result is a pair of equations with one unknown parameter. Then if the return flow can be computed the evaluation of water level drop would be an easy calculation. Originally, Schijf used limit speed in Bernoulli's equation, he derived equations for the limit drop and the return current and based on the ratio of the ship to channel cross section did a plot for the real return flow value.

○ (Janssen, 1953)

Tests that were held in 1953 at Delft Laboratories showed some deviations from the theory of (1949), probably due to the following simplifying assumptions. These assumptions also used from Bolt in 2003 and as such:

- a straight, infinitely long prismatic channel section
- a prismatic amidship cross section over the entire length
- a constant speed of the ship
- no trim of the ship
- Sinkage of the ship equal to the water level depression
- a uniform return current over the entire wet channel profile, next to and below the ship
- a uniform water level depression over the entire channel width

- no energy losses, i.e., shear stress and inertial losses are neglected.
- no influence of ship-initiated waves or phenomena caused by helical motion.

Subsequently, a correction factor has been introduced α_{Schijf} , that is multiplied by the first term. The physical meaning of this factor is for the correction of the non-uniform distribution of the return current as it was assumed to have a regular velocity distribution alongside and under the ship. The correction factor generally varies between 1.05 and 1.2 but a commonly used value is 1.1, which corresponds with $V_s = 0.75V_{lim}$. The effect of this correction is that the water level depression and the return current are larger than the original theory. Based on that new graphs and modified equations were constructed for the estimation of the remaining terms. It is mentioned that diagrams indicate what fraction of the limit speed each point concern.

$$\frac{V_s}{\sqrt{gh}} = \left(\frac{2 \frac{z}{h}}{a_{schijf} \left(1 - \frac{A_s}{A_c} - \frac{z}{h}\right)^{-2} - 1} \right)^{1/2} \left[\frac{m}{s} \right]$$

$$\frac{U_r}{\sqrt{gh}} = \frac{V_s}{\sqrt{gh}} \left(\frac{1}{1 - \frac{A_s}{A_c} - \frac{z}{h}} - 1 \right) \left[\frac{m}{s} \right]$$

○ (Bouwmeester, 1977)

A method was developed by Bouwmeester to determine the water level drop and the return current based on the principle of conservation of momentum. More specifically the method was developed for trapezoidal fairways and based on the second law of Newton, stated that the forces acting on the vessel are in equilibrium with the momentum of the flow. However, the basic conservation equations can be written in terms of energy conservation as well as of momentum conservation, the results of these two approaches should be the same. The full formulations, derivations and assumptions can be found also in (Verheij et al., 2008).

As previously referred, his approach was based on the trapezoidal shape, the transformation of which was done as follows. He schematized the original cross section into rectangular shape with the wet channel surface of the rectangular cross section equal to the trapezoidal and the width of the new area was selected equal to the larger width of the trapezoidal scheme. As far as the hydraulic depth for this theory the average was selected which is equal to the ratio of A_c/W_s . The deviations in the values of the area are strongly dependent on the slope gradient of the bank, the width of the water level and the magnitude of the drop. In the following picture the dimensions are presented.

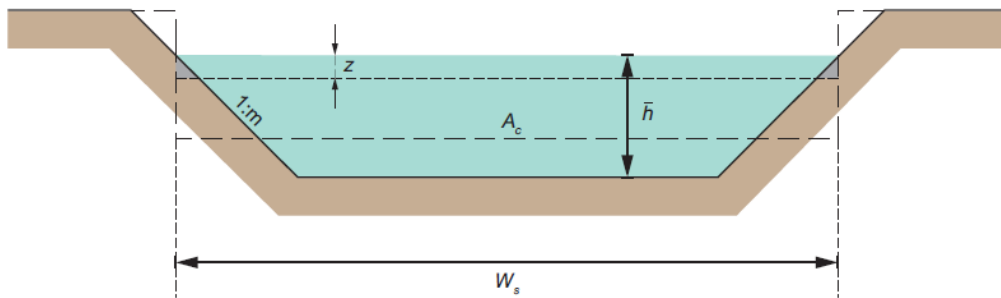


Figure G- 2: Schematization of a trapezoidal cross-section (Van Koningsveld, Verheij, Taneja & De Vriend, 2021)

Consequently, in Bouwmeester (1977) study was also proposed two simplified equations for return flow velocity and water level depression that originally developed by Tuck in 1966.

These simplified equations state when the $U_r/V_s \ll 1$ meaning that return flow is small compared to the sailing speed, second order term could be neglected. Given this assumption, equations for the water level depressions and the discharge are summarized as follow:

$$\left(\begin{array}{l} z = \frac{U_r \cdot V_s}{g} [m] \\ V_s \cdot (A_s + W_s \cdot z) = U_r \cdot (A_c - A_s) \end{array} \right)$$

By considering depth Froude number, eliminating z from the previous set of formulas and if $A_s/A_c \ll 1$ (unrestricted conditions) then the following equations were derived. It is mentioned that these two formulas were used in Bolt method.

$$U_r = \frac{A_m/A_c \cdot V}{1 - A_m/A_c - Fr_h^2} \left[\frac{m}{s} \right] \quad (G-1)$$

$$z = \frac{A_m/A_c \cdot Fr_h^2 \cdot h}{1 - A_m/A_c - Fr_h^2} [m] \quad (G-2)$$

Appendix H: Algorithms

Bolt method

- Friction resistance

Friction is caused by friction forces, acting tangentially on the surface of the submerged part of hull. This resistance component varies with respect to available depth and width, and it is strongly affected by the velocity profile in the boundary layer, which is determined by the Reynolds number and the roughness of the surface. It should be clear that if a ship sails in unconfined water without an ambient current, this part of the resistance is proportional to the ship's speed squared and its wetted surface area (Equation 0.1). In case of restricted water conditions as the available space of flowing water is limited the return current affects ship motion. So, the return current alongside the hull, cause significant increase in the friction. This is taken into account and the frictional resistance equation modified accordingly (Equation 0.2).

$$\text{Deep water: } R_f = \frac{1}{2} \cdot \rho_w \cdot V^2 \cdot C_f \cdot S \text{ [kN]} \quad (0.1)$$

$$\text{Shallow water: } R_f = \frac{1}{2} \cdot \rho_w \cdot (V + U_r)^2 \cdot C_f \cdot S \text{ [kN]} \quad (0.2)$$

As it referred previously, frictional resistance is characterized by a dimensionless coefficient and depends on parameters such as the roughness of the hull and the shape and dimensions of the ship. The proposed formula is presented next (Equation 0.3) as it was recommended by the ITTC57 (Morrall, 1970). This coefficient itself is again dependent on the sailing speed (velocity through water) that was made dimensionless through the Reynolds number.

$$C_f = \frac{0.075}{(\log_{10} Re - 2)^2} \xrightarrow{\text{yields}} C_f = \frac{0.075}{(\log_{10} \frac{V \cdot L_s}{\nu} - 2)^2} \quad (0.3)$$

The wet surface is approximated by Equation 0.4. Due to the curvature of the shape of the hull, the actual surface is larger than the value that arises from the formula. This extra surface is related to the area of appendages and rudders and leads to greater roughness that interfere with friction. Subsequently a surcharge of 20% on the total surface is usually applied to seagoing ships. As far as inland vessels a larger surcharge would be appropriate because the appendages are proportionally much larger than in seagoing vessels and the frictional resistance represents a larger share of the total resistance. So, a surcharge of 40% was applied to inland vessels. Nevertheless, the surcharge will again be smaller compared to seagoing vessels as it takes into account extra resistance due to waves and wind in the open sea.

$$S = L_s \cdot B_s + 2 \cdot L_s \cdot T_{avg} \text{ [m}^2\text{]} \quad (0.4)$$

T_{avg} : average current draft at the bow and the stern

Hence, by taking all the above mentioned into consideration a surcharge of 40% on the frictional resistance is predicted and result in the final formulation.

$$R_f = 53 \cdot (\log VL_s + 4)^{-2} \cdot (L_s \cdot B_s + 2 \cdot L_s \cdot T_{avg}) \cdot V^2 \text{ [N]} \quad (0.5)$$

- Residual resistance

Residual resistance is comprised of the wave resistance and the eddy resistance. More specifically, wave resistance refers to the energy loss caused by waves created by the vessel during its propulsion through water and eddy resistance refers to the loss caused by the flow separation particularly at the aft end of the ship. Wave resistance, similar to other resistance components such as friction, it is proportional to the square of the vessel's speed. At low sailing speeds, wave resistance is relatively small compared to friction. However, as the speed of the vessel increases, the magnitude of wave resistance becomes significant. The residual resistance normally represents 8-25% of the total resistance for low-speed ships and up to 40-60% for high-speed ships.

In general, there are two aspects that should be taken into account, first of all it has been shown that there is a speed limit where a further increase in the ship's propulsion power will not result in a higher speed as all the power will be converted into wave energy. Next, this effect or if the ship sails in shallow water, where the displaced water under the ship will have greater difficulty in moving, leads to higher waves with a great influence on the residual resistance and then should be considered in the calculations.

- Pressure resistance

Pressure resistance is caused by differences in the water pressure on the submerged part of the hull. Water pressure is omnidirectional, in the forward and the aft portion of the hull pressure act normal but the development of the boundary layer alongside the ship with maximum thickness at the stern, leads to reduction of the forward acting component of pressure (higher velocity, lower pressure). As a result, this reduction of the forward component causes a net resistance pressure or the different pressure between bow and stern may give rise to a net longitudinal component causing resistance against the ship's forward motion. Thus, this increase in resistance due to pressure is called "viscous pressure drag" or "form drag" and also referred to as the normal component of the viscous resistance.

The magnitude of the viscous pressure component is influenced of the shape of the ship's hull. To be more specific, vessels that are short in length with wide beams (a low length to beam ratio) will experience greater form drag than those with a larger length to beam ratio. Another important factor that affects pressure resistance is the dimensions of the fairway, so as the waterway is becoming more restricted, results in an increased sinkage and trim of the ship associated with the larger water level depression. Concerning the pressure coefficient is strongly determined by three factors the ship shape, the underwater dimensions of the hull and the sailing speed. So, a typical value is 0.1 but for loaded pusher tugs this value can reach up to 0.3, depending on the number of push-barge units. Bolt defined this coefficient equal to 0.15. This pressure resistance is approximately proportional to the wet amidships cross-section and the ship's speed squared, and the formula is presented next.

$$R_p = \frac{1}{2} \cdot C_p \cdot \rho_w \cdot V^2 \cdot A_m \text{ [kN]} \quad (0.6)$$

$$A_m = B_s \cdot T_{max} \text{ [m}^2\text{]} \quad (0.7)$$

$$T_{max} = \begin{cases} T_{bow} \\ T_{stern} \end{cases}$$

- Resistance due to limited water depth

The friction resistance of a ship on shallow water increases because the water speed along the ship increases. This increase in velocity is attributed to the return current velocity which in

turn causes a water level depression next to the ship. Accordingly, this effect is stronger as the waterway is narrower, and the blockage coefficient is then greater. In case of large or very large width this return flow, velocity is being substituted from the effective velocity (Equation 0.8) which again result in greater sailing speed. Usually, the resistance also increases if a vessel sails closely to a bank or when it encounters another ship, or during overtaking one. The return current between the vessel and the bank will increase and thereby the water-level depression and the sinkage and slows down the vessel. As it is addressed above this effective velocity is suitable in cases of very wide waterways but in the formula only the depth and the draft show the effect. Worded differently in wide waterways or unrestricted width conditions, limitations are attributed only to reduced depth.

$$V_{eff} = \frac{V}{1 - e^{4 \cdot (1-h)/T}} \left[\frac{m}{s} \right] \quad (0.8)$$

Schijf developed a theory for return flow on restricted fairways, which yields zero value in unlimited wide water, independent on the water depth. So, on shallow but wide water another approach is needed. Bolt was suggested the use of the return flow equation as it was developed from Tuck (1966) theory. Schijf in 1949 was the first that related the natural limit speed for ships which is reached when the Froude number is critical or when the sailing speed is equal to the wave propagation speed. He based on energy conservation to compute this maximum possible sailing velocity for a specific type of ship given shallow and restricted conditions, he worked by estimating the limit speed, the maximum return current velocity and the associated maximum depression and arranged a figure with known portion between cross section of ship and waterway. Some tests, that held from Delft hydraulic in 1953, showed some deviations (that attributed to simplifications) from the original theory and a correction factor was introduced to recalculate water level depression and the return current and thus new figures and equations that demand iterations were proposed. Bolt in his method proposed the use of equation 3.6 (Tuck, 1966; Bouwmeester, 1977) that can be solved algebraically.

As it previously referred, the local higher velocities around the ship hull, subsequently cause reduction in the pressure and extra increase in the water level drop. Part of the water level drop can be seen as an additional hydrostatic pressure term because the water level at the stern does not immediately return to the undisturbed level due to friction losses and disturbance by the propeller radius. The use of Appendix G, Equation G-1 represents the formula for the depression.

In general, this extra resistance term is like hydrostatic term and is described by the following equation. As far the value of C_z that is indicated in the equation, different values could be considered according to several literatures. In some books a value of 1 is proposed but this does not seem a realistic assumption as this would imply that the water level drop at the stern is still equal to the maximum water level drop alongside the ship and normally leads to a much too high required propulsion power. In reality, the value can strongly depend on the design of the stern and the propeller configuration so a value in the range of 0.1 - 0.4 is conceivable and finally was set at 0.2.

$$R_z = \rho \cdot g \cdot z \cdot C_z \cdot A_m \quad [kN] \quad (0.9)$$

- Total resistance

The total resistance is the sum of the resistance terms discussed above. For the frictional resistance, the flow speed along the ship must be used, which is higher than the ship's speed on limited water. For this, the maximum speed either for narrow or wide waterways, provided

limited water is used. It is mentioned that frictional resistance is predominant for (larger) unloaded inland vessels in comparison with loaded vessels where about half of the total resistance is friction dominated.

$$u_{rel} = \max \left\{ \frac{V + U_r}{V_{eff}} \left[\frac{m}{s} \right] \right. \quad (0.10)$$

$$R_{tot} = \frac{53}{(\log(u_{rel} \cdot L_s) + 4)^2} \cdot S \cdot u_{rel}^2 + \frac{1}{2} \cdot C_p \cdot \rho_w \cdot V^2 \cdot A_m + \rho \cdot g \cdot z \cdot C_z \cdot A_m \quad (0.11)$$

- Propulsive power

The main focus of Bolt method is the estimation of the required power. This is the type of power that a ship needs to sail or for propulsion and is related with several factors. The most important factors that affect power is the resistance of ship that needs to be overcome. The resistance an inland vessel experiences, depends on its dimensions and shape, the velocity of the ship and waterway characteristics. In turn the sailing speed is strongly connected with the resistance encountered during navigation, and of course with the installed engine power transferred by the propeller. To translate the resistance to total required power, you have to take into account propulsion characteristics and different losses in the system. Following section shows step by step which calculations are required to come up with the total required power for propulsion.

Concerning the development of this method, the effective power needed to travel and overcome the total resistance given specific speed is proportional to the total resistance times the ship speed. The effective power (Equation 0.12) is depicted in the following equation. In practice the velocity that was applied to the simulations for the derivation of the method is ship speed for the effective power and the relative velocity for the remaining terms, the selection of its suitable value was explained previously.

$$\text{Effective horsepower } P_e = V_s \cdot R_{tot} [kW] \quad (0.12)$$

The applied power is not the full installed power, because about 5-10% is used for systems on board such as lighting, heating, or other usages. Furthermore, there are various losses in the system (Chapter 5, Figure 5.2.2) and the total energy loss is the sum of all individual components. This schematization of a ship, illustrating different power components and efficiencies we are dealing with.

The total efficiency of the propeller behind the ship is around 0.55 depending on the propeller load and the power delivered to the propeller shaft. So, the delivered power is presented in 0.13. In turn, by taking into account the losses in the shaft line and the transmission the required motor power is produced (Equation 0.14).

$$\text{Delivered horsepower } P_d = \frac{u_{rel} R_{tot}}{0.55} [kW] \quad (0.13)$$

$$\text{Brake horsepower } P_b = 2 \cdot u_{rel} \cdot R_{tot} [kW] \quad (0.14)$$

Backer method

Backer calculated the limit speed for given ship and fairway dimensions. This limit speed would be used in order to check if the sailing speed is larger and if it is larger, the sailing speed will be substituted to the limit speed or if it is smaller can be maintained. This calculation will be done by solving Equation 2.11 iteratively. The iterations would be done in python notebooks, by using the Newton Raphson method a root-finding algorithm which produces successively better approximations to the roots. In turn after the estimation of limit speed, the check with

the sailing speed will be realized. Secondly, after selecting the limit or the sailing speed, the calculation of the return flow (Equation 2.12) will be achieved. Furthermore, given the sailing of the limit speed and the return and by using either Equation 2.15 or 2.16 depending on the channel dimensions, the water level drop will be derived. Then by applying Equation 0.9 the resistance due to water level drop is computed. Originally, in Backer van Ommeren review was proposed this resistance term do not compute in case of motor vessels but taken into account for inland barges. The motivation of this assumption was based on the fact that about that in case of motor vessels the propeller is at the stern where the water level depression is no longer present, and all the produced thrust is used entirely to overcome the pressure. Instead in case of push-barges, the propeller is at a small distance behind the drop and interaction is present. However, residual resistance indeed investigated for motor vessels and the results are relatively low compared to other terms.

Additionally, for the calculation of friction resistance the effective velocity was determined. The effective velocity reflects the summation of the sailing speed and the return current, and this velocity was also applied to Reynolds number computation and consequently in friction coefficient (Equation 0.3). The calculation of the frictional resistance is done with (Equation 0.2). The last resistance term that was computed is the pressure resistance by using (Equation 0.6).

The last step from Backer method has to do with the calculation of the power. Notably, he computed the effective power by multiplying sailing speed with the total resistance (Equation 2.4). Concerning the calculation of the propulsive power, it is achieved by dividing the effective power with the product of the open water efficiency, the hull efficiency and the transmission efficiency. The difference with Bolt theory regarding the propulsive power is that the calculation of the latter was done only by considering the open water efficiency only. As far as the power delivered, it tends to range from 90% to 95% of the propulsive power due to the losses from the gearbox.

Bolt method with speed correction

Two return flow formulas will be used, the first will reflect the shallow conditions (Equation 2.17 or 2.18) and the second the intermediate conditions (Equation 2.19). Therefore, in Bolt method with speed correction, the return flow is computed according to the aforementioned formulas and their limitations and then it was added to the sailing speed. The sailing speed or equivalent the adjusted speed is computed according to Bolt method (Equation 2.8). Then the relative velocity is computed based on Equation 2.9. Then for the calculations of the Reynolds number, the depth Froude number, the water level drop, the frictional resistance and the residual resistance, the relative velocity is used. The pressure resistance is determined with the adjusted velocity. After determining all resistance components, the total resistance is derived. The calculation of the effective power is based on the multiplication of the total resistance with the adjusted speed and then the delivered and the propulsive power were derived.

Bolt method modified by Backer

The limit speed, the adjusted, the return flow and the relative velocity are computed according to Bolt method as they are described in Chapter 2, Section 2.2 and Appendix H. Secondly, by using 0.15 & 0.16 formulas, it is determined the class of the waterway. Following the characterization of the fairway, the suitable equation for the calculation of the water level drawdown (Equation 2.15 or 2.16) is arranged.

$$\text{Normal, Narrow, Wide: } \frac{A_c}{A_s} \leq 5.45 \cdot h + 0.56 \cdot A_s - 17.68 \quad (0.15)$$

$$\text{Very wide: } \frac{A_c}{A_s} > 5.45 \cdot h + 0.56 \cdot A_s - 17.68 \quad (0.16)$$

Apart from these modifications, he also recommended the substitution of resistance coefficients. Especially, concerning the friction resistance the original surcharge by 40% in order to take into account the extra roughness that the curved hull shape and the appendages, it is suggested will be halved. Moreover, from tests that were done on M6 and M8 motor vessels, it is shown that a reduction from 0.15 to 0.1 in pressure coefficient had significant influence on the total resistance and in turn on the energy consumption. Additionally, in case of coefficient for water level drop, C_z , it is proposed to use the value of zero in case of motor vessels and 0.2 for inland barges. The equations for the calculation of the friction coefficient, the frictional, the pressure and the residual resistance are the one that were presented in Bolt method. Finally, for the calculation of the effective and the brake horsepower Equations 2.4 and 2.6 were applied respectively. The power efficiency coefficients that were used are as follows:

$$\eta_o = 0.55$$

$$\eta_h = 1.07$$

$$\eta_t = 0.91$$

Reference formula for implementing TU Delft method

- Friction resistance

The first component considered in Chapter 2, equation 2.1 is the frictional resistance while its computation was derived from Equation 0.1. The calculation of the wetted surface area of the vessel has a significant influence on the total frictional resistance and a detailed estimation is required. So, the wetted surface was computed as follows.

$$S_T = Ls(2T + B_S)\sqrt{C_M} \left(0.453 + 0.4425C_B - 0.2862C_M - 0.003467\frac{B}{T} + 0.3696C_{WP} \right) + 2.38\frac{A_{BT}}{C_B} \text{ [m}^2\text{]} \quad (0.17)$$

The block coefficient C_B expresses the “fullness” of the ship. Notably, it is the ratio of the underwater volume of the ship’s hull to the volume of a rectangular underwater block with a length and width equal to these of the ship, and the depth equal to the draft (Figure H-1). The block coefficient for inland vessels typically is relatively high, so a constant value of 0.85 is selected. Following that the midship coefficient C_M and the water plane coefficient C_{WP} are determined from Schneekluth and Bertram’s formula (Saha & Sarker, 2010), and both depend on the block coefficient.

$$C_M = 1.006 - 0.0056 \cdot C_B^{-3.56} \text{ [-]} \quad (0.18)$$

$$C_{WP} = \frac{1+2 \cdot C_B}{3} \text{ [-]} \quad (0.19)$$

As far as the A_{BT} the wetted transverse sectional area of the bulbous bow of the ship, the majority of inland ships do not have a bulbous bow and therefore A_{BT} was assumed equal to zero.

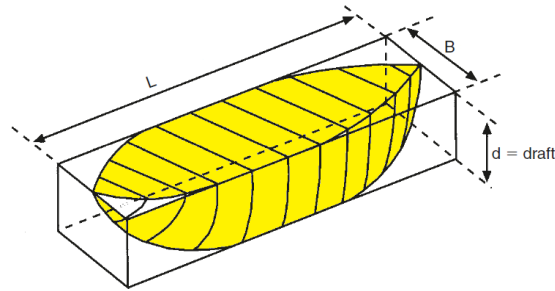


Figure H- 1: Visualization of block coefficient, displaced volume of the ship's hull is highlighted in yellow (Segers, 2021)

- Dimensionless friction coefficient C_f

Over the years, several methods have been developed to determine the friction coefficient C_f . The most popular formula is the ITTC57 correlation line, the simplicity and the relevant accuracy makes it frequently used to predict the frictional resistance of ships. However, the waterway restrictions (depth, width) and the unrestricted flow conditions were considered, cause limitations to the applicability of the formula .

The original resistance prediction method of Holtrop and Mennen (1982) uses the ITTC57 friction line as a starting point. Typically, inland shipping is strongly influenced by waterway limitations and as a consequence this influences the frictional resistance, which leads to decreasing accuracy of the prediction of the ITTC57 correlation line. Therefore, a modification of this correlation line by Zeng et al. (2018) is proposed, taking into account shallow water effects. Width and depth limitations both have influence on the resistance of inland vessels. This modification focuses on the effects of shallow water, since the effects from the lateral direction are in many cases much smaller than from the vertical direction. For simplification, waterways with no width, but only depth limitations are considered. In these cases, limited water depth mainly affects the bottom area of the vessel. The effects on other parts of the wetted surface are significantly smaller. Below, the effects of limited water depth are briefly discussed, followed by a fit of the numerical friction line proposed by Zeng et al. (2018) and a proposed method to be able to directly apply the theory to calculate the frictional resistance.

- 2D flat plate and velocity increase

Inland ships usually have a long parallel midbody with a large flat bottom, which is considered as a 2D flat plate (Figure H-2). The velocity of far-field incoming water is V (assuming no currents, this velocity is equal to minus the sailing speed). The water underneath the ship is accelerated by ΔV , caused by limited water depth and the displacement of the ship. This acceleration also occurs in deep water, but it is more significant in shallow water. Figure H-2 shows the following parameters: L_b is the length of the flat bottom (which is from now assumed to be equal to the ship length L), T is the draft of the ship and D is the distance between the flat plate of the ship and the bottom of the waterway.

Regarding the physical effects, when a vessel sails in shallow water, the flow will be accelerated for both reasons because of the reduced cross section that lead to higher velocity and due to the displacement of the boundary layer. This leads to a thinner boundary layer and the criterion to define the thickness is when D/L decreases which means shallower water:

- D = water depth minus ship draft ($h-T$)
- L = length of the flat plate

Entering shallow water consequently means that the velocity gradient normal to the 2D flat plate increases, which results in an increase of local friction. This means that the total friction, summing the local frictions, is also increased in case of limited water depths and depends on the ratio D/L .

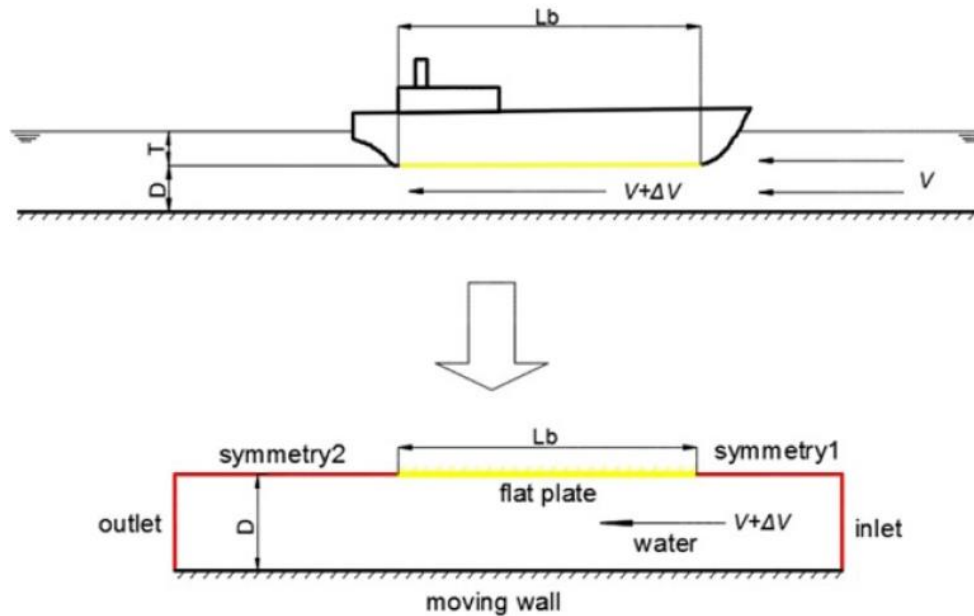


Figure H- 2: Simplification of the bottom of the ship in shallow water (Zeng et al., 2018)

- Fitting numerical line and method to apply the modified friction line

Zeng et al. (2018) proposed a numerical friction line, taking into account the shallow water effects. This friction line is based on Computational Fluid Dynamics (CFD) calculations. He applied a regression analysis, using the method of least squares. The results of the fitting give a function for the total frictional resistance coefficient in deep water $C_{f,deep}$ and in shallow water $C_{f,proposed}$. The deep water friction coefficient depends only on the Reynolds number and the ratio between underkeel clearance and ship length (D/L close or greater than 1). It should be mentioned that the coefficient for deep water has the same format as the ITTC57 correlation line but from the CFD calculations the value in numerator and denominator differs from the original values to 0.08169 and 1.717 respectively.

$$C_{f,deep} = \frac{0.08169}{(\log Re - 1.717)^2} [-] \quad (0.20)$$

For shallow water conditions ($D/L < 1$), the friction coefficient depends on the Reynolds number and on D/L and the following equation was derived. If the ratio of D/L is almost one, then only the first part for the deep water conditions is valid. Also, it had be seen the errors of this fitted line are most of the times less than 1% while in case of D/L equal to 0.01 the error increased to 3%. (Zeng et al., 2018).

$$C_{f,proposed} = \frac{0.08169}{(\log Re - 1.717)^2} \left(1 + \frac{0.003998}{\log Re - 4.393} \left(\frac{D}{L} \right)^{-1.083} \right) [-] \quad (0.21)$$

For the application of the new formulations in Holtrop and Mennen (1982) the proposed modification of the ITTC57 correlation line cannot directly be applied. The disadvantage of these formulas is that do not incorporate the non-horizontal wetted surfaces of inland ships. Consequently, this particularity should be taken into account. Therefore, the following

formula is proposed by Zeng et al. (2018) which includes a new friction line to calculate the friction coefficient of a flat plate in unrestricted water conditions.

$$C_f = C_{f0} + (C_{f,proposed} - C_{f,Katsui}) \left(\frac{S_B}{S_T} \right) \left(\frac{V_1}{V_0} \right)^2 [-] \quad (0.22)$$

C_f : Corrected total friction coefficient of a ship in shallow water [-]

C_{f0} : Conventional friction coefficient (ITTC57 correction line) [-]

$C_{f,proposed}$: Proposed friction line in shallow water [-]

$C_{f,Katsui}$: Katsui's line for friction coefficient of a flat plate in unrestricted conditions [-]

S_B : Area of the flat bottom [m^2]

S_T : Area of the total wetted surface [m^2]

V_1 : Vessel speed [m/s]

V_0 : Corrected velocity underneath ship's bottom [m/s]

In Equation 0.22 the conventional frictional coefficient by ITTC57 was used. The new friction line that is included in the proposed friction coefficient is the friction line as it is suggested by Katsui.

$$C_{f,Katsui} = \frac{0.0066577}{(\log Re - 4.3762)^\alpha} [-] \quad (0.23)$$

$$\alpha = 0.042612 \cdot \log Re + 0.56725 [-] \quad (0.24)$$

The area of the flat bottom can be approximated by the equation 5.41 and the average velocity underneath the ship at the edge of the flat bottom follows the formula 0.26 as it was formulated from Zeng et al. (2018). As it was derived the uncertainty of V_1 is only 2.5% and the applicability is limited to $h/T \leq 4$, otherwise V_1 is equal to sailing speed.

$$S_B = L \cdot B [m^2] \quad (0.25)$$

$$V_1 = V_0 + \Delta V = 0.4277 \cdot V_0 \cdot e^{\frac{h}{T}^{-0.07634}} \left[\frac{m}{s} \right] \quad (0.26)$$

In his research tested the formula 0.22 and it was shown that this formula agrees better with the values derived from CFD calculation instead of ITTC57. As it has an uncertainty less than 3%, makes it a successful to predict the friction including shallow water effects on the ship's flat bottom.

- Viscous resistance

In J. Holtrop and G.G.J. Mennen theory of 1982 the effect of viscosity is introduced to the total resistance via the form factor ($1+k_1$), No matter water has a relatively low viscosity, it still produces a significant viscous resistance force on the ship. The form factor is computed by Equation 0.27. It is mentioned that Equation 0.27 is a modification of an earlier form factor equation proposed by Holtrop and Mennen in Watson (1998) study. The form factor has to be multiplied by the frictional resistance to take into account the effect of viscosity.

$$1 + k_1 = 0.93 + 0.487 C_{14} (B_s/L_s)^{1.068} (T/L_s)^{0.461} (L_s/L_R)^{0.122} (L_s^3/\Delta)^{0.365} (1 - C_p)^{-0.604} [-] \quad (0.27)$$

$$\text{Specific shape coefficient for th afterbody: } C_{14} = 1 + 0.0011 C_{stern} [-] \quad (0.28)$$

$$C_{stern} = \begin{pmatrix} 0, \text{ for normal shape afterbody} \\ -25 \text{ to } -20, \text{ for barge - shaped forms} \end{pmatrix}$$

$$\text{Length of the run: } L_R = L_S(1 - C_p + \frac{0.06C_p l_{cb}}{4C_p - 1}) [m] \quad (0.29)$$

$$\text{Primstaic coefficient: } C_p = \frac{C_B}{C_M} [-] \quad (0.30)$$

$$\text{Longitudinal postion of the centre of buoyancy: } l_{cb} = -13.5 + 19.4C_p [-] \quad (0.31)$$

- Wave resistance

The fourth resistance component defined by Holtrop and Mennen (1982), is the wave resistance. Differently from Bolt (2003) theory, present method investigate also the third shallow water effect which is the ship waves. When a ship sails, it creates waves, which results in additional resistance. As the vessel speed increases (in shallow or narrow waterways or both), the height of the produced waves increases and therefore the wave resistance becomes higher. The magnitude of the wave resistance is strongly connected with the depth Froude number, so when it approaches critical discharge, the resistance increases even more. For estimating the wave resistance, a distinction is made between different ranges of Froude number while its calculation is based on the corrected velocity V_2 . The Equation 0.32 shows the wave resistance.

- Wave resistance for $Fn_{v2} < 0.4$:

$$R_{w1} = C_1 \cdot C_2 \cdot C_5 \cdot \Delta \cdot \rho_w \cdot e^{(m_1 \cdot Fn_{v2}^{-0.9} + m_4 \cdot \cos(\lambda \cdot Fn_{v2}^{-2}))} [kN] \quad (0.32)$$

$$\Delta = C_B \cdot L_S \cdot B_S \cdot T \quad (0.33)$$

In equation 0.33 the block coefficient is selected equal 0.85 as it is previously explained.

$$C_1 = 22,231,105 \cdot C_7^{3.78613} \frac{T^{1.07961}}{B_S} \cdot (90 - i_E)^{1.37165} [-] \quad (0.34)$$

Angle of the waterline at the bow:

$$i_E = 1 + 89 \cdot e^{\left[-\left(\frac{L_S}{B_S}\right)^{0.80856} (1 - C_{wp})^{0.30484} (1 - C_p - 0.225l_{cb})^{0.6367} \left(\frac{L_R}{B_S}\right)^{0.34574} \left(\frac{100\Delta}{L_S^2}\right)^{0.16302} \right]} [-] \quad (0.35)$$

$$C_7 = \begin{cases} 0.229577 \cdot \left(\frac{L_S}{B_S}\right)^{\frac{1}{3}}, & B_S/L_S < 0.11 \\ B_S/L_S, & 0.11 < B_S/L_S < 0.25 \\ 0.5 - 0.0625 \left(\frac{L_S}{B_S}\right), & B_S/L_S > 0.25 \end{cases} [-] \quad (0.36)$$

$$C_5 = 1 - \frac{0.8A_T}{C_M B_S L_S} [-] \quad (0.37)$$

$$\lambda = \begin{cases} 1.446C_p - 0.03 \frac{L_S}{B_S}, & L_S/B_S < 12 \\ 1.446C_p - 0.036, & L_S/B_S > 12 \end{cases} [-] \quad (0.38)$$

$$m_1 = 0.01140407 \frac{L_S}{T} - 1.75254 \frac{\Delta^{\frac{1}{3}}}{L_S} - 4.79323 \frac{L_S}{B_S} - C_{16} [-] \quad (0.29)$$

$$C_{16} = \begin{cases} 8.07981C_p - 13.8673C_p^2 + 6.984388C_p^3, & C_p < 0.8 \\ 1.02344, & C_p > 0.8 \end{cases} [-] \quad (0.30)$$

$$m_4 = 0.4 \cdot C_{15} \cdot e^{-0.034 \cdot Fn_{V2}^{3.29}} [-] \quad (0.41)$$

$$C_{15} = \begin{cases} C_{15} = -1.69385, & \frac{L_S^3}{\Delta} < 512 \\ C_{15} = -1.69385 + \frac{\left(\frac{L_S}{\Delta^{\frac{1}{3}}}\right)^{-8}}{2.36}, & 512 < \frac{L_S^3}{\Delta} < 1727 \\ C_{15} = 0, & \frac{L_S^3}{\Delta} > 1727 \end{cases} [-] \quad (0.42)$$

- Wave resistance for $Fn_{V2} > 0.55$:

$$R_{w2} = C_{17} \cdot C_2 \cdot C_5 \cdot \Delta \cdot \rho_w \cdot e^{(m_3 \cdot Fn_{V2}^{-0.9} + m_4 \cdot \cos(\lambda \cdot Fn_{V2}^2))} [kN] \quad (0.43)$$

$$C_{17} = 6,919 \cdot C_M^{-1.3346} \cdot \frac{\Delta^{2.00977}}{L_S^3} \cdot \left(\frac{L_S}{B_S} - 2\right)^{1.40692} [-] \quad (0.44)$$

$$m_3 = -7.2035 \cdot \frac{B_S^{0.326869}}{L_S} \cdot \frac{T^{0.605375}}{B_S} [-] \quad (0.45)$$

- Wave resistance for $0.4 < Fn_{V2} < 0.55$:

$$R_{w3} = R_{w1} + \frac{(10Fn_{V2} - 4) \cdot (R_{w2} - R_{w1})}{1.5} [kN] \quad (0.46)$$

- Appendage resistance

The appendage resistance as it was introduced by Holtrop and Mennen (1982), is attributed to the ship appendages such as rudders, shafts, skeg and etc. The result is an additional frictional resistance when a ship moves through the water. It can be expressed as follows.

$$R_{APP} = \frac{1}{2} \cdot \rho_w \cdot V_0^2 \cdot C_f \cdot S_{APP} \cdot (1 + k_2) [kN] \quad (0.47)$$

$$\text{Appendage factor: } 1 + k_2 = 2.5$$

$$\text{Wetted area of appendages: } S_{APP} = 5\% S_T \text{ for inland ships}$$

- Immersed transom resistance

The immersed transom of inland ships (vertical flat plate at the stern) results in an additional pressure resistance that should be considered. The magnitude of this resistance term is defined by the transom Froude number (Equation 0.49).

$$R_{TR} = \frac{1}{2} \cdot \rho_w \cdot V_2^2 \cdot C_6 \cdot A_T [kN] \quad (0.48)$$

$$\text{Transom Froude number: } F_{nT} = \frac{V_2}{\sqrt{2 \cdot g \cdot A_T / (B_S + B_S \cdot C_{WP})}} [-] \quad (0.49)$$

$$C_6 = \begin{cases} 0.2 \cdot (1 - 0.2F_{nT}), & F_{nT} < 5 \\ 0, & F_{nT} \geq 5 \end{cases} [-] \quad (0.40)$$

$$\text{Transom area: } A_T = 20\% B_s \cdot T$$

- Model-ship correlation resistance

The final resistance term is the model-ship correlation resistance which again takes into account the shallow water effect by applying the corrected velocity V_2 . The Karpov theory (van Terwisga, 1989) is used for this estimation. This theory was developed into a towing tank so through the correlation allowance coefficient the differences between measurements by full-scale experiments and the resistance estimated by model testing are normalized.

$$R_A = \frac{1}{2} \cdot \rho_w \cdot V_2^2 \cdot C_A \cdot S_T [kN] \quad (0.51)$$

$$\text{correlation allowance coefficient: } C_A = 0.006(L_s + 100)^{-0.16} - 0.00205 + 0.003 \sqrt{\frac{L_s}{7.5}} C_B^4 C_2 (0.04 - C_4) [-] \quad (0.52)$$

$$\text{Coefficient for the effect of bulbous: } C_2 = 1$$

$$C_4 = \begin{cases} \frac{T}{L_s}, \frac{T}{L_s} < 0.04 \\ 0.04, \frac{T}{L_s} > 0.04 \end{cases} [-] \quad (0.53)$$

$$\text{Ship wetted surface: } S_T [m^2]$$